ELECTROCHEMISTRY AND PHOTOPHYSICS

OF CARBON NANODOTS-DECORATED NIGS

(Ni(In, Ga)Se$_2$) QUANTUM DOTS

By

BANGILE NOEL ROLIHLAHLA

(BSc Honours)

A thesis submitted in partial fulfilment of the requirements for the degree

of

MAGISTER SCIENTIAE IN NANOSCIENCE

In the

Faculty of Science

University of the Western Cape, South Africa

Supervisor: Prof Emmanuel Iwuoha

Co-supervisor: Dr Unathi Sidwaba

November 2019

ABSTRACT

Currently, non-renewable sources are mostly used to meet the ever-growing demand for energy. However, these sources are not sustainable. In addition to these energy sources being not sustainable, they are bad for the environment although the energy supply sectors highly depend on them. To address such issues the use of renewable energy sources has been proven to be beneficial for the supply of energy for the global population and its energy needs. Advantageous over non-renewable sources, renewable energy plays a crucial role in minimizing the use of fossil fuel and reduces greenhouse gases. Minimizing use of fossil fuels and greenhouse gases is important, because it helps in the fight against climate change. The use of renewable energy sources can also lead to less air pollution and improved air quality. Although solar energy is the most abundant source of renewable energy that can be converted into electrical energy using various techniques, there are some limitations. Among these techniques are photovoltaic cells which are challenged by low efficiencies and high costs of material fabrication. Hence, current research and innovations are sought towards the reduction of costs and increasing the efficiency of the renewable energy conversion devices. This work developed and investigated the electrochemistry and photophysics of carbon nanodots-decorated quaternary quantum dots of nickel (Ni), indium (In), gallium (Ga) and selenium (Se) (NIGS) as potential material that can be efficiently convert light into useful energy. The carbon nanodots were synthesized using a greener route through microwave irradiation while the NIGS quantum dots were synthesized using solvothermal synthesis. These materials were then combined into a nanocomposite using the microwave synthesis. The properties of these materials (CNDs, NIGS and CND-NIGS nanocomposite) were investigated using spectroscopy (Fourier Transform Infrared (FT-IR) spectroscopy, ultraviolet-visible (UV-Vis)

i

spectroscopy, photoluminescence (PL) spectroscopy, Raman spectroscopy, small angle X-ray scattering (SAXS) spectroscopy and X-ray diffraction spectroscopy (XRD)), microscopy (transmission electron microscopy (TEM)), and electrochemistry (cyclic voltammetry (CV)).The FTIR spectrum of carbon nanodots revealed that the structure consisted of O-H, C-O-C and C=O bands originating from the glucose precursor. The UV-Vis spectroscopy revealed that the carbon nanodots absorb light in the UV region with a characteristic short-wavelength peak at 284 nm, attributed to the π-π* transitions. The carbon nanodots also exhibited intense photoluminescence with emission peaks at 445 nm and 636 nm. The shape of the carbon nanodots was found to be spherical with diameters 9-13 nm as determined from HRTEM analysis, and 15-20 nm as determined from SAXS analysis. Carbon nanodots exhibited an oxidation-reduction pair centered at 0.6 V and 0.01 V (vs Ag/AgCl). This pair was attributed to oxidation and reduction of the CNDs. XRD and SAED from HRTEM revealed an amorphous nature of the carbon nanodots. Similarly to CNDs, NIGS quantum dots had a spherical shape, but with estimated diameters of 11.55 nm from HRTEM analysis and 18-55 nm from SAXS analysis. The NIGS quantum dots absorb light at 547 nm with a broad band extending to 750 nm. From these results, an optical bandgap of 2.01 eV was determined. The PL analysis revealed that the NIGS quantum dots emit light at 397 nm. The NIGS quantum dots exhibited two oxidation peaks with maximum peak current of 29 μA and at 35 μA appearing at 0.53 V and 0.95 V, respectively. The carbon nanodots-decorated NIGS quantum dots absorbed light in the visible region of the solar spectrum at 400 nm and 750 nm from which an optical bandgap of 1.97 eV was determined. The carbon nanodots-decorated NIGS quantum dots exhibit maximum peak current of 98 μA at 0.63 V and 17 μA at 1.0 V (vs Ag/AgCl). The low bandgap of carbon nanodots-decorated NIGS quantum dots indicates potential applications in photovoltaic cells.

KEYWORDS

Bandgap

Carbon nanodots

Carbon nanomaterials

Electrochemistry

Green synthesis

Microwave irradiation

Nanomaterials

NIGS quantum dots

Photophysics

Photovoltaic cells

Renewable energy

ABBREVIATIONS

Ag: silver

Al: aluminium

Au: gold

Cd: cadmium

CdS: cadmium sulphide

CdSe: cadmium selenide

CdTe: cadmium telluride

CIGS: copper indium gallium selenide

CIS: copper indium selenide

CNDs: carbon nanodots

CNTs: carbon nanotubes

Co: cobalt

CV: cyclic voltammetry

EDS: energy-dispersive X-ray spectroscopy

Fe: iron

FT-IR: Fourier Transformed Infrared

GWh: gigawatt hours

HOMO: highest occupied molecular orbital

HRTEM   high resolution transmission electron microscopy

HRTEM: high resolution transmission electron microscopy

IR: infrared

LUMO: lowest unoccupied molecular orbital

MEG: multiple exciton generation

MW:	megawatts
NIGS:	nickel indium gallium selenide
Pb:	lead
PbS:	lead sulphide
PbSe:	lead selenide
PL:	photoluminescence
PV:	photovoltaic
QDs:	quantum dots
SAED:	selected area electron diffraction
SAXS:	small angle X-ray scattering
SWCNTs:	single walled carbon nanotubes
UV-Vis:	ultraviolet visible
XRD:	X-ray diffraction
Zn:	zinc
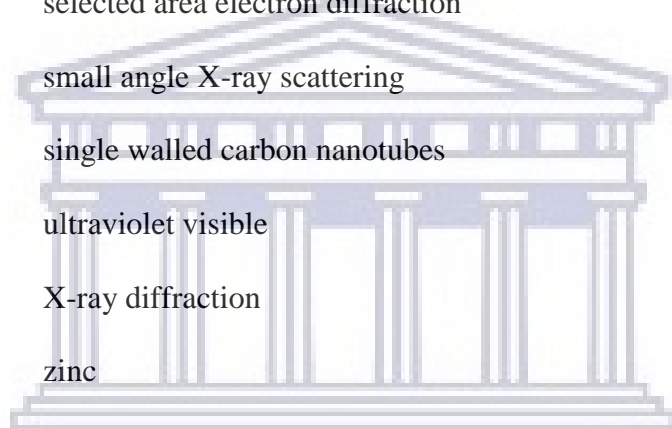
DECLARATION

I declare that **"Electrochemistry and photophysics of carbon nanodots-decorated NIGS (Ni(In, Ga)Se$_2$) quantum dots"** is my own work, that it has not been submitted before for any degree or examination in any other university, and that all the sources I have used or quoted have been indicated and acknowledged as complete references.

Signature_____

Bangile Noel Rolihlahla   **24 November 2019**

DEDICATION

I would like to dedicate this master's degree to my father Bafana Rolihlahla, and my mother Nosakhele Rolihlahla.

ACKNOWLEDGEMENTS

I would like to acknowledge the following people and institutions:

- I would like to express my gratitude to my supervisor Prof Emmanuel Iwuoha for giving me the chance to do this research project and for providing support in this physically and emotionally challenging project.

- I would like to send many thanks to my co-supervisor Dr. Unathi Sidwaba for expert advice and all the support provided in this project.

- I would also like to thank my fellow laboratory mates Mr Sabelo Sifuba, Mr Samuel Mkehlane, Miss Noniko Nqakala, Mr Siyabonga Mdluli, Miss Penny Mathumba, Miss Sixolile Mini, Mr Muziwenkosi Memela, Mr Emmanuel Ramoroka and Mr Christopher Nolly from University of the Western Cape Sensor Laboratories (SensorLab) for all the support provided.

- I would also like to express my gratitude to Miss Valencia Jamalie and Prof Dirk Knoesen from the University of the Western Cape MSc Nanoscience Postgraduate Programme for the support provided.

- I would to like to express my gratitude to the National Nanoscience Postgraduate Teaching and Training Platform for their financial support during the course of my studies.

- I would also like to thank Dr Remy Bucher & Mr Zakhele Khumalo from Ithemba LABS materials research department for all the assistance provided during XRD characterization.

- I would also like to thank Dr Subelia Botha and colleagues from the electron microscope unit (EMU) at the University of the Western Cape department of physics for all the assistance provided for HRTEM characterization.

LIST OF PUBLICATIONS

1. **Rolihlahla, B.,** Sidwaba, U. and Iwuoha, E. Electrochemistry and photophysics of carbon nanodots-decorated NIGS (Ni(In, Ga)Se$_2$) quantum dots.(*Manuscript under preparation).*

2. **Rolihlahla, B.,** Sidwaba, U. and Iwuoha, E. A short review on sugar-derived carbon nanodots: Green synthesis methods and applications (*planned manuscript*).

TABLE OF CONTENTS

LIST OF FIGURES

<div align="center">

CHAPTER 1

INTRODUCTION

</div>

1.1 Overview

In this chapter, the summary of the importance of carrying this project is stated. The background of the research is also discussed. This chapter also includes the problem statement, motivation for carrying out the study aims and objectives.

1.2 Introduction

1.2.1 Energy demand

Ever since the end of World War 2 in 1945, humans have become more dependent on non-renewable energy sources for energy supply [1]. In the modern world energy has become a burning issue, as we have been relying on unstainable sources of energy such as fossil fuels for a very long time [2]. Non-renewable energy is obtained from sources which are predicted to run out in the next 200 years [3]. These unrenewable sources of energy will not only run out soon they are also having adverse effects on the environment [4]. As the demand for energy supply increases, with the world's population increasing at an exponential rate, it is predicted that these non-renewable energy sources will not be able to handle this increasing demand in future [5]. Renewable energy most sources include natural gas, oil and coal which are limited [6]. The shortage of energy does not only negatively affect the environment, it has social impact as well. The competition for resources can lead to regional conflicts such as the case for oil while the burning of fossil fuels contributes to global warming [7]. As a results, the over use of these non-renewable energy sources can lead to them running out sooner than expected [8].

Renewable energy sources offer benefits to the environment and to human beings, because little or no toxic gases are emitted during their use [9]. Amongst the benefits of using these renewable sources of energy is that they are not going to run out anytime soon [10]. Renewable energy activities are situated in rural areas, this could provide economic opportunities for local residents [11]. Most countries around the world are moving into renewable energy but at a snail's pace [12]. In 2013, the use of renewable sources for the generation of energy around the globe was estimated to be 19.1% and this was expected to increase, the biggest growth was observed in solar energy technologies followed by wind power [13].

1.2.2 Solar energy

It is obvious that there is a need to move towards renewable energy sources to solve the problem of energy supply especially for a region like Africa. One of those renewable sources is solar energy, the energy from the sun [14]. Solar energy has many applications including electricity power production, solar propulsion and solar desalination [15]. The sun is a stable, cleanest and most reliable source of energy on earth, with no carbon emissions or product waste generated [16]. This abundant energy source is converted to useful energy utilizing various devices including solar cells (photovoltaic cells and concentrated solar cells). Photovoltaic (PV) cells are the popular of the two and will be the focus of our research [17].

The history of PV cell dates back to 1876 and it is recognized as the energy for the future, because the energy from the sun is expected to last for billions of years. South Africa is one of those African countries with the highest solar radiation, with an average of 8 and a

half hour of sunshine daily [18]. Most of this abundant solar radiation is found in the province of Northern Cape in Upington with a potential to generate 5000 megawatts (MW) of electricity from solar power using PV cells [19]. Clearly, South Africa has a big potential in generating energy using PV cells, following the fact in 2014 it was listed 9th in the world for the solar PV market [20]. Also one of the biggest solar PV cell in Africa is found in Northern Cape, with a potential of providing 180 GWh of electricity to 80000 households [19]. According to the Climatescope report of 2015, South Africa had invested more in PV cells than any other sub-Saharan African country [21]. However high costs and low efficiencies are hindering the development of these energy conversion devices [22]. As a result many research groups have recognized improvements in photovoltaic cells are needed to optimize the conversion of this fascinating energy from the sun [23].

1.2.3 Energy and nanotechnology

In age of renewable energy, most countries are moving towards green energy solutions, because it is being seen as the energy for the future [24]. Current approaches of improving the materials used for solar energy conversion to electricity have major drawbacks such as not being environmentally benign and economically feasible [25]. This is a problem especially in a country like South Africa which has so much inequality. Thankfully, nanotechnology has a potential to solve some of these problems, which in future can lead to equality access energy sources for everyone [26]. Particularly the use of nanoparticles holds a big promise of minimizing the costs in the current solar conversion technologies [27]. Among these nanoparticles, semiconductor nanocrystals such as quantum dots and the emerging carbon nanodots have attracted strong interest due to their novel optical and electronics characteristics which, apart from the diverse applications, can increase the efficiency of solar conversion devices at lower costs [28].

1.2.4   Energy conversion and challenges

Although, the sun is the cleanest and sustainable sources of energy, the biggest challenge is finding suitable materials to efficiently collect this energy [29]. Solar cell is one of the important energy conversion device, a photovoltaic cell is a type of solar cell that uses the principle of photo electric effect to convert solar energy into electrical energy [30]. The process (as illustrated in Figure 1.1) begins when photons of light fall on the cell free electrons are ejected, this results in the flow of electric current [31]. The majority of photovoltaic cells consist of semiconducting material which absorb and traps photons from the sun [32]. These absorbed photons generate electron-hole pair, the electrons flow in a similar direction being controlled by internal electric field originating from p-n junction material, and finally generate electric current [33].   The p-n junction is formed by combining positively charged (p) material with negatively charged (n) material [34].
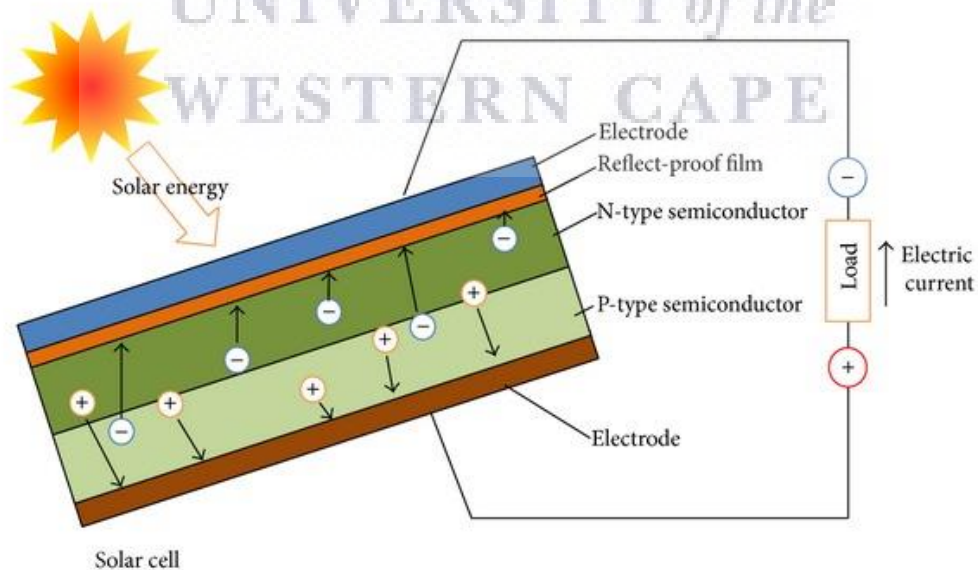
Figure 1.1: Visual representation of the working principle of PV cells [34].

1.2.5   Quantum dots

Semiconducting nanoparticles recently have become a hot topic in research, because of their unique properties [35]. Quantum dots were discovered about three decades ago and have attracted attention in solar cell technology because of their superior optical, electronic and photoluminescence properties [36]. Quantum dots are semiconductor nanoparticles that are small in size (with diameter between 2 nm and 10 nm). Quantum dots have size-dependent properties such as colour and their emission of light and this phenomenon is due to quantum confinement [37]. All these unique properties have made quantum dots useful in many applications [38]. These applications include solar cells, light emitting diodes, lasers, emitters for colour displays, sensors and bio-imaging [39]. Over the last ten years more new avenues have been explored to use quantum dots in optoelectronic applications, especially solar cell devices [40].

Although, silicon solar cells are commercial popular their fabrication processes are very expensive while their achievable maximum efficiency is restricted to 33.7% , some research groups have tried finding better alternatives such as dye-sensitized-solar cells, perovskite solar cells, organic solar cells and quantum dots-sensitized-solar cells [41]. These alternatives have reduced the manufacturing costs and have shown the potential to increase the maximum achievable efficiency to 44.7% [42]. Quantum dots solar cells have an edge over the other alternatives, because of unique optical and electrochemical properties which are size dependent [43]. One of the attractive properties of these nanoparticles which restrict movement of electrons in three dimensions is their potential to generate multiple excitons [44].

The chemical synthesis of quantum dots can be tricky and since their discovery, there has been improvements which lead to products that have controlled shape, size and composition [43]. In the 1980s, Ekimov and colleagues at the Loffe Institute in St. Petersburg, Russia, reported the size-controlled characteristics of ionic nanocrystals in a glass matrix [45]. Also in the same era, Brus discovered the size-controlled behaviour of colloidal CdS nanocrystals using the measurement of size-dependent redox potentials [46].

In solar cell devices, quantum dots are used as absorber material (a material that absorbs light). Lead (Pb) chalcogenides (lead sulphide (PbS) and lead selenide (PbSe)) and cadmium (Cd) chalcogenides (cadmium selenide(CdSe), cadmium sulphide (CdS) and cadmium telluride(CdTe)) quantum dots are popular solar cell sensitizing material utilized [47]. The biggest problem when using these Pb and Cd chalcogenides is that they are very toxic, making it clear that a shift towards green quantum dots is needed. These environmentally friendly quantum dots include compounds of group I–III–VI$_2$ elements such as CuInS$_2$(CIS), CuInSe$_2$ (CISe), CuInSeS(CISeS) and Cu(In,Ga)Se (CIGS) [48]. Amongst these copper indium gallium selenide (Cu(In,Ga)Se, CIGS) quantum dots are popular for their good stability and absorption close to the infrared (IR) spectrum of sunlight [49]. Another property of CIGS that make them superior when compared to crystalline silicon (another widely used solar cell material), is that they are a direct band gap semiconductor, meaning that CIGS have the potential to result in higher efficiency than silicon [50]. This efficiency was found to be 22.8%, as compared to 19% of silicon. However CIGS (efficiency, performance or properties) is still inferior to Pb and Cd chalcogenide quantum dots because their mechanism and engineering is not yet fully understood [51]. Hence, there is need for integration of various molecules or materials to

these semiconducting quantum dots to yield novel nanostructures with unique chemical and physical properties [52].

1.2.6   Carbon nanodots

Carbon nanodots (C-dots) (also referred to as carbon quantum dots) are an emerging type of nanocarbon, and usually consist of quasi-spherical nanoparticles with sizes less than 10 nm. Carbon nanodots generally have a large number of carboxylic acids groups on their surface, a property which makes them highly soluble in water with a good photoluminescence [53]. They have become a hot topic in research not only because of their potential to be used as substitute for the toxic conventional metal-based quantum dots, but also for the potential to replace conventional semiconducting quantum dots for many applications. This arises from their solubility in water, good photoluminescence, photostability and less toxicity [54].

Interestingly, C-dots were discovered by luck 13 years ago, during the purification of single walled carbon nanotubes (SWCNTs) synthesized by arc-discharge method. After the purification process the researchers also obtained a novel nanomaterial which later became known as carbon nanodots or carbon dots [55]. Since their fascinating discovery, they have attracted strong interest from researchers, because of their dominant photoluminescence (PL) property among others. The mechanism of this PL property is not yet fully understood, but is believed to result from the radiative recombination of excitons found on the surface energy traps [56].

1.2.7   Problem statement

Quantum dots are known for their fascinating light harvesting properties with applications in energy-based devices such as solar cells. However, the full potential of the quantum dots for this property is not yet realized. The major problem lies with the instability of quantum dots which results in low efficiency when they are applied in solar cells. Currently, crystalline silicon is the mostly widely utilized material for commercial solar cells, because it offers relatively better efficiency [57]. However, this comes at higher manufacturing costs, because obtaining silicon is not cheap. Also, silicon solar cells are not flexible and they suffer from low charger carrier mobility.

Amongst various available alternatives, nanoparticles characterized by large surface area can help to alleviate this problem. Examples include quantum dots which are known for their attractive light harvesting properties with applications in energy-based devices such as solar cells. These semiconducting nanoparticles have the potential to increase the efficiency of solar cells, possible through better engineering and finding to of ways to stabilize the quantum dots. However, there are major environmental concerns with regards to the starting materials used in preparation of these semiconducting nanocrystals [58]. Most popular quantum dots use toxic chemicals as such lead and cadmium. This is where it becomes important to utilize environmentally benign precursors during preparation of these nanomaterials. Hence, production of quantum dots that contain less-toxic chemicals while the electronic and optical properties are maximized for excellent solar cell efficiency is of vital importance.

To address the issues associated with the low efficiency of solar cells, the use of harsh chemicals that endanger the environment and the use toxic element-based quantum dots, this study adapted the green preparation route of microwave irradiation to develop a nanocomposite of quantum dots and carbon dots. The chalcogenide quantum dots were made from nickel, indium and gallium while the carbon dots were derived from a sugar precursor. The yielded nanocomposite is expected to have enhanced performance for future solar cell applications.

1.2.8   Rational and motivation

The energy from the sun is the most abundant form of renewable energy which expected to last for over billion years. When this abundant form of renewable energy from the sun is efficiently harvested, it can lead to easy access to electricity even for those people in remote areas. Photovoltaic cells are a fast- growing sector in the alternative energy industry owing to abundance of radiation from the sun. Most developing and developed countries are investing a lot in photovoltaic cells, because they have the potential to offer relatively cheaper renewable energy. While providing us with useful energy, they are causing minimum or no damage to the environment. Some solar cells occupy large space of land and hence, with the use of nanomaterials smaller solar cells, that will not occupy a large space of land can be produced.

Quantum dots are very small particles and they also have tuneable a bandgap which depends on the size. Quantum dots exhibit the unique multi exciton generation phenomenon and distinctive charge transfer property. However, despite the amazing properties of quantum dots, there are still some challenges such as their instability and the

use of toxic precursors when preparing quantum dots. Also, some of the properties of quantum dots such as the origin of the multi exciton generation is not yet fully understood. It is these challenges that motivated us to study the photophysical and electrochemical properties of carbon nanodots-decorated NIGS quantum dots prepared using environmentally benign precursors and synthesis methods.

1.2.9 Aims and Objectives

The main aim of this research was to develop and investigate the photophysical and electrochemical properties of selenium-based ternary quantum dots comprising nickel, indium and gallium ($Ni(In,Ga)Se_2$), NIGS) decorated with sugar-derived carbon nanodots (CNDs).

The objectives of this study included:

• Microwave-assisted synthesis of sugar-derived carbon nanodots and their characterization for optical, morphological, structural and electrochemical properties.

• Synthesis and characterization of ternary NIGS quantum dots using solvothermal methods.

• Synthesis of a nanocomposite comprising the ternary NIGS quantum dots and carbon nanodots using the microwave irradiation technique.

• Investigating the effects of the NIGS and CNDs on the photophysics and electrochemistry of the nanocomposite using spectroscopy (ultraviolet visible spectroscopy (UV) and photoluminescence spectroscopy (PL) spectroscopy) and electrochemistry (cyclic voltammetry (CV)).

1.2.10   Thesis outline

The outline below gives a brief insight about what is discussed in each chapter.

Chapter 1

This chapter gives a brief introduction on the energy supply challenge and a brief discussion on how nanomaterials have been proven to address known challenges towards meeting the escalating energy demand. This chapter also includes the problem statement and motivation while it also covers the objectives conducted towards achieving the main aim of the project.

Chapter 2

This chapter gives a detailed literature review on quantum dots and carbon nanodots. Different synthesis methods for these nanomaterials and their applications, specifically in energy-harvesting devices, are described.

Chapter 3

This chapter covers the synthesis of carbon nanodots, the experimental procedure followed and a detailed analysis and discussion of the results obtained.

Chapter 4

This chapter of the thesis deals with NIGS quantum dots and their detailed analysis. This section of the thesis includes analytical methods, experimental procedure, results and discussion.

Chapter 5
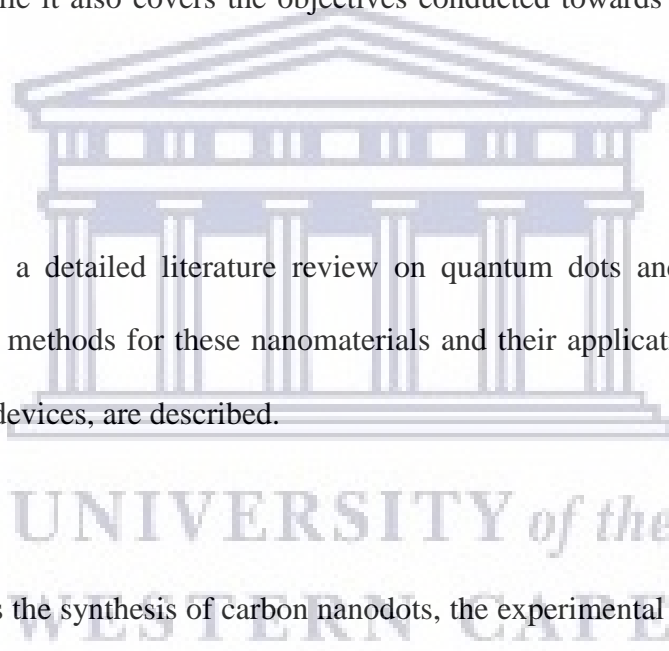
This chapter of the thesis deals with the carbon nanodots-decorated NIGS quantum dots nanocomposite. The effect of fusing together the CNDs and NIGS to form the nanocomposite are investigated and discussed.

Chapter 6

This chapter summarizes the findings of this research and future recommendations.

CHAPTER 2

LITERATURE REVIEW

2.1 Overview

Research in nanomaterials is increasing exponentially, because these materials have the potential to play an important role in improving the quality of life for the modern society. Nanomaterials are very important in both nanoscience and nanotechnology, because they can radically change the ways in which materials are made. In this section of the work important concepts and theories relating to quantum dots and carbon nanodots are described. Also in this chapter, work from other researchers is analysed and scrutinized and finally, characterization techniques used to study the properties of different quantum dots and carbon nanodots are explained.

2.2 Nanomaterials

Nanomaterials offer huge benefits for third-generation solar cells while utilizing low cost materials for reduced manufacturing cost. Despite their extraordinary properties the full potential of quantum dots has not been realized, because of issues with their stability [59]. Although quantum dots (metallic or carbon-based) were discovered about three decades ago, quantum dots have not yet provided strong competition to conventional material to harvest light in solar cells, this is partly due to lack of understanding of their surface chemistry. In this paper we will evaluate work done by other research groups on these zero dimensional nanoparticles especially for application in solar cells [60].

2.3   Metal-based nanomaterials

Inorganic solids generally consist of three distinct classes which are metals, semiconductors and insulators. Semiconductors are well known for having the valence band and the conduction band, where the valence band has the highest occupied molecular orbital (HOMO) while the conduction band has lowest unoccupied molecular orbitals (LUMO) [59]. Normally in a semiconductor the electrons are excited from HOMO to LUMO. When inorganic solids are in nanoscale dimensions their electronic properties change, the electrons at nanometer scale generally follow the "particle in-a-box" model and the band structure can be explained using this model [61].

Semiconducting nanoparticles are one of the most significant materials in nanoscience and nanotechnology, because these nanoparticles have fascinating optical, electronic, catalytic and magnetic properties which are unique from their bulk counterparts. These types of nanomaterials are prepared from metals using top down or bottom up approach. The metals used to synthesize metal nanomaterials usually include aluminium (Al), cadmium (Cd), cobalt (Co), copper (Cu), gold (Au), iron (Fe), lead (Pb), silver (Ag) and zinc (Zn). It has been proven that the size and morphology of nanomaterials are related to their applications [62].

2.4   History of quantum dots

Research on nanoparticles was started in 1857 by Michael Faraday when he was investigating the thin film of gold. Ever since then these unique materials have generated strong interest from the research community, these interest is largely due to their large

surface area as compared to their bulk counterparts [63]. This unique property increases the reactivity of materials, the increase in surface area is due to the small size of nanoparticles which is typically 1-100 nm. Quantum dots are very small particles of semiconductors in the nanometer scale. Quantum dots emerged from several research laboratories. About three decades ago, Alexei Ekimov identified these semiconducting nanoparticles in a glass matrix while Louis Brus is widely credited with their discovery in colloidal solutions [64].

Quantum dots are generally semiconductor colloidal crystals of II–VI, III–V and IV–VI of the periodic table of elements. These nanoparticles are special because their optical and electronic properties depend on their size which is typically 2-10 nm. The changes in the electronic and optical properties occur as the electron, hole and exciton is quantum confined in zero dimension [65]. It is for this reason that these colloidal nanocrystals are popularly known as quantum dots and their physical and chemical properties are greatly influenced by quantum confinement effects. This natural phenomenon results in these semiconducting nanoparticles having size tuneable and discrete energy levels [66]. The quantum confinement phenomenon also leads to the increase in the bandgap of quantum dots which is also dictated by size as well [67].

Although quantum dots are not historically popular in nanotechnology like carbon based nanoparticles, quantum dots have recently attracted a lot of interest in the scientific community for obvious reasons. Quantum dots have fascinating properties such as quantization of energy levels filled by charge carriers, the size is wavelength dependant, novel magnetic properties and multiple generation of electron-hole pairs (excitons) for light harvesting properties [67].

2.5 Different types of quantum dots

2.5.1 Quantum dots containing cadmium

Quantum dots (QDs) have become a hot topic in research over the last ten years due to their unique properties and many different applications such as solar cells. Widely established quantum dots include Cadmium telluride (CdTe), Cadmium sulphide (CdS) and Cadmium selenide (CdSe). Although these nanomaterials exhibit superior electronic and optical properties, they are toxic since they all consist of cadmium. Their toxicity hinders their application in various fields [68,69]. Also, although these QDs exhibit good light harvesting properties for solar cells, we cannot turn a blind eye to their adverse environmental effects. The challenge is to try to offer other QDs that do not contain the toxic Cd. At the same time, these non-toxic and environmentally friendly alternatives must be able to efficiently convert light into electricity [70,71].

2.5.2 Chalcogenide semiconducting nanostructures

Metalloid chalcogens belong to group 16 of the periodic table. These chemical elements generally include tellurium (Te), polonium (Po) selenium (Se) and sulfur (S).These elements are utilized when preparing colloidal semiconducting nanoparticles such as CdS, ZnS, CdTe and CdSe. Chalcogenide semiconducting quantum dots have attracted a lot attention from researchers who are pursuing environmentally friendly materials for the absorber layer of photovoltaic cells [72]. Chalcogenide nanoparticles gained popularity in the scientific community because they have significant applications while alterations in their physical and chemical properties are dependent on size, allowing their manipulation to meet requirements of various applications [72].

2.5.3   Quaternary chalcogenide quantum dots

Ternary and quaternary chalcogenide such as copper indium selenide (CIS) and copper indium gallium selenide (CIGS) materials have been widely studies over the last twenty years, but research on their formation using nanoparticles has been at its infancy. Yoon and co-researchers synthesized CIS material utilizing the nanoparticle based-approach using core-shell structured nanoparticles as a starting material [73]. Their reason for using that kind of precursor material was to optimize the kinetics of CIS reaction mechanism. They observed that the loss of selenium (Se) can be reduced by utilizing core-shell structures together with a compound consisting of two different elements and high heating rates. It is known that the formation of a bilayer structure between two binary compounds like Cu-Se and In-Se in the nanometre range can lead to the reaction time being shortened.

2.6   Multiple exciton production in quantum dots

The generation of multiple electron-hole pairs for each absorbed photon has known for over five decades in semiconductors that have continuous energy levels (bulk semiconductors). This process is not so efficient in bulk semiconductors, however in semiconducting nanoparticles (quantum dots) the multiple exciton generation process becomes very efficient [74]. About more than a decade ago, Nozik was the first scientist to theorize that the efficiency of multiple exciton generation process can be improved by employing nanomaterials such as quantum dots. Multiple exciton generation has been frequently notice in PbSe and PbS quantum dots, this phenomenon has also been observed in carbon nanoparticles such as graphene and carbon nanotubes [75].

The size-dependency of quantum dots properties makes it possible for photovoltaic devices to collect light in the wider regions of the solar spectrum. In traditional solar devices most of the light absorbed is lost through electron-hole recombination. The multiple exciton generation (MEG) phenomenon occurs in quantum dots when a sole high energy photon absorbed results in the generation of more than one electron–hole pairs (excitons). Such phenomenon has been identified as being particularly advantageous for photovoltaic cells, because of the potential to enhance light conversion efficiencies [76]. Latest researcher endeavours have demonstrated that multiple excitons for every single photon absorbed can be obtained through the utilization of quantum dots in the active layer of photovoltaic cells. Intensive studies on lead chalcogenide quantum dots have been done for applications in solar cells, because of their wider exciton Bohr radius [77].

2.7   Bandgap and quantum confinement

Bandgap is one of the unique fundamental features of quantum dots. It is defined as the distance between the valence band and conduction band. The band gap of quantum dots can be adjusted by altering the size due to the effects of quantum confinement [78]. This can only happen   when the size of the quantum dot is less than the size of the electron-hole pair (exciton). The quantum confinement phenomenon causes the bandgap to increase and the photoluminescence (PL) to shift to shorter wavelength (blue shifted) [79]. One way of tuning the bandgap of quantum dot is by manipulating its size. Also it has been reported that quantum confinement makes it possible to tune the absorbance and emission spectral properties [80]. Controlling the size of quantum dots over the years has been a tricky task especially in CIGS quantum dots. This is due to the lack of understanding of the precise molecular reactive species of metal and precursors of the chalcogenide [81].
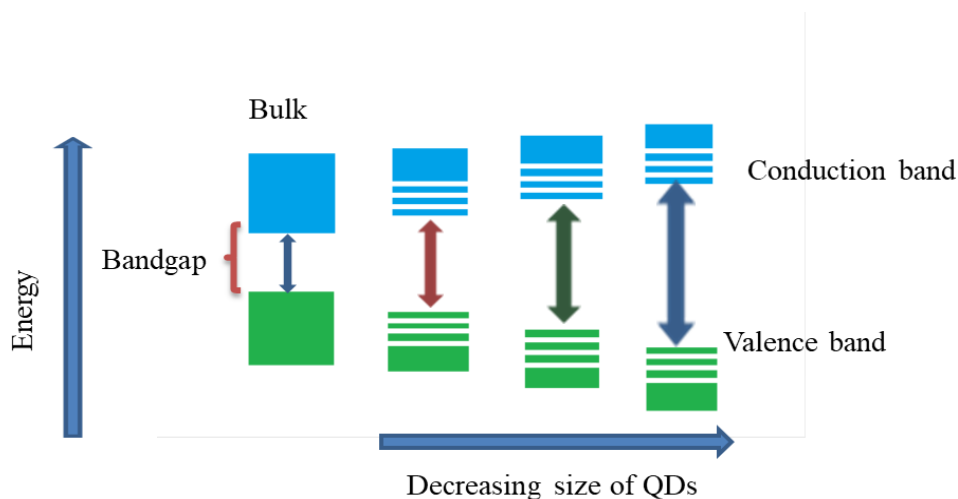
Figure 2.1: Illustration of the quantum confinement effect [81].

2.8 Photophysical properties of quantum dots

Current studies on quantum dots strive to find ways of tuning and enhancing their optical properties by finding ways of controlling their surface. One of the strategies that is employed is the alloying of core and shell quantum dots which reduces single particle PL blinking [82]. The photophysical properties of these colloidal semiconducting nanocrystals can be adjusted by wave function manipulation which is given by type I and type II heterostructures and ligands from metalloids which alter the PL over wider wavelength range. These type II heterostructures can be made through the use of multiple or different compositions in the same structure [83]. The precursors used to make quantum dots have an effect on the photophysical properties, but the size of these nanoparticles remains a decisive factor on their optical properties [84].

2.9   CIGS nanoparticles

CuInSe$_2$ (CIS) and CuInGaSe (CIGS) are chalcopyrite materials that have big potential in third-generation energy conversion devices. CIS nanocrystal is a direct bandgap material (1.04 eV) and research has shown that its bandgap can be tuned by the addition of gallium (Ga) to its crystal lattice which leads to the bandgap increasing up to 1.14 eV [85]. One of the most important characteristic of CIGS nanocrystals as like any quantum dot is that the bandgap is controlled by the nanocrystal size. Another added advantage of these compounds is that their high bandgap can be obtained without depending on toxic heavy metals [86].

2.10   Methods of preparing QDs

2.10.1   Hydrothermal

Generally physical and chemical methods are employed to synthesize QDs. However the chemical approach is preferred over the physical approach because it allows better control of size and functionality. While physicists prefer employing epitaxial technique to make quantum dots, chemists prefer using the so-called wet chemical methods to produce quantum dots [87]. The hydrothermal method has been utilized for many decades to prepare nanomaterials of particular size and shape. In this method, the solvent (usually water), precursors and organic surfactants are heated at a temperature greater 100ºC using an autoclave [88].The QDs crystals start forming when the precursors are decomposing. After waiting for a certain period of time, the QDs crystals start to precipitate out of the solution [89].

2.10.2 Solvothermal

The solvothermal method involves the reaction of the starting materials under carefully monitored temperature and pressure, employing a solvent with a higher than its boiling point. This method allows for more sophisticated control of size and shape distributions. In solvothermal method, the temperature can be increased to much higher temperatures compared to hydrothermal method [90]. Over the last 10 years, elemental salts and metallic salts have been utilized with desired results to prepare metal chalcogenide quantum dots using this method. However, this method has some major drawbacks as, sometimes, the solvent used can lead to environmental pollution [91].

2.10.3 Microwave

Microwave synthesis is a fast synthesis method and a technique which was first utilized in 1986 during organic synthesis of benzoic acid from benzamide [92]. Since then, it is being slowly applied in other material science fields for the synthesis of various nanoparticles and nanostructures [93]. The interest towards its use in the synthesis of nanoparticles, arose due to its efficiency and precision-controlled parameters such as reaction time and heat. Furthermore, this synthesis method does not only significantly decrease reaction times, it can also prevent side reactions which can lead to high yields [94]. The microwave reactors used for this method have built-in magnetic stirrers and direct temperature and pressure monitoring probes and sensors [95].

During microwave synthesis, microwaves penetrate the material and supply energy. Heat can be produced throughout the volume of the material leading to volumetric heating. This technique is useful, because higher yields can be obtained and it allows the synthesis of

compounds which are not available by traditional methods. The microwave technique results to the synthesis of materials with smaller particle size, narrow particle size distribution, high purity, and enhanced physicochemical properties [96]. Microwave reactors use reaction vessels consists of microwave transparent materials such as borosilicate glass, quartz or Teflon. Radiation goes through the walls of the vessels and the temperature rises uniformly throughout the sample [97].

There are two types of microwave heating equipment that have been employed for research; a multimode oven (most common) and single mode oven. A multimode oven has the benefits of being cheap but it is not flexible in controlling and monitoring reactions. As a result, other multimode ovens are designed for laboratory use. However, although they are expensive, they are preferable as they allow stirring of reaction mixture and constant temperature and pressure monitoring. In single mode ovens, microwave energy is piped into the reactor through waveguide [98].

2.10.4 Green synthesis

Green chemistry encourages green, safer and alternatives method of fabricating materials as compared to dangerous chemical methods. This approach uses the principles of green chemistry to design and produce various nanoscale products or develop methods for the production of nanomaterial based on potential applications. Green synthesis methods endeavour to ensure that synthesis processes minimize the use of harmful chemical reagents and increase the efficiency of synthesis processes, while at the same time the quantity and the quality of the required material is not compromised [99].

In the field of nanotechnology, the use of wet chemical methods for the fabrication of quantum dots has attracted interest in academia and industry. These methods mostly focus on size distribution and monodispersity based on. Unfortunately due to their lack of flexibility and use of large amounts of organic solvents, this delay their development and commercialization. Design of a facile, clean and effective nanoparticle synthesis routes which can lead to precursor separation and recycling [100]. Green chemistry synthesis methods have recently been utilized to solve these hindrances in the production of nanoparticles through the use of bio-based materials and elimination of the use of toxic organic solvents and chemicals [101].

2.11   Carbon-based nanomaterials

Carbon is one those elements which are available in abundance on earth. Carbon is generally found in nature in its basic structure as diamond, graphite and coal. This sixth element of the periodic table exists in numerous unique hybridization states; namely sp^3, sp^2 and sp [102]. These different hybridization states allow carbon to form straight chains, tetrahedral structures and planar sheets. The mechanical, electrical and physical properties of the allotropes of carbon depend on their structure and hybridization [103]. This opens up the likelihood to use the carbon material for different fascinating applications. The widely recognized chemical bonds in nanocrystalline and amorphous carbon are sp^3 and sp^2 hybridization [104]. Up until the year 1985, graphite, diamond and amorphous carbon were the only forms of carbon widely known to be found easily in nature. After 1985 research into carbon nanoparticles experienced a rapid rise, resulting in the discovery of carbon nanotubes (CNTs) in 1991, and graphene and carbon nanodots in 2004 [103].
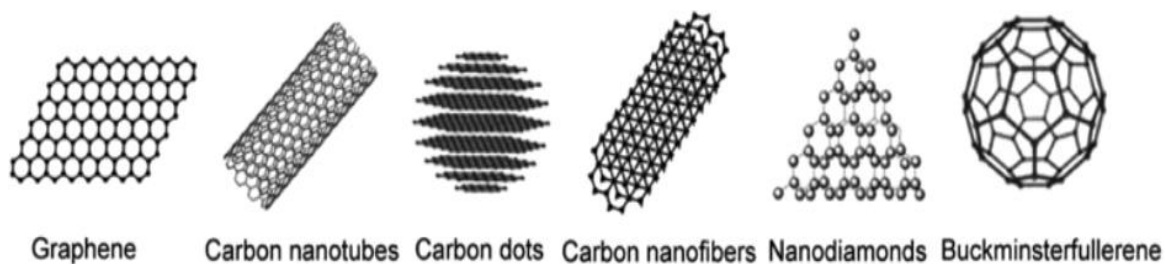
Figure 2.2: Some examples of carbon nanomaterials, revealing different conformational structures such as sheets, tubes and bulky balls [103].

2.12   Carbon nanodots discovery

Carbon nanodots were accidentally discovered by Xu and co-researchers during the purification of single walled carbon nanotubes using permeative electrophoresis more than decade ago. These carbon particles which belong to the quantum dots family and have attracted strong interest from the scientific community because of their strong and tunable photoluminescence [105]. However, carbon nanodots synthesis is facile when compared to conventional semiconductor quantum dots; the starting materials is relatively cheap and environmentally benign. What makes these tiny fluorescent carbon nanoparticles unique compared to quantum dots is their chemical stability, high water solubility and the ease of functionalization [106].
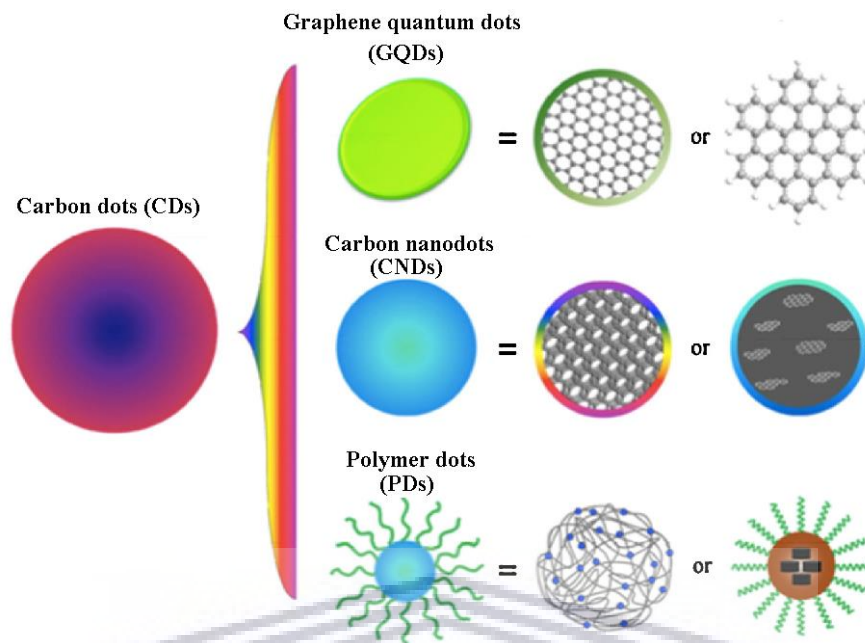
Figure 2.3: Examples of carbon-based quantum dots classified according to sources such as graphene, sugars and polymers [107].

These quasi-spherical nanoparticles have dimensions which are less than 10 nm. They are sometimes called carbon quantum dots since they share similar properties to quantum dots. Carbon nanodots have distinctive electrochemical properties of giving and receiving electrons, resulting in electrochemical luminescence and chemiluminescence. These distinct electrochemical properties can be important when carbon nanodots are used in sensors, catalysis and optoelectronics. In addition, carbon nanodots have good photophysical and chemical properties [107].

2.12.1 Electronic properties

The electronic properties of carbon nanodots have been well studied by many different research groups. Mandal and co-researchers investigated the influence of size, surface modification and shape on the electronic properties of carbon nanodots [108]. Mandal et al. discovered that because of quantum confinement effects the HOMO of these unique carbon nanoparticles shifted to higher energy, while the LUMO shifted to lower energy. The observed shifts happen with increasing particle size, this results in the reduction of HOMO-LUMO gap. They also observed that the introduction functional groups such as electron donating groups or electron withdrawing groups fine tune the HOMO and LUMO levels of carbon nanodots [109]. The research group also observe that the electron donating groups can shift both the HOMO and the LUMO levels to higher energy, while the electron withdrawing groups shift the HOMO and the LUMO levels to lower energy. Some studies have suggested that the functionalization of carbon nanodots has an impact on their electronic properties [110].

2.12.2 Photoluminescence

Carbon nanodots are popular for their unique and tuneable photoluminescence properties and non-toxicity. It comes as no surprise then that most people see them as a future substitute for quantum dots in many applications. In the early stages after carbon nanodots discovery, most scientists had a strong interest in fully understanding the photophysical properties and improving the photoluminescence efficiency of these carbonaceous nanomaterials [111]. Different approaches have been attempted by many research groups to obtain high photoluminescence efficiency using different synthesis methods and many diverse precursors. These approaches include both top down methods (such as chemical

oxidation and electrochemical) and bottom-up (hydrothermal and microwave synthesis) as discussed in this section of the thesis [112].

Although carbon nanodots with high quantum efficiency have been synthesized, however there is lack of understanding when it comes to their photoluminescence mechanism. Many studies have reported the dependency of photoluminescence on the excitation wavelength [113]. Generally, the photoluminescence of carbon nanodots exhibits a blue shift at longer excitation wavelengths and, a red shift at shorter excitation wavelengths. Wang and co-researchers revealed that carbon nanodots can emit light at distinct longer wavelength when the excitation wavelength is kept constant due to their different sizes [114].

2.12.3   Synthesis of carbon nanodots

2.12.3.1   Carbon source

Many carbon nanodots are prepared from environmentally benign precursors. These include carbon sources like ground coffee, candle soot, used tea, glucose, egg shells and grass. These precursors can be employed to synthesize carbon nanodots that are economical and abundant. The facile synthesis and surface passivation methods clearly indicates the potential and versatility of carbon nanodots materials for different applications [115]. Research into these nanoparticles is still in its infancy compared to other carbon nanoparticles such as carbon nanotubes and graphene. Although they are not as popular as other carbon nanomaterials, these zero dimensional nanomaterials can be

prepared from relatively cheap and environmentally benign precursors such as carbohydrates [116].

2.12.4   Microwave-assisted preparation of carbon nanodots

Carbon nanodots can be synthesised by microwave synthesis, which has been proven to be efficient and rapid when preparing carbon nanodots. In this method, quantum dots precursors are mixed in one reaction vessel of the microwave reactor system [117]. This method has many advantages as compared to traditional methods of making carbon nanoparticles. Also, this method generally offers better size control of nanoparticles [118]. Microwave chemistry is predicted to play an important role in the field of nanoscience and nanotechnology. This synthesis technique provides controlled and efficient heating which is important for the growth of nanoparticles which are sensitive to reaction conditions. Microwave irradiation eliminates side reactions, this leads to improved yields and the ability to reproduce results. This technique has also been proven to produce high quality carbon nanodots [119].

2.13   Working principle of a photovoltaic cell

A photovoltaic cell is a type of solar cell that uses the principle of photo electric effect to convert solar energy into electrical energy. When photons of light fall on the cell free electrons are ejected, this results in the flow of electric current [120]. The majority of photovoltaic cells consist of semiconducting material which traps photons from the sun. These absorbed photons generate electron-hole pair, the electrons flow in a similar direction being controlled by internal electric field [121]. In the process they generate electric current, the electric field originate from p-n junction material [122].

The p-n junction is normally formed through the combination of p-type semiconductors (positively charged) and n-type semiconductors (negatively charged). The combination of these two junctions leads to the creation of an energy barrier has electric field caused by the diffusion of electrons from the n-type semiconductor into the holes p-type semiconductor [123]. When a particle of light (photon) collides with the atom of n-type semiconductor in the energy barrier it absorbs the photon producing an exciton (electron-hole pair) [124].

2.14   Quantum dot solar cell

A photovoltaic cell is a type of solar cell that uses the principle of photo electric effect to convert solar energy into electrical energy. When photons of light fall on the cell free electrons are ejected, this results in the flow of electric current [125]. The majority of photovoltaic cells consist of semiconducting material which traps photons from the sun. These absorbed photons generate electron-hole pair, the electrons flow in a similar direction being controlled by internal electric field. In the process they generate electric current, the electric field originate from p-n junction material [126].

The p-n junction is normally formed through the combination of p-type semiconductors (positively charged) and n-type semiconductors (negatively charged). The combination of these two junctions leads to the creation of an energy barrier has electric field caused by the diffusion of electrons from the n-type semiconductor into the holes p-type semiconductor [127]. When a particle of light (photon) collides with the atom of n-type

semiconductor in the energy barrier it absorbs the photon producing an exciton (electron-hole pair) [128].

2.14.1   Why quantum dots for PV cells

Nanotechnology has a big potential to exponentially accelerate the development of novel absorber material for solar cells. This type of technology creates exciting novel materials for PV cells with less negative effects to environment and lower costs Quantum dots (QDs) are sophisticated inorganic semiconducting dimensionless nanomaterials, their dimensionless is cause by a natural phenomenon known as quantum confinement [129]. This phenomenon tightly confines the electrons in the conduction band and holes in the valence band in all three spatial directions. QDs are an ideal absorber material for solar cells owing to their fascinating and unique properties, these semiconductor nanocrystals can make it possible for solar cells to absorb light in ultraviolet(UV)-near infrared (NIR) regions of electromagnetic spectrum [130]. The band gap of these zero-dimensional nanoparticles can be adjusted according to their size and can produce more than one exciton per photon. The multiple exciton production can results in greater quantum yield which in turn can results in better efficiency, the achievable theoretical efficiency of these third materials can be up to 44% [131].

2.14.2   Working principle of a quantum dot solar cell

A typical QD solar cell consists of a wide bandgap semiconductor, electrolytes, counter electrodes and superconducting material. This superconducting material collects left over charge carriers at much faster rate [132]. The wide band gap semiconductor is made up of mesoporous nanocrystalline semiconducting layer joined to a substrate which is

conductive. This layer is sensitized with QDs complete the photo electrode and the effective charge injection can be enhanced through semiconductor material that have energy-level alignment with the QD [133]. The principle of QD solar cell is based on dye synthesized solar cell, when the QDs are exposed to photons of light they are excited. This excitation results in the generation of electron-hole pair, the isolated electrons penetrate the lowest unoccupied molecular orbital (LUMO) while positively holes are left behind in the highest occupied molecular orbital (HOMO) [134].

2.15   Characterization

2.15.1   Electrochemistry of quantum dots

Electrochemistry uses energy in greenest form, by transporting electrons through electrodes. It is for this reason that electrochemistry is at the heart of many energy conversion and storage devices, sustainable energy production is one the current challenges faced by the global community [135]. Research has revealed that electrochemical response of quantum dots exhibits discrete electronic response and decomposition reactions after oxidation and reduction. About two decades ago Bard and co-researcher extensively studied the relationship between the electrochemical bandgap and electronic spectra of quantum dots [136]. This research group used CdSe quantum dots to reveal that these quantum dots can function as multiple electron donors or multi electron acceptors at a specific potential, this is because of quantum confinement effect [137].

2.15.2   Cyclic voltammetry (CV)

Cyclic voltammetry (CV) has for many decades been used to obtain quantitative information of the HOMO and LUMO levels electro-active molecular species soluble in

appropriate solvents. Like other nanoparticles, quantum dots do not have continuous levels instead they have discrete energy levels. It is for this reason that quantum dots are expected to undergo transfer of electrons which is determined through the conduction band edge and the valence band edge [138].

The cathodic and anodic peaks in the cyclic voltammetry graph are cause by these two band edges and these peaks are not greatly influenced by the solvent, capping agent and the type of ligand used. Haram and co-researchers were the first group to reveal the relationship between optical and electrochemical bandgap of quantum dots [139]. Poznyak and co-researchers investigated the electrochemical response of thiol-capped CdTe quantum dots using water as a solvent. Kucur and co-researchers studied the relationship between optical bandgap and electrochemically controlled redox peak difference for CdSe quantum dots adsorbed on a gold disk microelectrode [140].

2.15.3   Transmission electron microscopy (TEM)

Despite growing interest in using nanomaterials to solve our energy problems, the accurate determination of the structure and properties of nanoparticles especially those with very small sizes is still a difficult task. Transmission electron microscopy (TEM) is a direct characterization technique employed to image nanoparticles, this electron microscopy is becomes useful when studying the basic properties of nanoparticles [141]. This electron microscopy technique is often used to investigate the morphology and size of quantum dots. TEM measurements rely on the difference between intensities of the incident and direct beam [142]. Therefore, if the semiconductor nanocrystals are in the same pathway as

the beam this will results in contrast and the quantum dot in the image would appear as a dark spot [143].

When the resolution of TEM is increased the lattice fringes become visible, this is caused by interference effects and these details can be useful when investigating the crystal structure of nanoparticles. It is well known in the research community that non-crystalline nanoparticles do not exhibit lattices fringes [144]. Normally those images with low magnification are used to construct histograms of the binned size versus frequency for at least 50 particles. Thereafter the histogram can be used to calculate the standard deviation and average size [145]. Many research studies do not provide a clear explanation on how many and how they determine the particle sizes. Selected area electron diffraction (SAED) is used to obtain information on the crystal phase of the sample. Energy dispersive X-ray spectroscopy (EDS) is utilized to analyse elemental composition of the nanoparticles [146]

2.15.4   X-ray diffraction (XRD)

In depth understanding of the atomic-scale structure is required in order to accurately determine the properties off nanocrystals. X-ray diffraction (XRD) is spectroscopic technique complimentary that is used by researchers to study the structural arrangement of quantum and carbon nanodots [147]. This X-ray technique is a powerful and non-destructive to the sample, this means that you can use the sample again for other characterization techniques. XRD is generally used for the characterization of all types solid particles which include also nanoparticles. This characterization technique yields information on structures, phases, preferred crystal orientations and crystal defects [148]. In carbon nanodots this technique is used to check if the XRD patterns of carbon nanodots

are amorphous in nature. On the other hand in quantum dots, the XRD technique is used to probe the crystallinity and lattice parameters [149].

2.15.5   Small angle X-ray scattering (SAXS) spectroscopy

Accurate determination of the dimensions of nanoparticles is very crucial for the growth of nanoscience and nanotechnology. Currently the average diameter of nanoparticles is normally predicted using transmission electron microscopy (TEM). The use of TEM technique has some major drawbacks, the analysis of TEM images hindered by the simultaneous appearance of contrast-forming phenomenon and also particle-background boundary is prone to the operator bias [150]. SAXS is an emerging characterization technique used to investigate the size of nanoparticles, this technique provides information about the structure and properties of nanoparticles such as particle shape, size distribution and specific surface area.

When compared to TEM, SAXS has many benefits these include the performance of measurements in solution form which circumvent drying artefacts like evaporation induced aggregation. It has been proven that in SAXS measurement, the data collection is highly similar even if is collected by different users. This X-ray technique is very important when probing the particle size (which is pivotal) and size distribution of quantum dots [151]. The SAXS technique becomes crucial when you want to precisely determine the size and size distribution of particles, research has proven that properties such as optical and electronic properties depend on the size of quantum dots [152].

2.15.6   Ultraviolet visible (UV-Vis) spectroscopy

The absorption of visible and ultraviolet light is related to the promotion of electrons from lower energy levels to higher energy levels. We know that energy levels are quantized meaning that only light with the right amount of energy can cause the excitation of electrons [153]. An instrument known UV-visible spectrometer is utilized to measure the ultraviolet or visible light absorbed by the sample. The absorbed light is measure at a single wavelength or performed a scan over the UV region (190-400 nm) and visible region (400- 800 nm). Ultraviolet visible (UV-Vis) Spectroscopy is a very important in the characterization of quantum dots and carbon nanodots, as it provides information on optical properties of these zero dimensional nanomaterials [154]. The bandgap, which is very important when these nanomaterials are applied in photovoltaic cells, can be calculated from the obtained UV-Vis spectra using the Tauc plot [155].

2.15.7   Fourier-Transform Infrared (FT-IR) spectroscopy

Fourier-Transform Infrared (FT-IR) spectroscopy is a resourceful analytical technique for characterizing nanomaterials. Infrared (IR) spectroscopy was one of the earliest structural characterization technique used to describe bonding structure after the interaction of infrared radiation with matter [156]. IR spectroscopy is frequently used to analyse the functional groups of nanoparticles such as metallic nanoparticles, carbon nanomaterials and hybrid nanoparticles. Fourier-Transform Infrared (FT-IR) spectroscopy is the first characterization of choice after obtaining synthesized your nanomaterial. FT-IR is suitable for identifying functional groups in a molecule, this technique is often used to detect functional groups on the surface of carbon nanodots and quantum dots [157].

CHAPTER 3

Microwave-assisted synthesis of sugar-derived carbon nanodots

3.1   Overview

Carbon nanodots have recently become an important member of carbon nanomaterial family which has drawn strong interest in the nanoscience and nanotechnology research community. Research into these carbon nanoparticles is relatively at its infancy when compared to their counterparts such as carbon nanotubes, fullerenes etc. Over last decade, significant advances have been made to better understand the unique properties of carbon nanodots. This chapter includes the synthesis method used to prepare the carbon nanodots materials and the results obtained are discussed.

3.2   Abstract
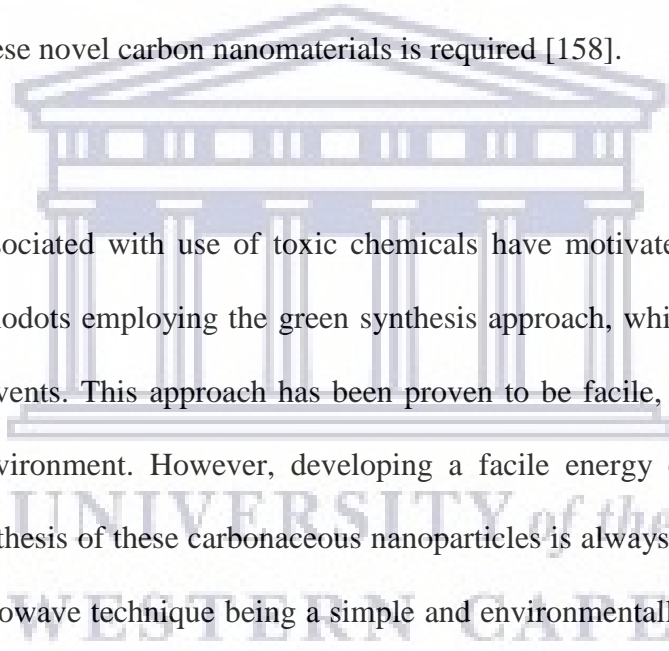
Research into carbon nanodots still lags behind when compared to other carbon nanomaterials such as carbon nanotubes, but this is fast changing at an exponential rate. Although carbon nanodots are relatively a new class in the family of carbon nanomaterials, they have found applications in many fields due to their unique properties and easy preparation from diverse carbon sources using different synthesis methods. However, the current challenge is choosing a carbon source and a synthesis method that is environmentally friendly in order to mitigate the release of harsh and toxic chemicals from harsh precursors and waste into the environment. This work presents the synthesis of glucose-derived carbon nanodots using the microwave synthesis technique. The carbon nanodots were prepared from glucose which is a cheap and environmentally friendly starting material. Fourier Transformed Infrared (FT-IR) spectroscopy was used to study the

structural composition of the carbon nanodots. Ultraviolet visible (UV-Vis) spectroscopy, Raman spectroscopy and photoluminescence (PL) spectroscopy were employed to study photophysical properties, while the high-resolution transmission electron microscopy (HR-TEM), X-ray diffraction (XRD) and small-angle X-ray scattering (SAXS) were used to evaluate the size and size distribution of the carbon nanodots. Cyclic voltammetry (CV) was used to study electrochemistry of the carbon nanodots. The FT-IR technique revealed that the structure of synthesized carbon nanodots consisted of O-H, C-H and C-O-C bonds originating from the starting material, glucose. The UV-Vis spectroscopy revealed that the carbon nanodots absorb light at 284 nm while it was observed from PL spectroscopy that the carbon nanodots strongly emit light at 636 nm. Confirmed using Raman spectroscopy, these nanomaterials had a D and G band, which are typical of materials consisting of carbon in their structure. HR-TEM revealed that the size of the spherical carbon nanodots was 11.55 nm. XRD and HR-TEM also revealed that the carbon nanodots had an amorphous structure entailed by the broad peak at 25° of the 2θ scale. The SAXS showed that the carbon nanodots consisted of different sizes where the individual nanospheres exhibit a size of 15-20 nm while the bigger particles of agglomerated nanodots exhibit a size of approximately 80 nm and 100 nm from distribution-by-volume plots.

3.3   Introduction

Research into nanomaterials of carbon family significantly increased over the last decade due to their attractive properties and the versatile applications they have. Carbon nanodots belong to the family of carbon nanoparticles and, unlike their well-known counterparts such as carbon nanotubes their physical and chemical properties are not fully understood. These fortuitously-discovered carbon nanoparticles have properties which are similar to those of semiconductor quantum dots. For this reason carbon nanodots are considered as

emerging quantum dots [115]. Ever since the discovery of carbon nanodots more than a decade ago, there are many diverse methods that have been explored to prepare these carbon quantum dots. Current synthesis methods used to prepare carbon nanodots, such as solvothermal or hydrothermal synthesis techniques use toxic chemical reagents and organic solvents as starting materials. These synthesis techniques employ harsh conditions such as high temperatures, usually temperatures which are above 200 ºC. Additional drawbacks of the conventional synthesis approaches include the use of expensive precursors and time consumption. Hence, the exploration of novel synthesis methods and molecular precursors for synthesizing these novel carbon nanomaterials is required [158].

The challenges associated with use of toxic chemicals have motivated nanoscientists to prepare carbon nanodots employing the green synthesis approach, which involves the use of non-organic solvents. This approach has been proven to be facile, efficient and is not harmful to the environment. However, developing a facile energy efficient and green method for the synthesis of these carbonaceous nanoparticles is always a tricky task [159]. Although, the microwave technique being a simple and environmentally benign process is among promising techniques to address the preparation challenges of carbon nanodots, its use still at its infancy. This method can be employed to prepare and modify carbon nanodots because throughout the reaction the microwaves can greatly penetrate the materials precisely, yielding nanoparticles of uniform size and distribution [117].

Herein, this chapter reports the preparation of polyethylene glycol-functionalized carbon nanodots from glucose using the microwave technique. The properties of these materials were investigated and analyzed for structural, morphological, photophysical and

electrochemical response using photoluminescence spectroscopy (PL), ultraviolet-visible spectroscopy (UV-Vis), small angle X-ray scattering (SAXS), X-ray diffraction (XRD) spectroscopy, high-resolution transmission electron (HR-TEM) microscopy and cyclic voltammetry (CV).

3.4   Experimental

3.4.1   Reagents

D-(+)-glucose (ACS reagent grade) and polyethylene glycol-200 (PEG-200) (reagent plus grade) were obtained from Sigma- Aldrich (South Africa) and used without further purification. Distilled water, used throughout the experiment, was passed through and collected from a Millipore Milli-Q system (Milford, USA).

3.4.2   Preparation of polyethylene glycol-stabilized carbon nanodots

The carbon nanodots were synthesized using the microwave irradiation, a green synthesis economical method mostly preferred when one wants to obtain highly fluorescent carbon nanodots. In a typical microwave-assisted experimental procedure, 2.0017 g of D-glucose was dissolved in 25 mL ultrapure distilled water and the solution was ultrasonicated for 10 min, resulting in a clear and homogeneous solution. Thereafter, 100 μL of polyethylene glycol-200 (PEG-200) was added to the clear and transparent solution. The mixture was then transferred into 100 mL Teflon vessel and put inside a microwave reaction system (Microwave Reaction System SOLV, Multi PRO from Anton Paar, Graz, Austria). The reaction was carried at 10 min using a power of 600 W. The carbon nanodots were obtained as a brown suspension which was then stored at room temperature for analysis.

Similarly, another batch of carbon dots was synthesized at half the reaction time (5 min) to observe the effect of reaction time on the obtained carbon nanodots.

3.4.3   Characterization

The Fourier Transformed Infrared spectroscopy (FT-IR) investigations of the synthesized materials were carried out using FT-IR spectrometer (Model spectrum Two, Perkin Elmer, Massachusetts, USA) with KBr pellet technique in the range between 500 cm^{-1} and 4000 cm^{-1}. The light absorption properties of the brown CNDs suspension were investigated using ultraviolet visible (UV-Vis) spectroscopy (Nicolet Evolution 100 spectrometer, Thermo Electron Corporation, Massachusetts, USA) from 200 nm to 600 nm. The photoluminescence spectrum of the carbon nanodots was recorded using photoluminescence spectrometer (IGA-521 X 1-50-1700-1LS, Horiba Jobin Yvon, Horiba scientific, Kyoto, Japan) at an excitation wavelength of 284 nm. The Raman spectroscopy of the brown CNDs suspension was recorded using Raman spectrometer (Xplora, Horiba Scientific, Kyoto, Japan). The morphology of the prepared carbon nanodots nanomaterials was probed using TEM spectroscopy (Tecnai F20 emission transmission electron microscope, FEI, Oregon, USA). The shape and size distribution were further investigated using SAXS spectroscopy (small and wide-angle scattering system, Anton-Paar, Graz, Austria) To study crystalline nature of the carbon nanodots, the XRD spectrum was recorded using Bruker AXS D8 Advance diffractometer (voltage 40 KV; current 40 mA) from Bruker, Massachusetts, USA. All electrochemistry experiments were conducted using potentiostat CH work station (PalmSens BV, Houten, Netherlands) and a conventional three-electrode system with a glassy carbon working electrode, Ag/AgCl reference electrode saturated in 3M NaCl and a platinum wire counter electrode. All the electrodes were obtained from BASi, Lafayette, USA. Prior to all electrochemistry experiments, the

working electrode was prepared by polishing in alumina slurries of 1 μm, 0.3 μm and 0.05 μm, respectively, followed by successive ultrasonication in ethanol and water. A solution of 0.5M tetrabutylammonium perchlorate (for electrochemical analysis, 99.0% purity) was used an as electrolyte. For all electrochemical measurements, the glassy carbon electrode was modified by drop-coating with 5μL of the brown the brown CNDs suspension, followed by air-drying overnight at room temperature.

3.5   Results and Discussion

3.5.1   Fourier-Transform Infrared (FT-IR) spectroscopy

Fourier-Transform Infrared (FT-IR) spectroscopy is an important quantitative and qualitative tool for characterizing the structural composition of nanoparticles by identifying diverse functional groups such as carbonyl, hydroxyl, epoxy and amine on the surface of different materials. In this work, FT-IR spectroscopy was used to confirm the composition of the synthesized carbon nanodots by identifying changes in the stretching, bending or vibration modes and bond formations or deformations of functional groups of the starting material [160,161]. Figure 3.1 below displays the FT-IR spectra of the synthesized CNDs (at a reaction time of 10 min) and glucose (the starting material). The spectrum of glucose exhibits characteristic O-H, C=O , C-O-C and C-H at 3306 cm^{-1}, 1826 cm^{-1}, 1035 and cm^{-1} and 2800 cm^{-1} respectively [162].

In the carbon nanodots spectrum, the O-H and C-H functional groups are shifted to higher wavenumbers at 3436 cm^{-1} and 2947 cm^{-1} respectively, while the C-O-C functional group is observed at the same wavenumbers. However, it is worth notable that the C-H and C-O

peaks are more pronounced in the CNDs than in glucose. Therefore, the formation of the CNDs is confirmed by the presence of the characteristic O-H, C-H and C-O-C bonds accompanied by the respective shifts to higher wavenumbers and pronunciation of the bonds. This shift may be attributed to interactions between the carbon nanodots and polyethylene glycol whose main functional groups are O-H, C-C and C-O. The existence of these rich hydrophilic functional groups implies that the prepared carbon nanomaterials have decent water solubility [163].
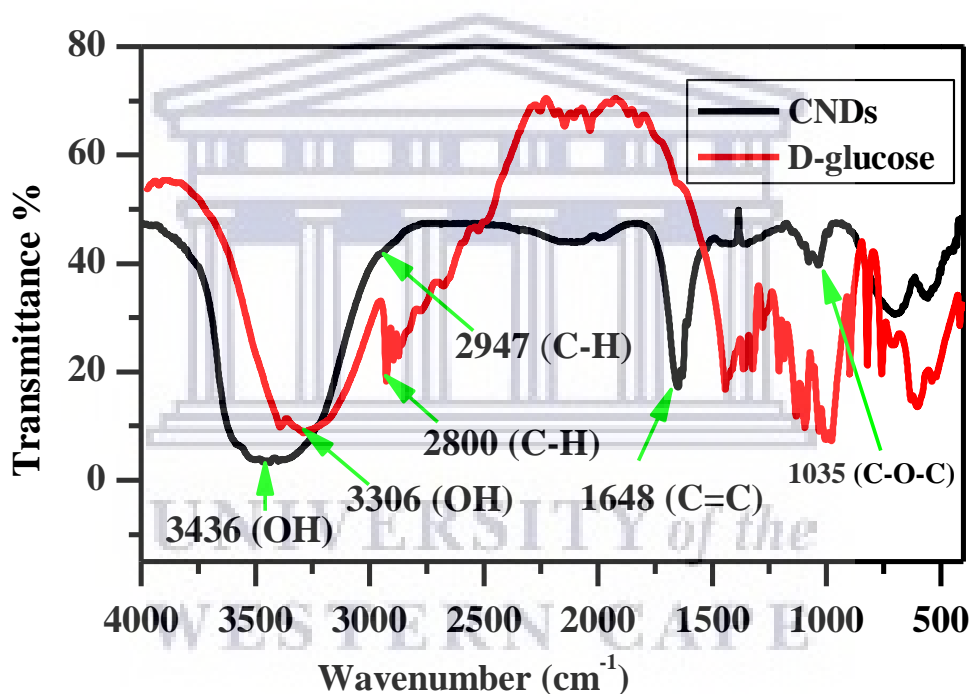
Figure 3.1: FT-IR spectrum revealing the functional groups of CNDs and glucose.

3.5.2   Ultraviolet-visible (UV-Vis) spectroscopy

Ultraviolet-visible (UV-Vis) spectroscopy has become a popular method in the characterization of carbon nanomaterials. Carbon nanodots generally exhibit optical absorption in the ultraviolet (UV) range with absorption peaks between 260 nm and 320

nm with the tail sometimes extending into the visible region [164]. The absorption patterns depend on the type of method employed during synthesis and moreover, research has shown that oxygen content has influence in determining the position of the absorption band of these unique carbon nanomaterials [165,166].

Figure 3.1a below displays UV-Vis spectrum of the CNDs, exhibits absorption peaks at 228 nm and 284 nm that are attributed to the π- π* transition of C=C and n-π* transition of C=O respectively. The bandgap which is defined as the gap between the valence band and conduction band, was calculated using the Tauc plot (Figure 3.2b) and was found to be 4.2 eV [167]. This bandgap value means that the prepared carbon nanodots cannot be used for solar cell application as pristine, and, therefore, need to be modified or incorporated into a composite fit for application in solar cells.
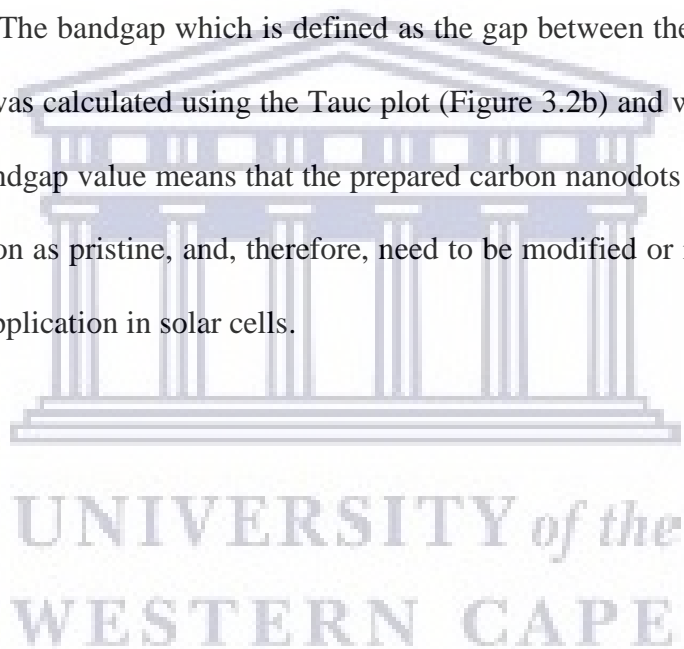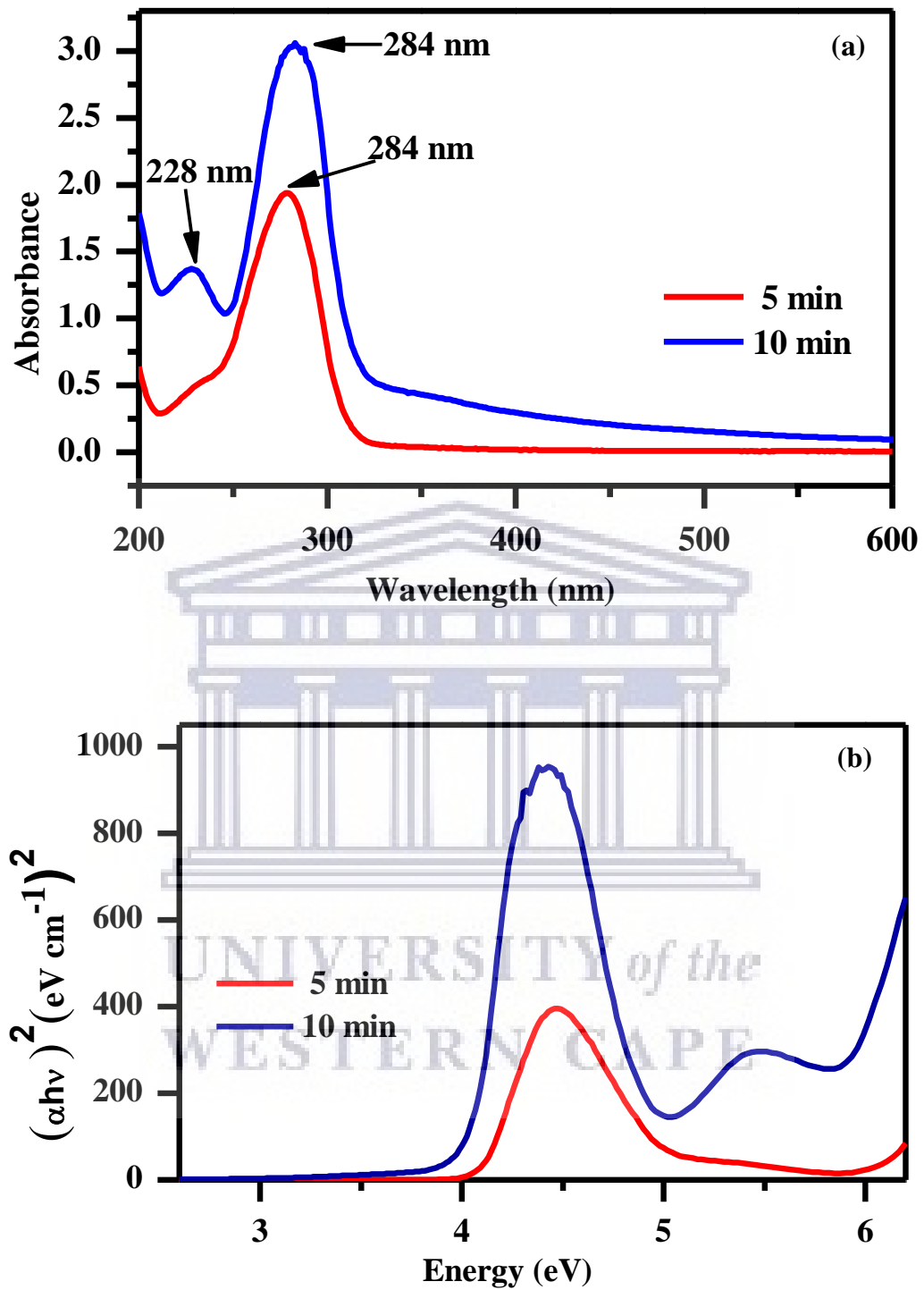
Figure 3.2: UV-Vis spectrum (a) and Tauc plot (b) of CNDs prepared at 5 min and 10 min

reaction times.

3.5.3 Photoluminescence spectroscopy

The photoluminescence spectrum of the prepared carbon nanodots materials was recorded by measuring the intensity of emitted radiation as a function of emission wavelength. Carbon nanodots are classically known for their good photoluminescent property, a fascinating property which makes these carbon nanomaterials have versatile applications [107]. The photoluminescence mechanism of carbon nanodots is still a debating topic in the scientific community, and in the past some researchers had suggested that the mechanism is not primarily influenced by quantum confinement effects. Rather, it was suggested that other factors like functional groups, surface defects and heteroatom functionalization have a big influence on the photoluminescence mechanism of carbon nanodots [168]. To investigate the fluorescent properties of the carbon nanodots, the photoluminescence (PL) spectrum is displayed in Figure 3.3. The PL spectrum of carbon nanodots synthesized at two different time intervals (5 and 10 min) was obtained using an excitation wavelength of 284 nm. The carbon nanodots showed good photoluminescence in the visible region, with two emission peaks observed for the CNDs prepared at both time intervals (5 min and 10 min).These peaks are centred at 445 nm and 636 nm for the 5 min interval and at 494 nm and 636 nm for the 10 min interval. The carbon nanodots PL spectrum exhibit different photoluminescence response intensities for the different time intervals. Carbon nanodots prepared at 10 min show higher intensity than carbon nanodots prepared at 5 min. This reveals that the more one increases the time, the more the photoluminescence-intensity of carbon nanodots. The carbon nanodots PL spectra exhibited red shift since the emission wavelengths are longer than the absorption wavelengths [169].
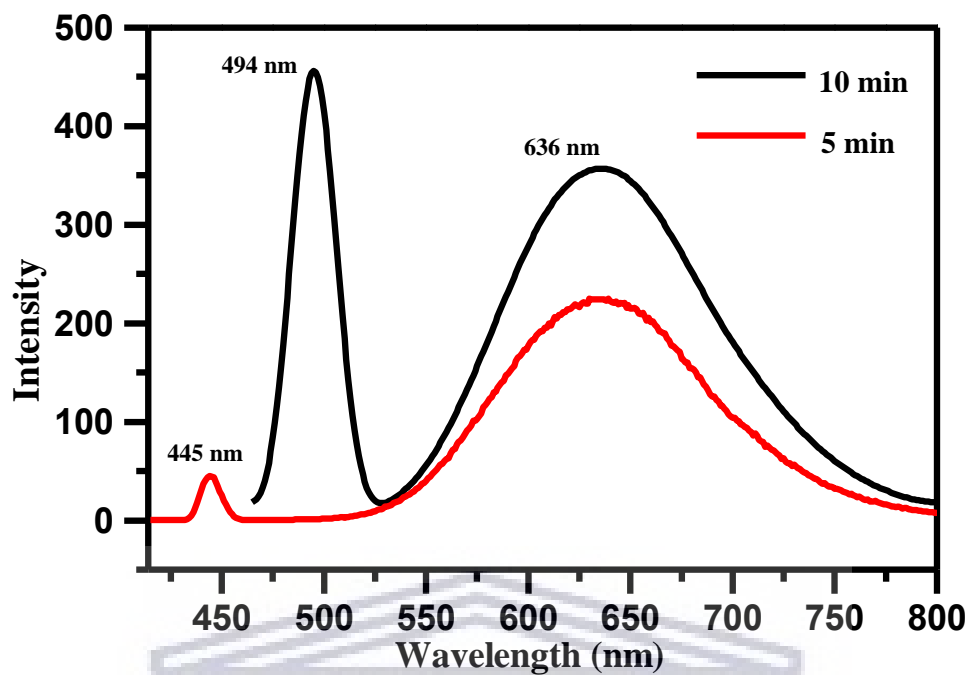
Figure 3.3: Photoluminescence spectra of carbon nanodots prepared at different reaction times. The spectra were acquired with an excitation wavelength of 284 nm.
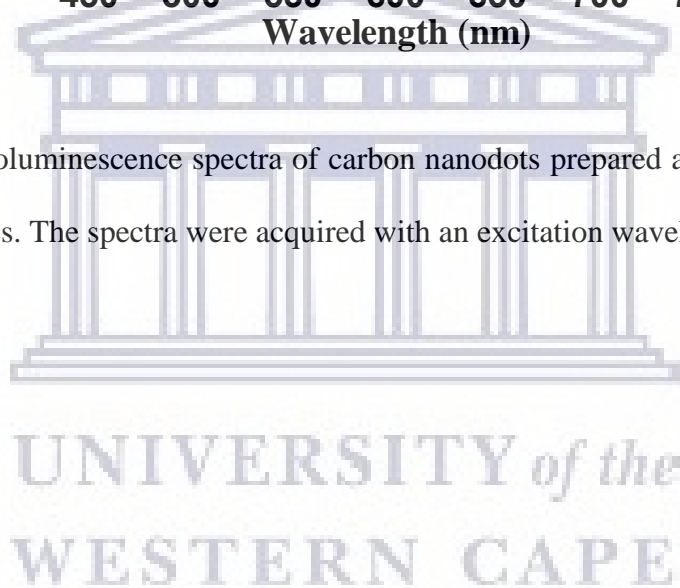
3.5.4 Raman spectroscopy

Raman spectroscopy can be employed to characterize the surface of partially ordered carbon materials in the nanometre scale regime. This spectroscopic technique is more sensitive to symmetric covalent bonds which have small dipole moment [162]. Carbon materials are known to consist of carbon-carbon bonds, this make the Raman spectroscopy a valuable technique when probing the structure of carbon materials. Generally each Raman band that is visible in the Raman spectra correlates to a particular vibrational frequency of a bond in the molecule. The position of the Raman band and the vibration frequency are very responsive to the orientation of bands. There are two characteristics Raman bands that are typically observe in the Raman spectrum of carbon nanomaterials [118,170].

The two bands are known as the D band and the G band, the D band is a defect-initiated band found generally in sp^2 hybridized carbon materials. On the other hand, the G band is a result of a first order Raman band of all sp^2 hybridized carbon materials. The appearance of the D band in the Raman spectrum is usually observed around 1580 cm^{-1} and the G band around 1350 cm^{-1} [171]. The obtained Raman spectra of the carbon nanodots prepared at a reaction time of 10 min is shown in Figure 3.4. The Raman bands at 1763 cm^{-1} and 1932 cm^{-1} might be the D and the G bands, respectively. The appearance of these two bands is dependent on the excitation wavelength. As observed from the PL spectra the prepared carbon nanodots have high fluorescence, and it is known that obtaining the Raman spectra of highly fluorescent carbon nanomaterial is not an easy process since these materials are sensitive to excitation wavelength [172]. The intensities of the observed two bands are similar suggesting that the prepared carbon nanodots have a single layer and amorphous in

nature. This also suggests the synthesized carbon nanodots have many reactive sites. The appearance of the additional bands at 2435.27 cm^{-1} and 2953.03 cm-1 were identified as the 2D and D+G respectively. The appearance of these additional bands is indicative that there are some carbon bonds which have different bonding energies, this suggest that the structure is not uniform.
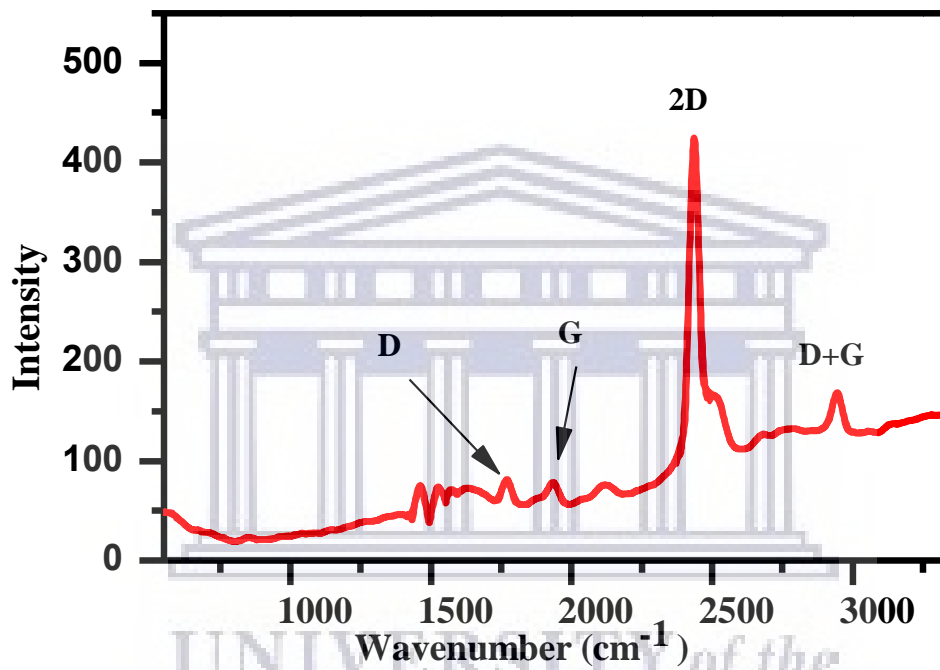
Figure 3.4: Raman spectra of carbon nanodots.

3.5.5 High-resolution transmission electron microscope (HRTEM)

The transmission Electron Microscope (TEM) technique is a very useful tool in material science. Through this microscopic technique features, such as crystal structure and lattice imperfections can be characterized. TEM can also be employed to probe the growth of layers and surface defects in semiconducting nanoparticles [173]. This can also be used to investigate the shape, quality and size of carbon nanodots. Figure 3.5displays the high-resolution TEM images (low magnification on left and high magnification on the right) of amorphous CNDs with diameters between 9.54 nm and 12.59 nm and an average diameter of 11.55 nm. The inserted SAED image also reveals amorphous carbon nanodots. The TEM microgram shows aggregated and nearly spherical particles of the synthesized CNDs. The appearance of dark clear spots in the TEM images is an indication of the formation of confined clusters of carbon atoms, nanoparticles which gives characteristic amorphous nature. The highly magnified TEM image in figure 3.5 does not exhibit any significant lattice fringes, further confirming the amorphicity of the nanoparticles.
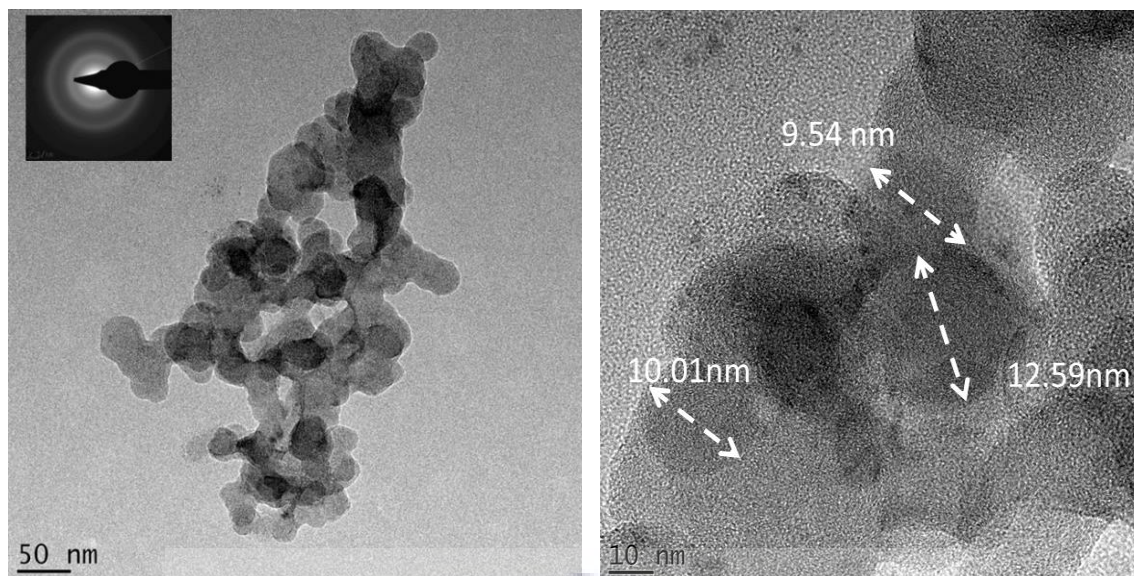
Figure 3.5: HRTEM images of carbon nanodots at lower (left) and higher (right) magnification. Spherical nanodots of sizes ranging from 9 nm to 15 nm were identified. The insert is the SAED graph revealing the amorphous nature of the CNDs.

3.5.6 Energy Dispersive X-ray Spectroscopy (EDS) of Carbon nanodots

Energy Dispersive X-ray Spectroscopy (EDS) which is generally used together with HRTEM is utilized to assist in the investigation of the chemical composition of carbon nanodots in the nanometer scale regime. This TEM technique creates elemental composition plot over broader raster area. Figure 3.6 displays the elemental composition of carbon nanodots, the structure consists mostly of carbon (C) and oxygen (O). The EDS clearly shows that the carbon is the most abundant element in the prepared carbon nanodots structure, with a small percentage of oxygen ccontent. The presence of copper (Cu) and silicon (Si) originate from grid used during the TEM experiments.
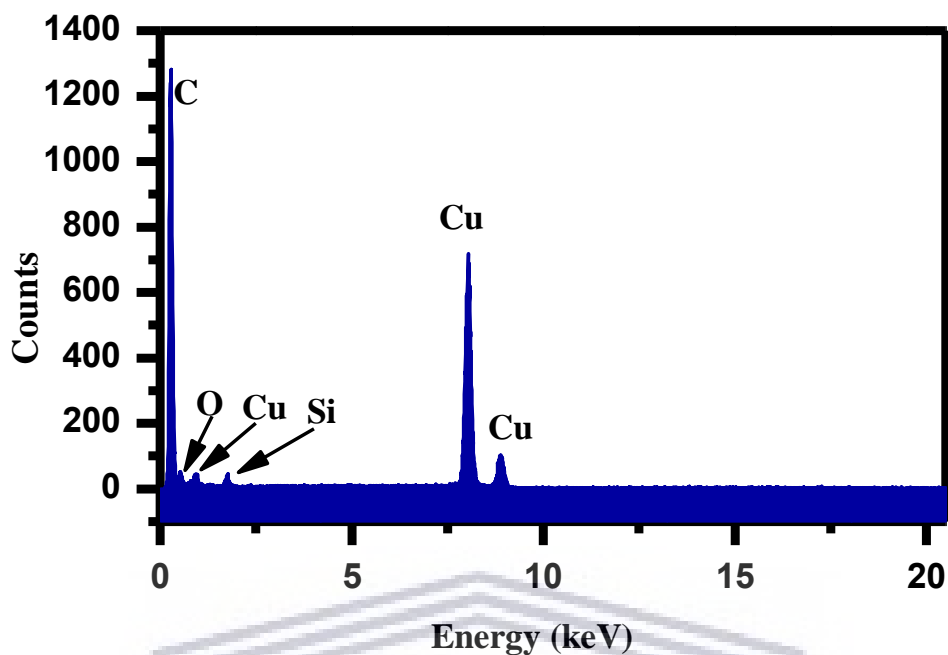
Figure 3.6: EDS spectrum for the elemental composition of carbon nanodots.

3.5.7   X-ray diffraction (XRD)

The size and crystal structure of the prepared carbon nanodots (at reaction time of 10 min) were investigated using X-ray diffraction (XRD), which is a rapid and non-destructive analytical tool. The XRD pattern of carbon nanodots generally exhibit broad peak (generally around 20º-30º) which is due to highly disordered carbon atoms [174]. Figure 3.7 below displays the XRD pattern of the prepared carbon nanodots. The XRD pattern displays a broad peak around 25º which corresponds to miller indices of 002. This broad peak is characteristic structure of amorphous carbon. Carbon nanodots are known to exhibit a structure of graphitic carbon, this is consistent with previous reported properties of carbon nanodots [175]. The other peaks which are visible in the pattern below might be because of some impurities.
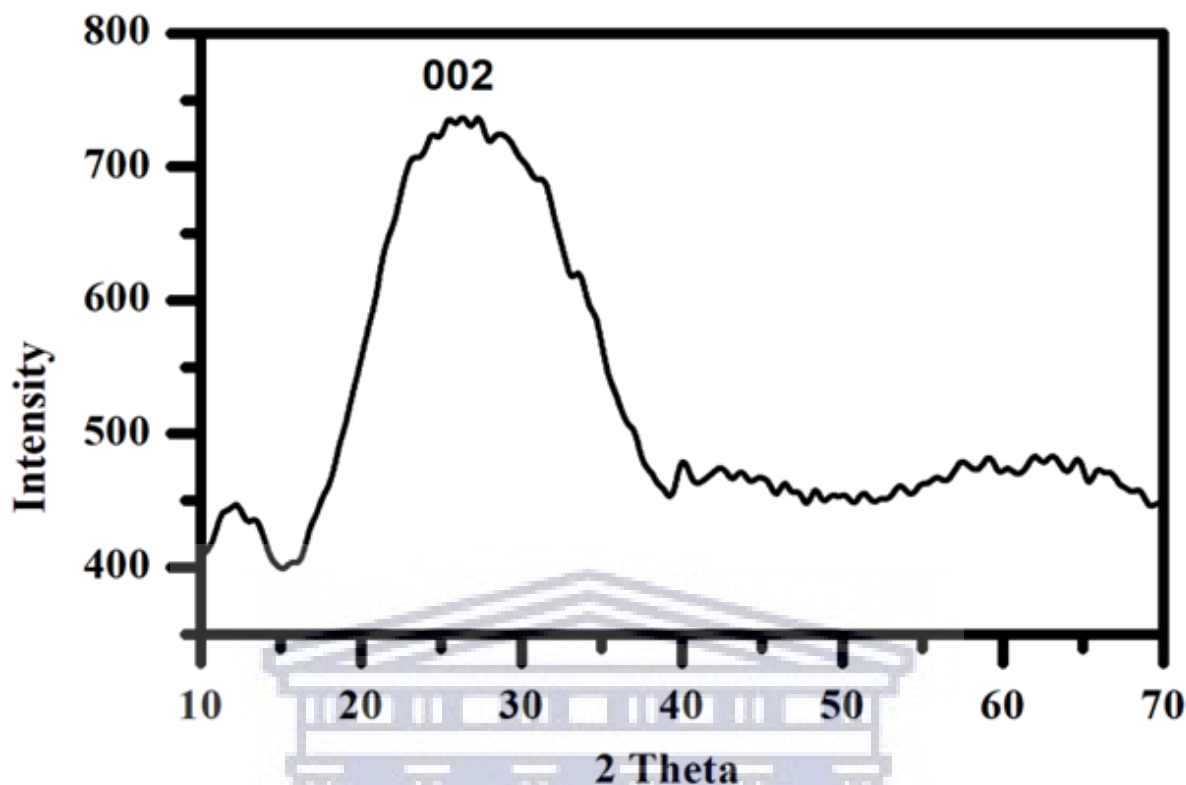
Figure 3.7: XRD pattern of the amorphous sugar-derived carbon nanodots prepared using microwave irradiation with a power of 600 W for 10 min.

3.5.8 Small-angle X-ray scattering (SAXS) spectroscopy

Among many parameters that can be studied using the small-angle X-ray scattering (SAXS) technique, this technique becomes reliable when one wants to analyse shape, size, size distribution and surface structure of nanoparticles. This small angle scattering technique provides reliable characterization of nanostructure materials [147]. The SAXS technique has become useful in determining the particle size, size distribution, surface structure and shape. It comes as no surprise that SAXS has gained increasing popularity in nanoscience research [151].

The size distribution of the prepared carbon nanodots material was investigated using SAXS method, accurate determination of particle size distributions is vital when studying the properties of nanoparticles. The PDDF spectrum in Figure 4.8(a) was used to determine the shape of carbon nanodots, the spectrum revealed that the carbon nanodots were covered by a shell since one curve overlaps to the negative y-axis. The distribution by volume graph (Figure 3.8(d) reveals that particles with size below 25 nm are more prevalent although larger particles are also present. The intensity graph (Figure 3.8(b)) of the prepared nanomaterials revealed that the nanoparticles are polydispersed with nanoparticles of sizes below 25 nm showing low intensity while nanoparticles centred around 80 nm show higher intensity due to their size.
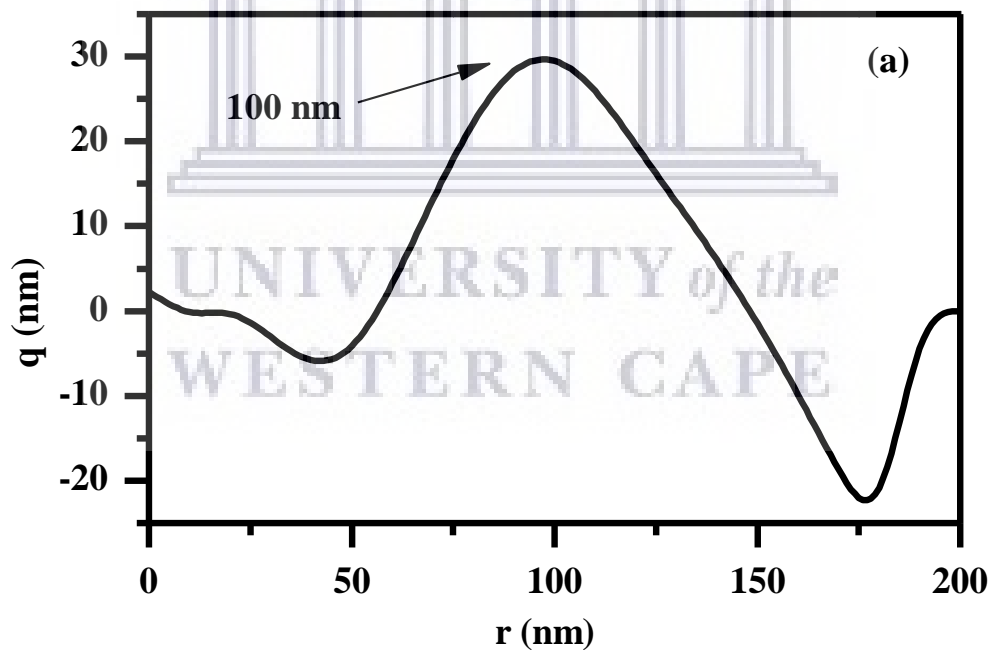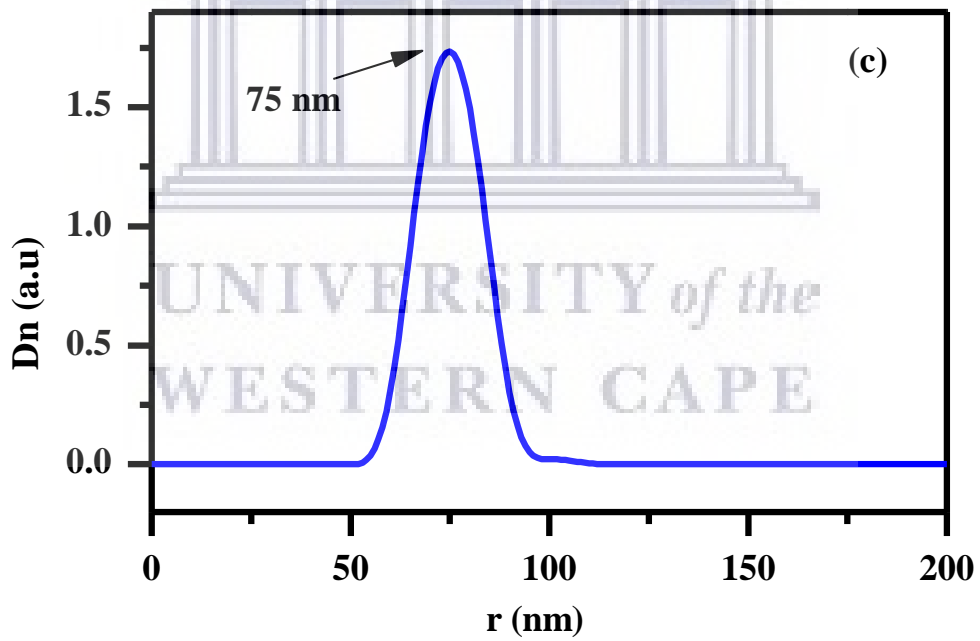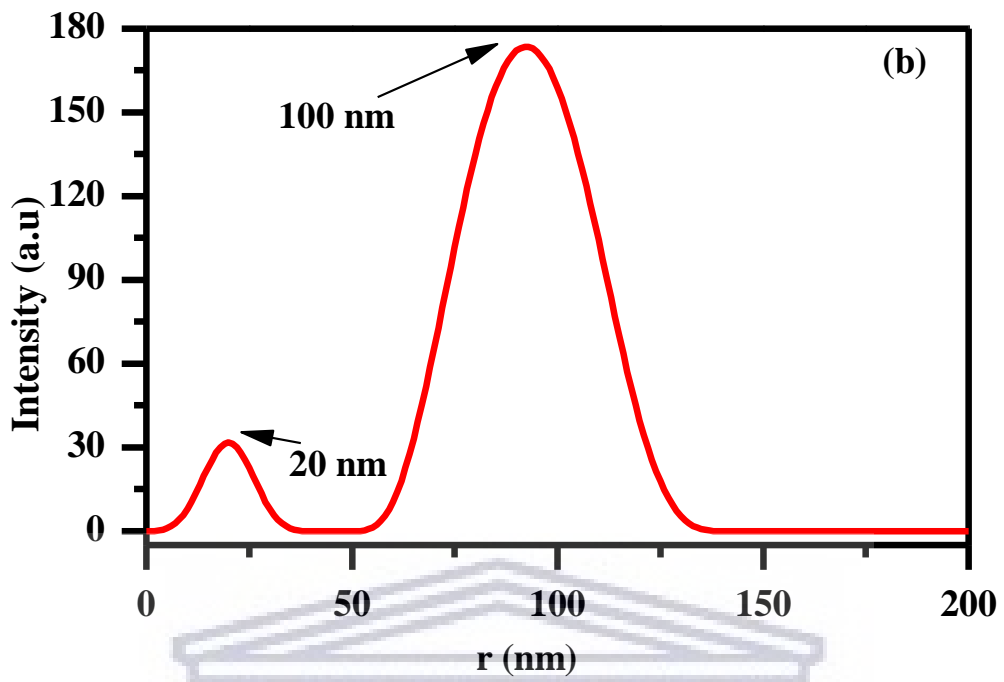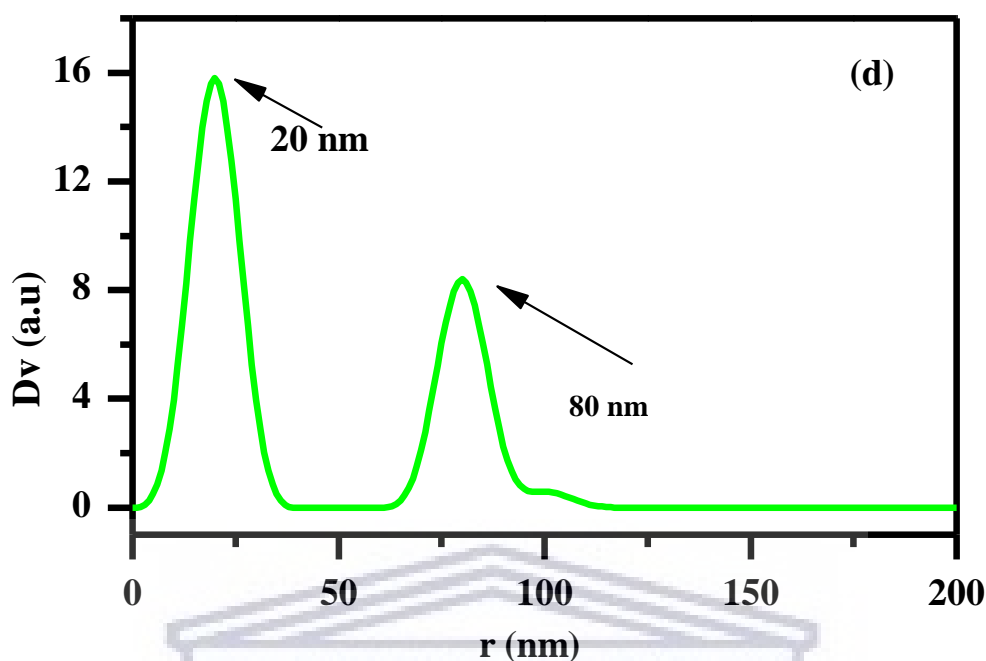
Figure 3.8: SAXS spectrum of carbon nanodots prepared at reaction time of 10 min analysed by (a) PDDF, (b) by distribution intensity, (c) distribution by number and (d) distribution by volume.

3.5.9 Cyclic voltammetry (CV)

The CV graph of the CNDs reveals one redox pair, labelled I/I'. This pair, centred at -0.01 V and 0.6 V vs Ag/AgCl) is ascribed to the reduction and oxidation of the CNDs through its reactive hydroxyl-terminated functional groups. The additional reduction peak (II) is assigned to the adsorbed oxygen at the electrode surface. As the scan rate is increased from 0.01 V/s to 0.05 V/s (Figure 3.10(a)) and from 0.06 V/s to 0.13 V/s (Figure 3.10(b)), an increase in peak current is observed. This is also accompanied by an observable shift in the peak potentials towards more negative values for the reduction peak and towards more positive values for the oxidation peaks (Figure 3.10(c)). This peak shift for lower scan rates shows a well separated pattern while the higher scan rates show a clustered pattern. This

indicates that the reduction-oxidation process of the CNDs prefers slower kinetics. At both high and low scan rates, the process reveals a quasi-reversible process indicated by a large deviation of the anodic to cathodic ratio of the peak currents from unity ($I_{pa}/I_{pc} \neq 1$) [176].
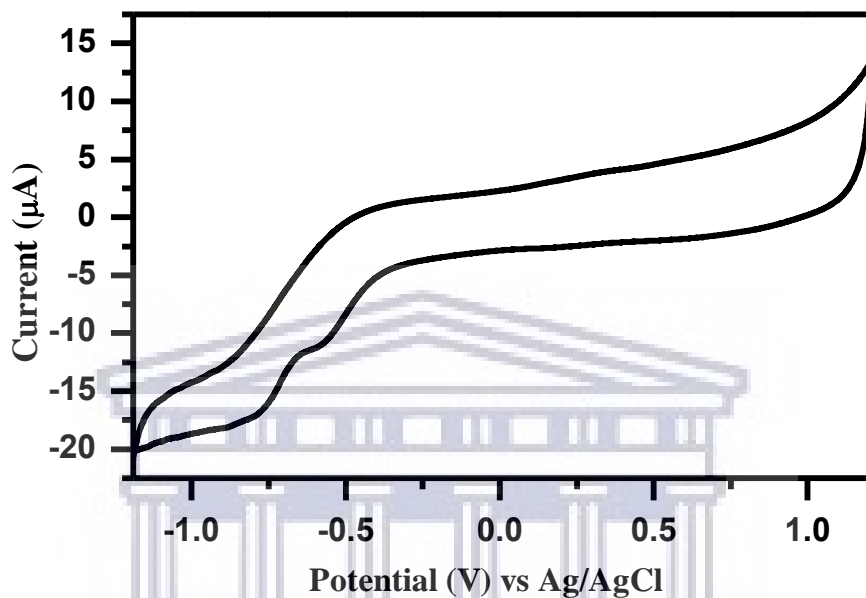
Figure 3.9: CV scan of the bare glassy carbon electrode in 0.5 M tetrabutylammonium perchlorate at scan rate of 0.05 V/s between -1.20 V and +1.20 V.
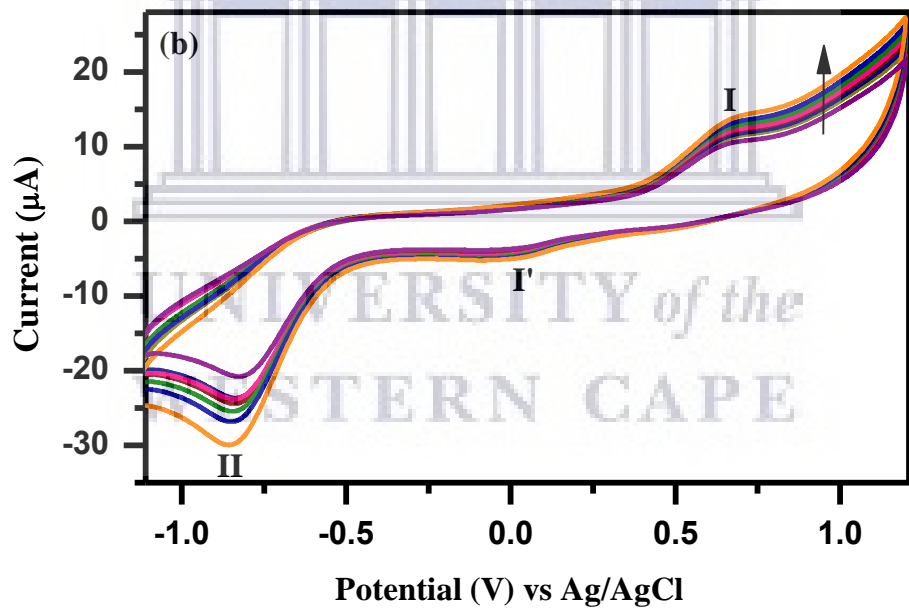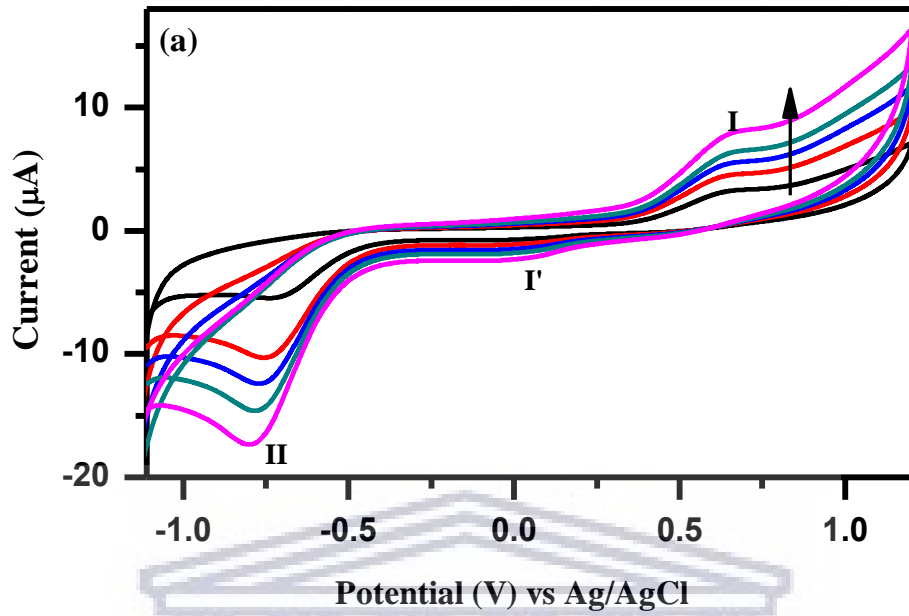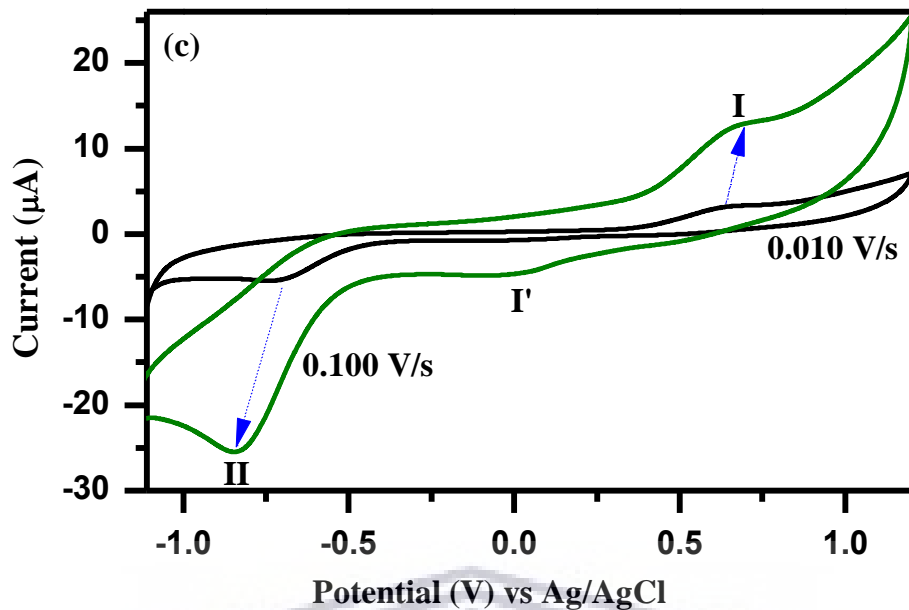
Figure 3.10: CV graph of the carbon nanodots-modified GCE between -1.10 V and +1.10 V in 0.5 M tetrabutylammonium perchlorate at (a) lower scan rates from 0.010 to 0.050 V/s and (b) higher scan rates from 0.050 to 0.130 V/s in increments of 0.01 V/s (black arrows indicate direction of scan rate increase), (c) reveals response differences of the CNDs (indicated by dashed blue arrows) at the lowest scan rate (0.010 V/s) and highest scan rate (0.100 V/s).

3.6 Conclusion

Highly photoluminescent carbon nanodots were prepared using the green chemistry approach. This approach was chosen as it is an alternative towards remediating the drawbacks associated with both the use of harsh, costly and toxic chemicals and exhaustive synthesis procedures that require high temperature conditions for long periods. Hence, the carbon nanomaterials were prepared from the cost effective precursor, glucose using the fast energy-friendly microwave synthesis procedure.

Classical and sophisticated material science characterization techniques were used to carefully study the unique properties of the obtained sugar-derived carbon nanodots. The FT-IR spectroscopy revealed that these carbon nanodots consisted of carbon and oxygen. The formation of CNDs was witnessed by the observed shifts in the stretching and vibration bands of different functional groups and changes in their intensities. HRTEM and SAXS were used to identify the size and particle distribution. HRTEM revealed that the obtained spherical carbon nanodots have an average size of 11.55 nm while the SAXS individual nanospheres of sizes between 15 and 20 nm. The distribution-by-volume plot of SAXS also revealed presence of bigger particles of approximately 80 nm and 100 nm. The presence of these big particles may be attributed to agglomerated nanoparticles and/or contribution by the polyethylene-glycol used as a stabilizing agent. The PEG contribution is also evidenced by the downward curve around 150 nm, characteristic of a shell formed around the nanoparticles.

The XRD technique revealed an amorphous structure of the carbon nanodots. This amorphous nature is exhibited by the broad peak of 002 miller indices observed 25° of the 2-theta scale. This behaviour was also revealed by the SAED results. During optical

characterization, the carbon nanodots absorbed light at a wavelength of 284 nm which is in the UV region of the solar spectrum. It was also found that emission of carbon nanodots occurs at 636 nm. In addition to the high photoluminescence exhibited by the carbon nanodots, Raman spectroscopy revealed that these nanomaterials have many reactive sites (mainly the D and G bands), which makes them good electron donors.

CHAPTER 4

Synthesis of NIGS quantum dots

4.1   Overview

Quantum dots have attracted strong interest from nanoscience researchers over the past couple of years, due to their versatile applications in medicine and opto-electronics. It is easy to see that quantum dots are very important in nanoscience and nanotechnology. Research into quaternary chalcogenide quantum dots is still at infancy, and this motivated this research to prepare and investigate these unique nanomaterials. This chapter includes the synthesis approach used to synthesize the NIGS quantum dots and the results obtained are analyzed.

4.2   Abstract

Quantum dots are a unique class of metal nanoparticles which have attracted huge interest in nanoscience and nanotechnology. The challenge encountered when preparing these tiny nanocrystals is the use of toxic precursors and solvents. In this research study nanocrystal semiconducting materials known as NIGS quantum dots have been prepared and their photophysical and electronic properties were carefully analysed. Fourier Transformed Infrared spectroscopy (FT-IR) was used to study the structural composition of NIGS quantum dots. Ultraviolet visible (UV-Vis) spectroscopy, Raman spectroscopy and photoluminescence (PL) spectroscopy were used to study photophysical properties. High resolution transmission electron microscope (HRTEM), X-ray diffraction (XRD) and small-angle X-ray scattering (SAXS) spectroscopy were employed to evaluate the size of the NIGS quantum dots. Cyclic voltammetry (CV) was used to study electrochemistry of

the NIGS quantum dots. The UV-Vs spectroscopy revealed that the NIGS quantum dots absorb light in the visible with a broad peak at 547 nm and the absorption extends to 700 nm. The PL spectroscopy revealed that the NIGS quantum dots emit light at 397 nm. The optical bandgap of the NIGS quantum dots estimated using Tauc plot was found to be 2.01 eV, while the electrochemical bandgap estimated using CV graph was 1.91 eV. The HRTEM revealed that the average size of the NIGS quantum dots was 11.25 nm, SAXS revealed polydispersity of spherical nanoparticles of NIGS quantum dots.

4.3   Introduction

Intensive research is being done on zero-dimensional nanoparticles popularly known as quantum dots, have sizes which are typically from 2 nm to 10 nm. Quantum dots have attractive optical properties which are dependent on their size and these optical properties can be exploited in applications such as photovoltaics, light emitting diodes (LEDs), lasers and medical imaging. The small size of the nanomaterials is caused by a natural phenomenon known as quantum confinement. During synthesis, the size is normally controlled by various approaches which include varying the amount of precursors, changing reaction conditions and use of stabilizing or capping agents [70].

As the quantum confinement effect becomes strong, the quantum dots size decreases. The size of the quantum dots increases as the effect becomes weaker. The bandgap of these nanoparticles is size dependent. Most quantum dots that have the desired properties are prepared from heavy metals such as cadmium (Cd), lead (Pb) etc. Quaternary quantum dots are an emerging class of quantum dots, these compounds do not depend on toxic elements unlike well-known quantum dots. There are many methods that have been report

in literature for preparing these nanocrystalline materials, but to the best of our knowledge there are few reports on quantum dots synthesized using a greener route such as microwave synthesis [177].

4.4   Experimental

4.4.1   Reagents

All the chemicals were using as received, indium acetylacetonate (99.99%), nickel acetylacetonate (99.99%), gallium acetylacetonate (99.99%), selenium (Se) (99.99%), methanol (99.99%), toluene (95%), tetrabutylammonium perchlorate (for electrochemical analysis, 99.0%) were obtained from Sigma-Aldrich (Modderfontein, South Africa). The diethylene triammine (99.99%) was obtained from Kimix (Cape Town, South Africa).

4.4.2   Preparation of NIGS quantum dots

The quantum dots were synthesized utilizing the solvothermal technique, using nickel (III) acetylacetonate (Ni (acac)$_3$,0. 2475 g), indium (III) acetylacetonate (In(acac)$_3$), 0.3871 g), gallium (III) acetylacetonate (Ga(acac)$_3$, 0.2755 g) and selenium (Se, 0.3950 g) as starting materials and diethylene triammine (DETA) as a solvent. In the experimental procedure, the four precursors were mixed with 20 mL of diethylene triammine at ambient temperature in a 100 mL round bottom flask. A reflux condenser was connected to flask which contained the reaction mixture, and the reaction was carried out at a temperature of 200 ℃ at a reaction times of 3 h with stirring at 3000 rmp under a continuous flow of nitrogen. The products were purified by centrifugation at 10000 rpm for 10 min, followed by successive washing three times with methanol and three times with toluene, respectively.

4.4.3   Characterization

The Fourier Transformed Infrared spectroscopy (FT-IR) investigations of the synthesized materials were carried out using FT-IR spectrometer (Model spectrum Two, Perkin Elmer, Massachusetts, USA) with KBr pellet technique in the range between 500 cm^{-1} and 4000 cm^{-1}. The light absorption properties of the NIGS quantum dots were investigated using ultraviolet visible (UV-vis) spectroscopy (Nicolet Evolution 100 spectrometer, Thermo Electron Corporation, Massachusetts, USA) from 200 nm to 600 nm. The photoluminescence spectrum of the NIGS quantum dots was recorded using photoluminescence spectrometer (IGA-521 X 1-50-1700-1LS, Horiba Jobin Yvon, Kyoto, Japan) at an excitation wavelength of 284 nm. The Raman spectroscopy of the NIGS quantum dots was recorded using Raman spectrometer (Xplora, Horiba Scientific, Kyoto, Japan). The morphology of the prepared NIGS quantum dots was probed using TEM spectroscopy (Tecnai F20 Emission Transmission Electron Microscope, FEI, Oregon, USA). The shape and size distribution were further investigated using SAXS spectroscopy (small and wide-angle scattering system, Anton-Paar, Graz, Austria. To study crystalline nature of the NIGS quantum dots, the XRD spectrum was recorded using Bruker AXS D8 Advance diffractometer (voltage 40 KV; current 40 mA) from Bruker (Massachusetts, USA). All electrochemistry experiments were conducted using potentiostat CH work station (PalmSens BV, Houten, Netherlands) and a conventional three-electrode system with a glassy carbon working electrode, Ag/AgCl reference electrode saturated in 3M NaCl and a platinum wire counter electrode. All the electrodes were obtained from BASi (Lafayette, USA). Prior to all electrochemistry experiments, the working electrode was prepared by polishing in alumina slurries of 1 μm, 0.3 μm and 0.05 μm, respectively, followed by successive ultrasonication in ethanol and water. A solution of 0.5 M

tetrabutylammonium perchlorate (for electrochemical analysis, 99.0%) was used an as electrolyte. For all electrochemical measurements, the glassy carbon electrode was modified by dropcoating with 5µL of the NIGS quantum dots that were dissolved in ethanol.

4.5 Results and Discussion

4.5.1 Fourier Transformed Infrared (FT-IR) spectroscopy

Fourier Transformed Infrared (FT-IR) spectroscopy was used to investigate the functional groups appearing on the surface of the NIGS quantum dots. The Figure 4.1 below displays the FT-IR of carbon NIGS quantum dots synthesized at a reaction of 3h using solvothermal synthesis. The following functional groups some of O-H, C=O, C-O and C-H in the structure of the synthesized quantum dots material. The synthesized NIGS QD material FTIR has some peaks that are identical to the solvent, meaning that DETA is used as capping agent [178].
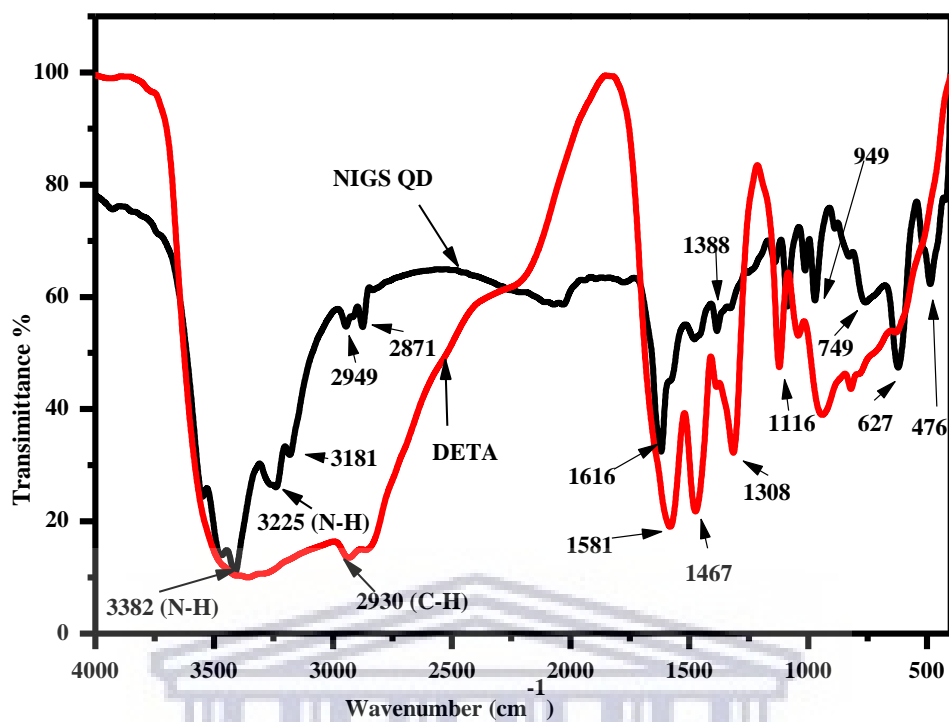
Figure 4.1: FT-IR spectrum of diethylenetriamine (DETA) and NIGS quantum dots.

4.5.2   Ultraviolet-visible (UV-Vis) spectroscopy

UV-Vis studies were done to investigate the optical properties the prepared quantum dots material, it is expected that when quantum dots are exposed to a light source in the UV-Vis region electrons are promoted from lower energy state (valence band) to higher energy state (conduction band). The region between these bands is known as the optical bandgap, bandgap is useful when scrutinizing the optical properties of quantum dots [179]. Figure 4.2 displays UV-Vis spectrum of the NIGS quantum dots. The synthesized QD material exhibited an absorption peak centred on 547 nm and absorbs light up to 700 nm, this means that the prepared material does absorb light in the visible region which is ideal for solar cell applications. The bandgap was calculated using the Tauc plot and found to be 2.42 eV. The optical bandgap of the prepared NIGS quantum dots is close to the bandgap that a material must have when one want to apply it to solar cells. The range of the optical

bandgap value in order for a material to be applied in solar cell devices is generally 1.0 eV-2.4 eV [180,181].
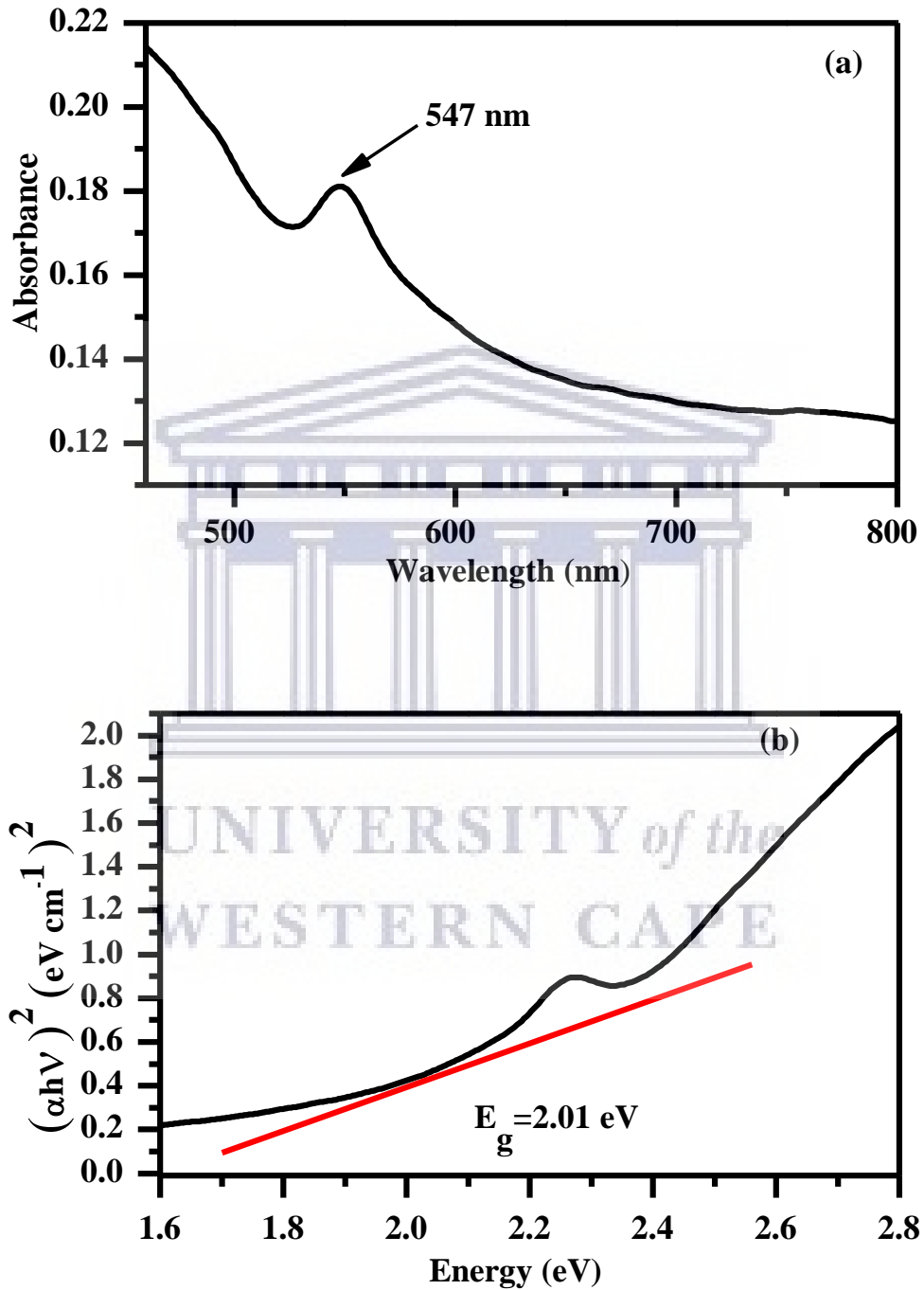
Figure 4.2: UV-Vis spectrum (a) and Tauc plot (b) of NIGS quantum dots.

4.5.3   Analysis of photoluminescence spectroscopy

The optical properties of semiconductors are strongly affected when they are reduced to nanoscale regime. The emission of quantum dots can go from 200 nm up to 850 nm in theory [182,183]. The photoluminescence (PL) spectra of the synthesized NIGS quantum dots was recorded in Figure 4.3, it is observed from the PL spectra that there was only one emission peak located at 397 nm and the peak has strong intensity of 800 counts per second. The solvent used to record the PL spectra was benzene which is non-polar, the reason for the peak appearing at this wavelength region might be because of the weak interaction between the polar groups of the solvent and the prepared NIGS quantum dots [184].
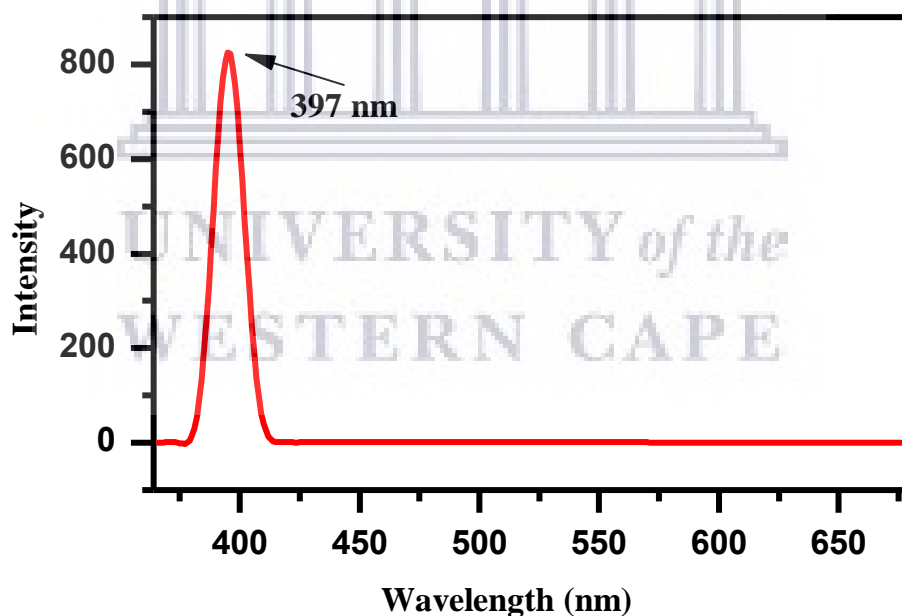
Figure 4.3: Photoluminescence spectra of NIGS quantum dots.

4.5.4   Analysis of Raman spectroscopy

The Raman spectroscopy is a useful tool when one wants to better understand crystalline properties of nanomaterials. Generally a highly crystalline material is centered at 580 cm^{-1}, a highly crystalline materials is desirable for solar cell applications [185]. The Raman spectra of the prepared NIGS carbon nanodots was obtained in Figure 4.4 below, there was a sharp peak observed at 488.62 cm^{-1}. The observed broad peak is known as A_1 mode, this dominant mode is generally caused by vibrating selenium (Se) anions in the x-y plane interacting with the cation at rest [186].
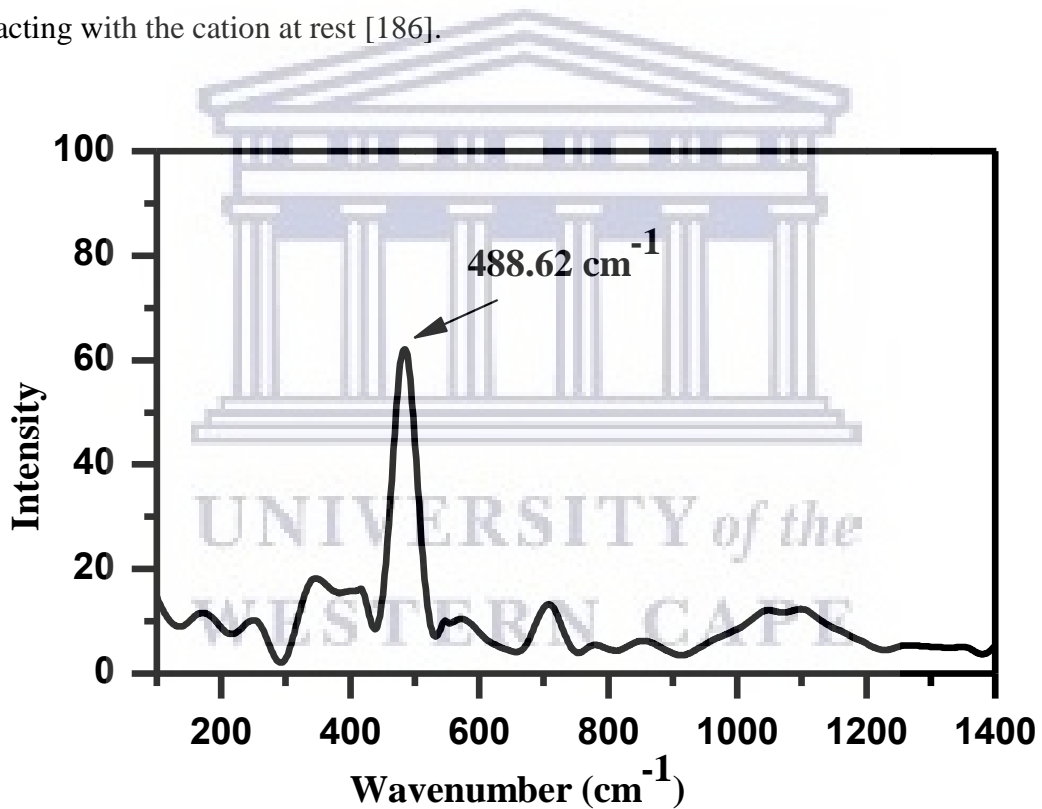
Figure 4.4: Raman spectra of NIGS quantum dots.

4.5.5   High resolution transmission electron microscopy (HRTEM)

The structural and chemical characterization of quantum dots need a technique that has suitable spatial resolution, since quantum dots are zero dimensional nanoparticle (compound semiconductors have a size of only some nanometers in all spatial directions). The TEM investigations of these quaternary nanostructured semiconductors mainly focus on structural properties such as size, shape, surface defects and strain [187,188]. The HRTEM images in Figure 4.5(a) (low magnification) and Figure 4.5(b) (high magnification) of crystalline NIGS quantum dots with diameters between 9.50 nm and 13 nm and an average diameter of 11.25 nm. The inserted SAED image shows that the prepared quantum dots are crystalline with lattice fringes.
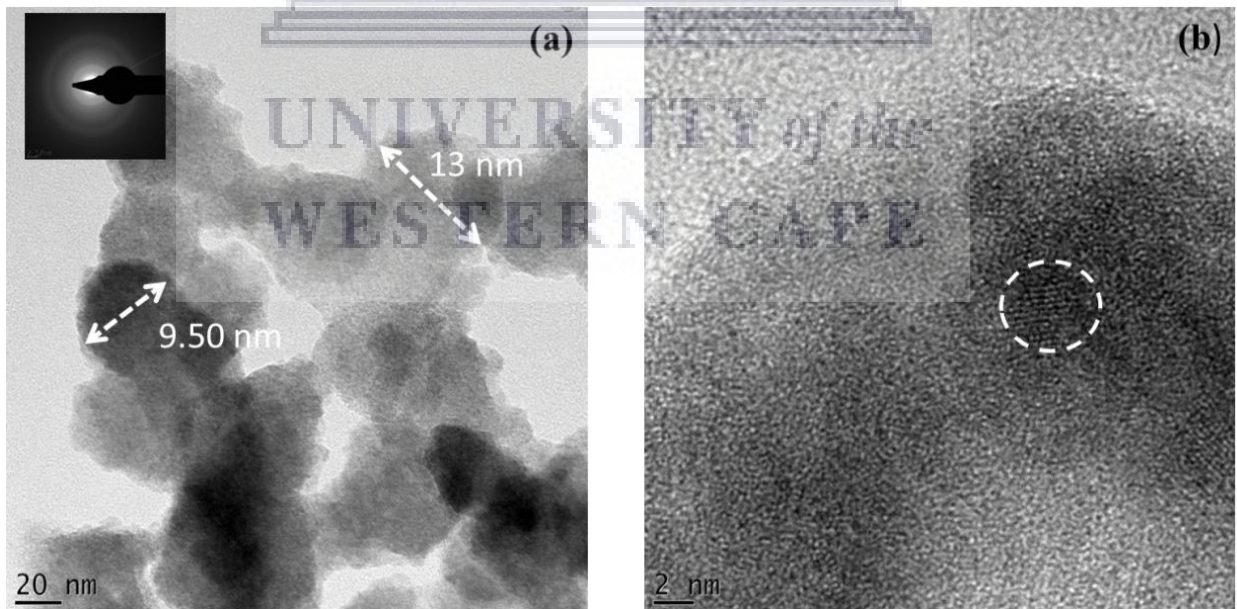
Figure 4.5: HRTEM images of NIGS quantum dots.

4.5.6 Energy dispersive X-ray spectroscopy (EDS)

The energy dispersive X-ray spectroscopy (EDS) of the prepared NIGS quantum dots was obtained together with TEM, from the EDS graph it can be observed that nickel (Ni) has the highest composition as expected. The next element having highest composition after Ni is indium (In) followed by gallium (Ga) and finally selenium (Se).
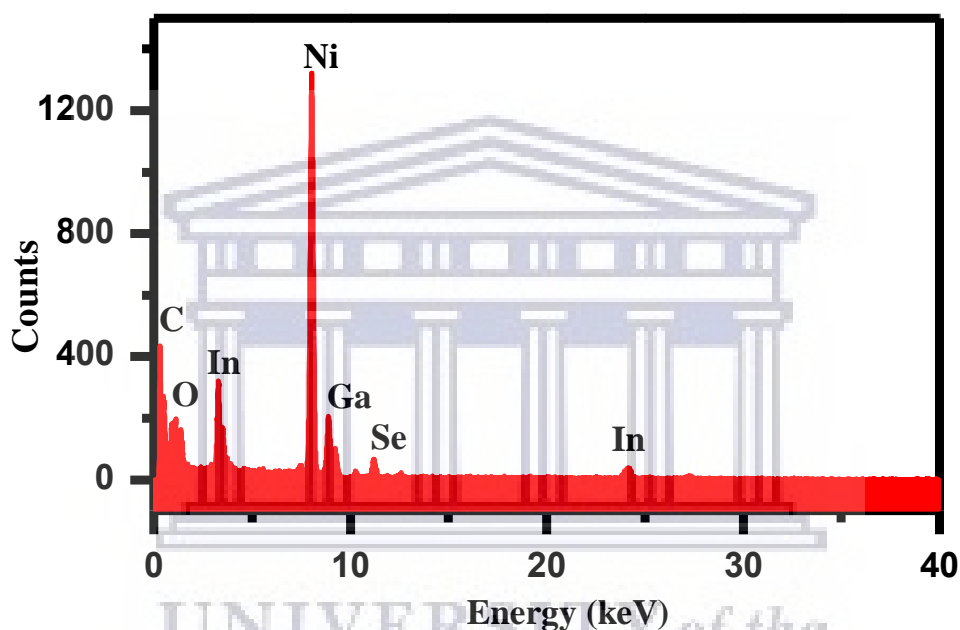
Figure 4.6: EDS of NIGS quantum dots.

4.5.7 X-ray diffraction (XRD)

The X-ray diffraction (XRD) patterns of the synthesized of the prepared quantum dots at reaction time of 2 h materials are displayed in Figure 4.7 below. The XRD pattern reveals crystalline quantum dots which in agreement with the TEM results. The XRD pattern also show two distinct peaks at 2 theta =22º which corresponds to miller indices of 112, and 2 theta= 30º which corresponds to miller indices of 211. These two distinct peaks exhibit a

degree of high crystallinity, the broad peaks are broader. The crystal structure was found to be orthorhombic using the miller indices.
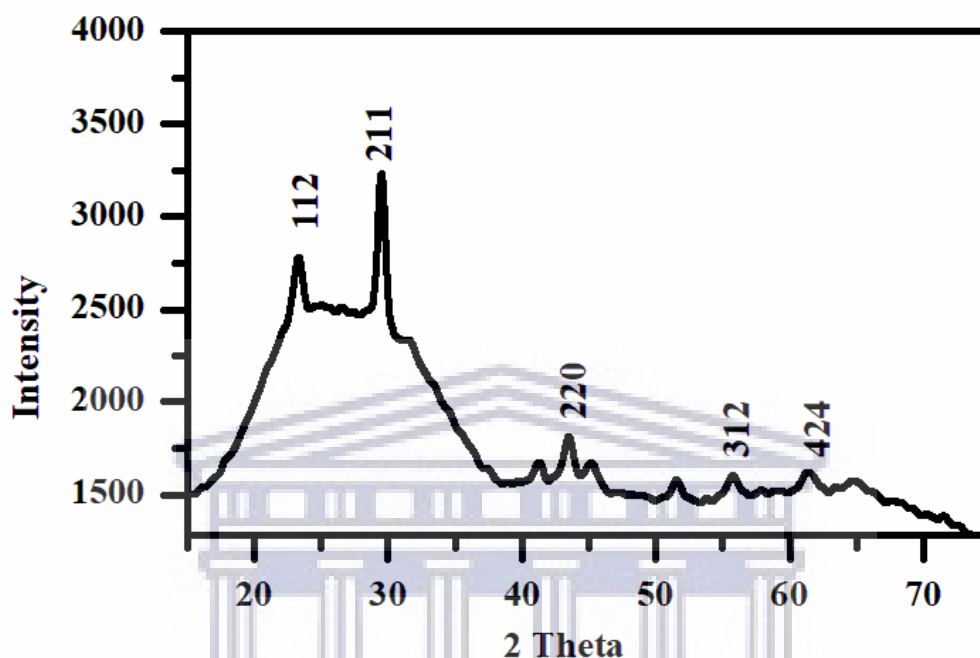
Figure 4.7: XRD patterns of NIGS quantum dots synthesized.

4.5.8   Small angle X-ray scattering (SAXS) spectroscopy

The small angle X-ray spectroscopy (SAXS) technique is generally capable of providing structural information for particles having sizes between 5 and 25 nm of repeat distance and up to 200 nm. SAXS can also be used to evaluate the inner structure of quantum dots, quantum dots are very unstable when exposed to air. SAXS is performed in solution this becomes useful when characterizing nanoparticles such as quantum dots, because this minimizes particle agglomeration [152,189].

The pair-distance distribution function (PDDF) spectrum in Figure 4.8(a) was used to identify the shape of the prepared NIGS quantum dots, and the PDDF spectrum showed

that the NIGS quantum dots have a spherical shape [190]. The intensity spectrum in Figure 4.8(b) and volume by distribution in Figure 4.8(d) reveals polydispersity. The volume by distribution spectrum in Figure 4.8(d) showed that particles with sizes below 25 nm are dominant. The distribution by number spectrum in Figure 4.8(c) showed more presence of particles with sizes below 25 nm, than particles with size around 100 nm.
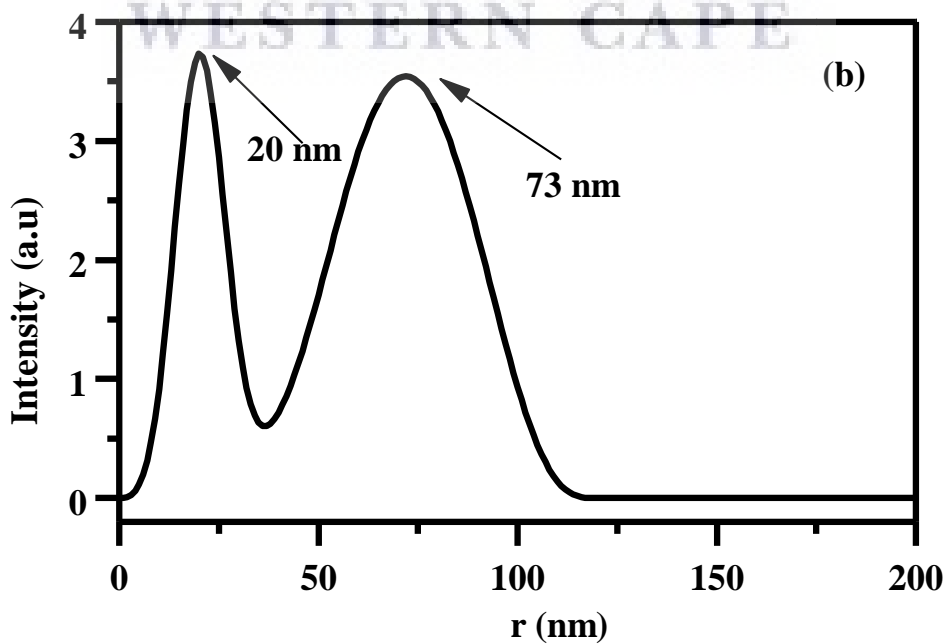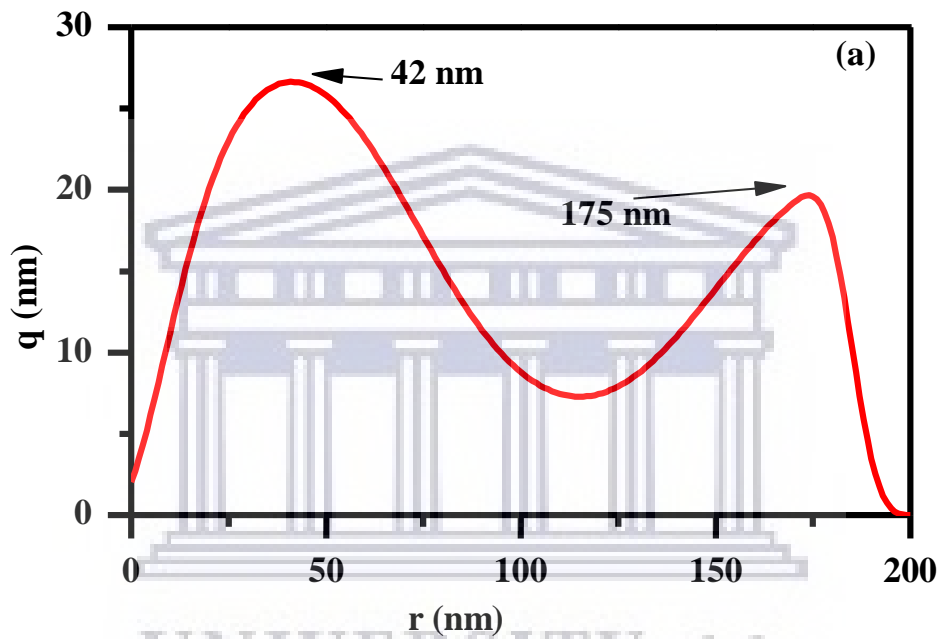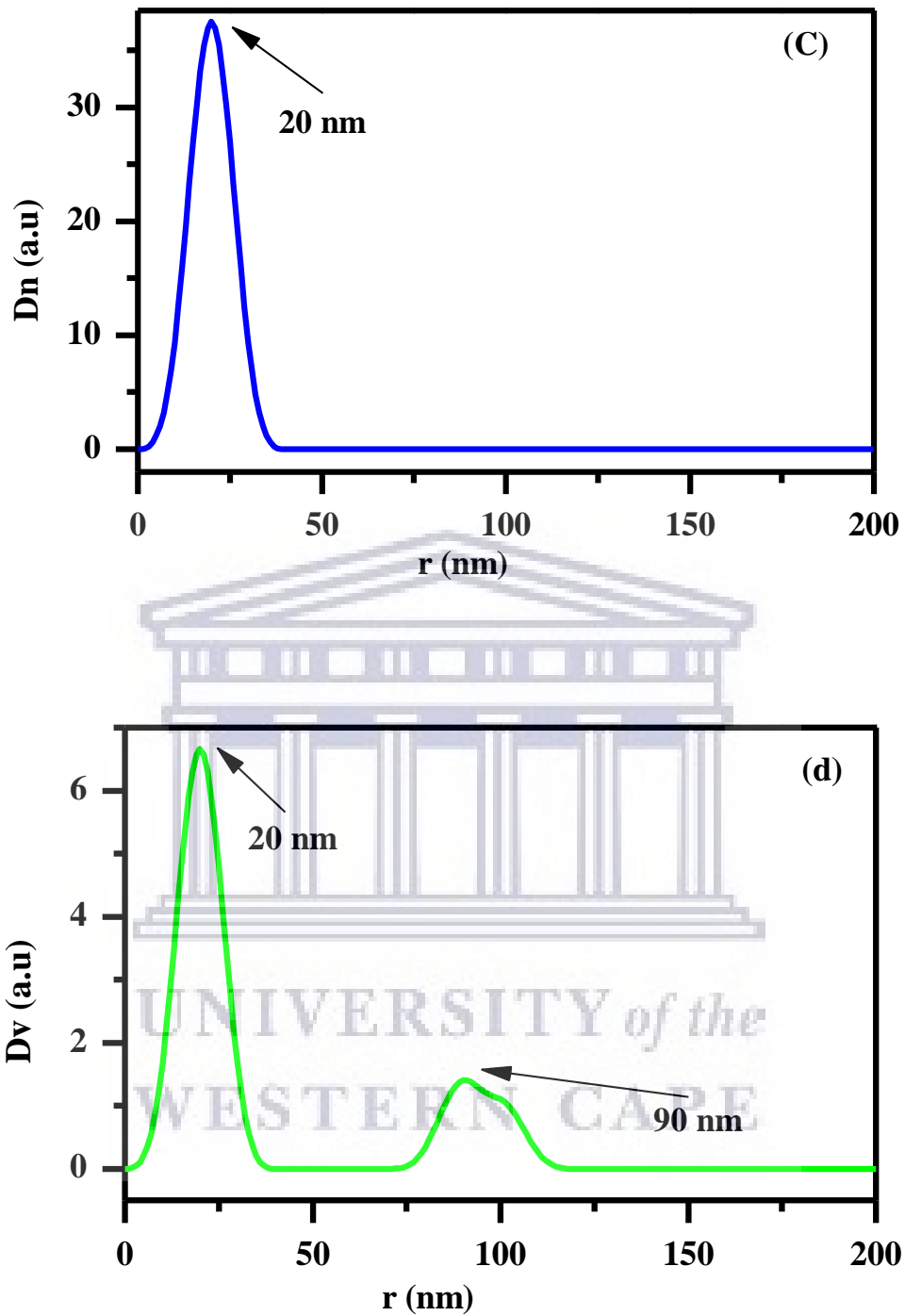
Figure 4.8: SAXS of NIGS quantum dots analysed by (a) PDDF, (b) by distribution intensity, (c) distribution by number and (d) distribution by volume.

4.5.9   Cyclic voltammetry (CV)

Figure 4.10 displays the cyclic voltammetry (CV) of NIGS quantum dots using, while figure 4.9 displays the bare glassy carbon electrode (GCE). All the electrochemistry experiments were performed using a solution of 0.5 M tetrabutylammonium perchlorate as an electrolyte. The cyclic voltammetry of the NIGS quantum dots modified glassy carbon electrode (GCE) was performed using a potential window from -1.10 V to 1.10 V, while the CV of bare GCE was performed using potential window from -1.20 V to 1.20 V.

The CV graph of the prepared NIGS quantum dots revealed two oxidation peaks, labelled I/I'. These peaks, centred at 0.49 V and 0.91 V vs Ag/AgCl is ascribed to the oxidation of NIGS quantum dots. The peaks can be assigned to the oxidation of Ga to Ga^{3+}. The CV graph also revealed that the reduction (labelled II) of NIGS quantum dots occurred at -0.89 V vs Ag/AgCl. It is also observed that at a scan rate of 0.010 V/s, there was one oxidation peak observed at 0.83 V vs Ag/AgCl. The Figures 4.10(a) and 4.10(c) were plotted to clearly show the NIGS quantum dots had two oxidation peaks at all other scan rates, except at a scan rate of 0.010 V. As the scan rate is increased from 0.01 V/s to 0.05V/s (Figure 4.10(a)) and from 0.06 V/s to 0.13 V/s (Figure 4.10(b)), an increase in peak current is observed. The electrochemical bandgap was calculated using the formulae 4.1.

$$Eg= E(HOMO)- E(LUMO) \qquad\qquad 4.1$$

$$E(HOMO)=-e[E_{Ox}^{onset}- 4.4] \qquad\qquad 4.1(a)$$

$$E(LUMO)=-e[E_{Red}^{onset}- 4.4] \qquad\qquad 4.1(b)$$

With an onset oxidation potential of 0.98 V and an onset reduction potential of -0.93 V, the HUMO and LUMO were estimated using equations 4.1 (a) and 4.1 (b), respectively. The HOMO and LUMO were found to be 3.42 eV and 5.3 eV. This led to an estimated band gap of 1.91 eV for the NIGS quantum dots.
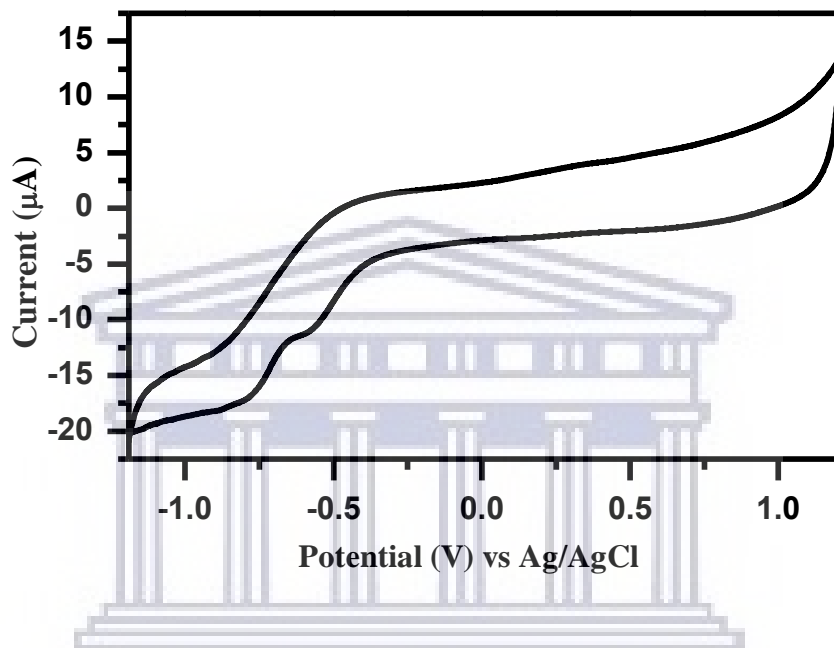
Figure 4.9: Glassy carbon electrode in 0.5 M tetrabutylammonium perchlorate at a scan rate of 0.050 V/s between -1.20 V and +1.20 V vs Ag/AgCl.
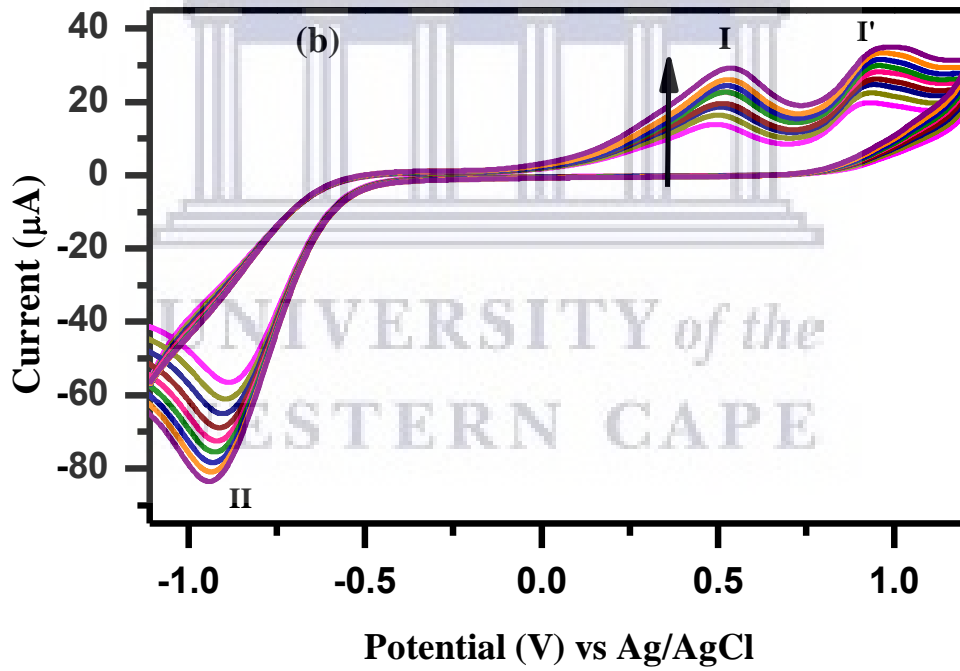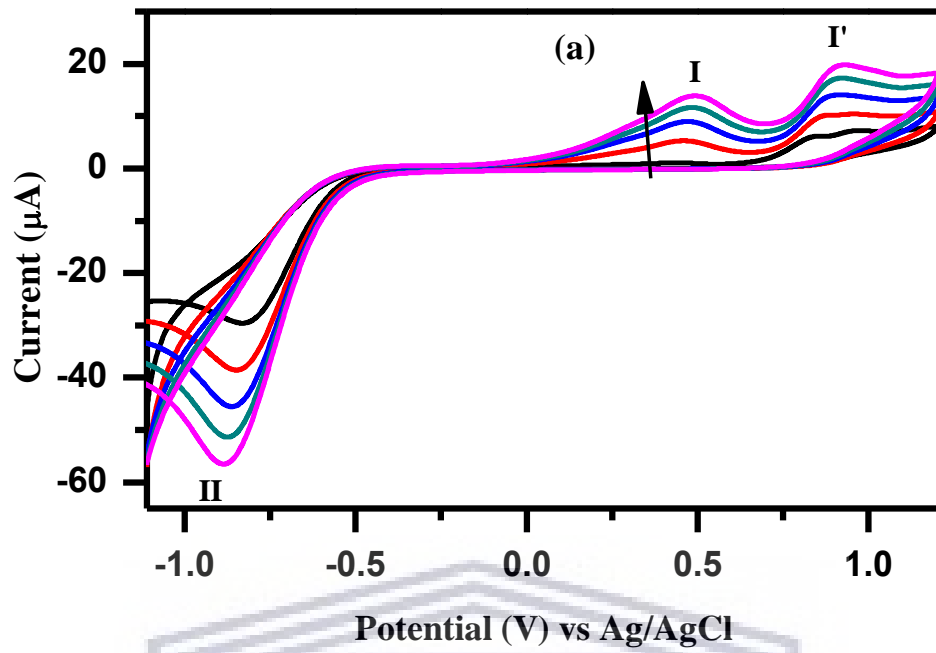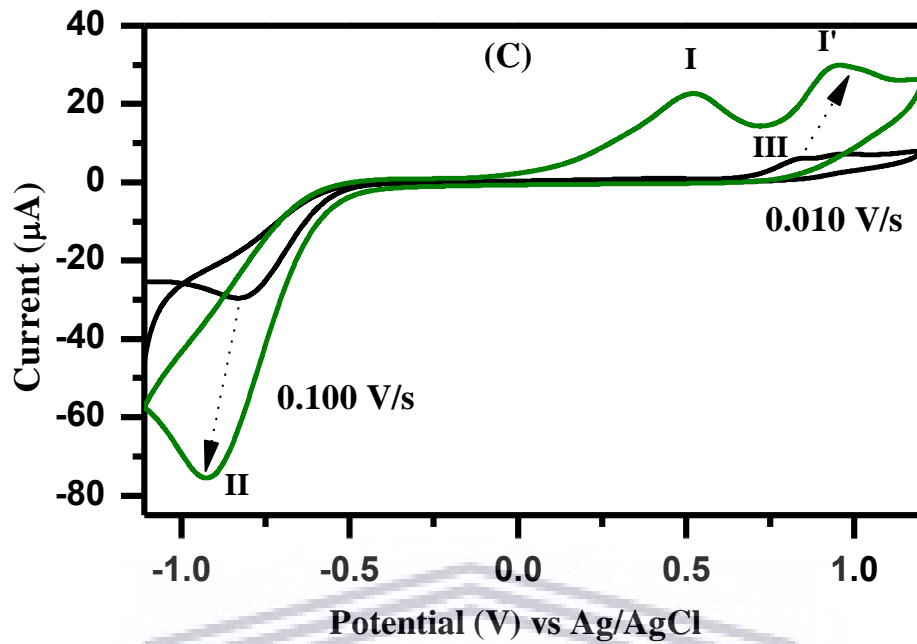
Figure 4.10: CV graph of NIGS quantum dots -modified GCE between -1.10 V and +1.10 V in 0.5 M tetrabutylammonium perchlorate at (a) lower scan rates from 0.010 to 0.050 V/s and (b) higher scan rates from 0.050 to 0.130 V/s in increments of 0.01 V/s (black arrows indicate direction of scan rate increase), (c) reveals response differences of the NIGS quantum dots (indicated by dashed blue arrows) at the lowest scan rate (0.010 V/s) and highest scan rate (0.100 V/s).

4.6   Conclusion

Novel NIGS quantum dots were synthesize using solvothermal synthesis. The NIGS quantum dots prepared showed good absorption in the visible region of the solar spectrum. The absorption first occurred at 547 nm and extended to 700 nm, we then using the UV-Vis spectrum to obtained Tauc plot. Tauc plot was employed to estimate the optical bandgap of 2.01 eV. This bandgap value is higher than the bandgap of materials applied in solar cells. Cyclic voltammetry was employed to estimate the electrochemical bandgap of NIGS quantum dots, the bandgap was 1.91 eV. The light emission of NIGS quantum dots occurred at a wavelength of 397 nm, this meant that the NIGS quantum dots underwent blue shift.

HRTEM and XRD revealed that the NIGS quantum dots have high degree of crystallinity, HRTEM revealed that the NIGS quantum dots have a size of 11.25 nm. On the other hand SAXS revealed polydispersity of spherical nanoparticles of NIGS quantum dots. The cyclic voltammetry revealed that the NIGS quantum dots had two oxidation peaks centred at 0.49 V and 0.91 V. The NIGS quantum dots had one reduction peak centred at -0.89 V.

CHAPTER 5

Novel carbon nanodots- decorated NIGS quantum dots

nanocomposite

5.1 Overview

In this chapter the carbon nanodots-decorated NIGS quantum dots synthesis method is described in detail. Also the results obtained are presented in graphs and explained in detail. The results obtained for the carbon nanodots -decorated NIGS quantum dots are discussed and their implications are explained.

5.2 Abstract

The integration of nanomaterials with different properties can lead to novel nanomaterials with versatile application. In this work we have synthesized novel carbon nanodots decorated NIGS quantum dots using microwave synthesis. We have studied the structural composition of these novel nanomaterials using Fourier Transformed Infrared spectroscopy (FT-IR). The photophysical properties were studied ultraviolet visible (UV-vis) spectroscopy, Raman spectroscopy and photoluminescence (PL) spectroscopy. High resolution transmission microscopy (HRTEM), X-ray diffraction (XRD) and small angle X-ray spectroscopy (SAXS), were employed to investigate the size of the carbon nanodots-decorated NIGS quantum dots. The electrochemical properties of carbon nanodots-decorated were investigated using cyclic voltammetry (CV).

The UV-vis spectroscopy showed that the carbon nanodots decorated quantum dots absorb light in the visible region starting at 400 nm to around 750 nm, while we deduced from the

PL spectroscopy analysis that they emit light at 444 nm. The optical bandgap was estimated to be 1.97 eV using the Tauc plot, this bandgap value make these nanomaterials potential candidates for photovoltaic applications. Optical properties such as the photoluminescence, absorption of light in the visible region and Raman spectroscopy improves when the NIGS quantum dots are decorated with carbon nanodots.

5.3 Introduction

Nanotechnology and nanoscience is progressing at an exponential rate, this makes it possible for scientists and engineer to design sophisticated nanomaterials that have tuneable and unique optical and electronic properties. Quantum dots are one typical example of nanomaterials that offer many advantages. It comes as no surprise that quantum dots have attracted strong interest from researchers. Quantum dots have impressive electronic and optical properties. However, when used pristine quantum dots are not for suitable solar cell applications and cannot compete with conventional materials for similar applications. There are many disadvantages encountered when quantum dots are used alone, these include instability when exposed to air and toxicity. It is a great challenge in the field of nanoscience to find plausible solutions to these problems [191].

Carbon nanodots are a novel class of carbon nanomaterials which have attracted strong attention, because they are cheap to make, have high conductivity and small size. Carbon nanodots are known to be good electron conductors when integrated with semiconducting nanocrystals [45]. In this work carbon nanodots-decorated quantum dots were prepared, and their electrochemistry and photophysics was investigated.

5.4   Experimental

5.4.1   Reagents

All the chemicals were using as received, indium acetylacetonate (99.99%), nickel acetylacetonate (99.99%), gallium acetylacetonate (99.99%), selenium (Se) (99.99%), methanol (99.99%), toluene (95%), tetrabutylammonium perchlorate (for electrochemical analysis, 99.0%) and ethylene glycol (99.99%) were all obtained from Sigma-Aldrich (Modderfontein, South Africa).

5.4.2   Synthesis of carbon nanodots- decorated NIGS quantum dots

The synthesis of the nanocomposite material was prepared utilizing the microwave synthesis approach, the carbon nanodots material (which was prepared in chapter 3) was mixed with the precursors of the NIGS quantum dots employing ethylene glycol as a solvent. In the synthesis nickel acetylacetonate (Ni(acac)$_3$, 0.2100 g) and indium acetylacetonate (In(acac)$_3$, 0.2461 g) were added together and sonicated for 10 min to form a solution, while gallium acetylacetonate (Ga(acac)$_3$, 0.3200 g) and selenium (Se) (0.3417 g) were mixed as well and sonicated for 10 min to form a solution. Thereafter, the two solutions were transferred to 100 mL Teflon vessel containing 25 mL of ethylene glycol and 1.2 mL of carbon nanodots was added, the vessel was then placed inside a microwave reaction system (Microwave Reaction System SOLV, Multi PRO from Anton Paar, Graz, Austria). The reaction was irradiated at 160 ℃ using temperature control at different reaction times (15 and 20 min). The products were purified by centrifugation at 10000 rpm, followed by washing (for 10 min) with ethanol, toluene and ethanol conservatively.

5.4.3   Characterization

The Fourier Transformed Infrared spectroscopy (FT-IR) investigations of the synthesized materials were carried out using FT-IR spectrometer (Model spectrum Two, Perkin Elmer, Massachusetts, USA) with KBr pellet technique in the range between 500 cm^{-1} and 4000 cm^{-1}. The light absorption properties of were investigated using ultraviolet visible (UV-Vis) spectroscopy (Nicolet Evolution 100 spectrometer, Thermo Electron Corporation, Massachusetts, USA) from 200 nm to 800 nm. The photoluminescence spectrum of the carbon nanodots decorated NIGS quantum dots was recorded using photoluminescence spectrometer (IGA-521 X 1-50-1700-1LS, Horiba Jobin Yvon, Kyoto, Japan) using an excitation wavelength of 350 nm. The Raman spectroscopy of carbon nanodots decorated NIGS quantum dots was recorded using Raman spectrometer (Xplora, Horiba Scientific, Kyoto, Japan). The morphology of the prepared carbon nanodots decorated NIGS quantum dots nanomaterials was probed using TEM spectroscopy (Tecnai F20 Emission Transmission Electron Microscope, FEI, Oregon, USA). The shape and size distribution were further investigated using SAXS spectroscopy (small and wide-angle scattering system, Anton-Paar, Graz, Austria. To study crystalline nature of the carbon nanodots, the XRD spectrum was recorded using Bruker AXS D8 Advance diffractometer (voltage 40 KV; current 40 mA) from Bruker (Massachusetts, USA). All electrochemistry experiments were conducted using potentiostat CH work station (PalmSens BV, Houten, Netherlands) and a conventional three-electrode system with a glassy carbon working electrode, Ag/AgCl reference electrode saturated in 3M NaCl and a platinum wire counter electrode. All the electrodes were obtained from BASi (Lafayette, USA). Prior to all electrochemistry experiments, the working electrode was prepared by polishing in alumina slurries of 1 µm, 0,3 µm and 0.05 µm, respectively, followed by successive ultrasonication in ethanol and

water. A solution of 0.5M tetrabutylammonium perchlorate (for electrochemical analysis, 99.0% purity) was used an as electrolyte. For all electrochemical measurements, the glassy carbon electrode was modified by dropcoating with 5µL of the brown the brown CNDs decorated NIGS quantum dots.

5.5   Results and discussion

5.5.1   Fourier transformed infrared (FT-IR) spectroscopy

The Fourier transformed infrared (FT-IR) spectroscopy spectrum in Figure 5.1 below displays of the synthesized carbon nanodots decorated quantum dots, NIGS quantum dots and carbon nanodots. The FT-IR spectra show a significant peak at 3353 nm which is due to the presence of O-H functional group and show a significant peak at 2910 nm [192]. There is also a peak around 700 nm, which might be from bonding between nickel and oxygen.
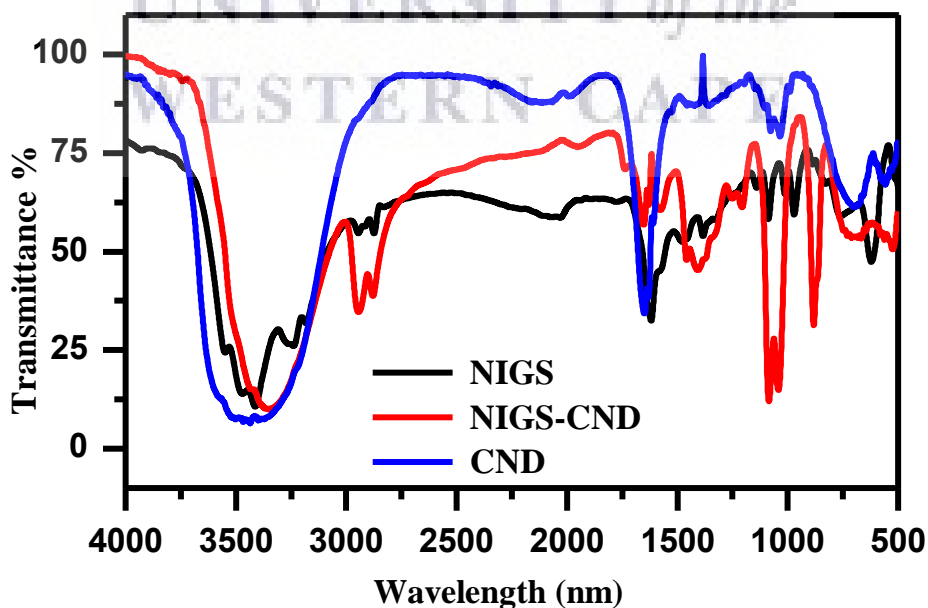
Figure 5.1: FT-IR of CND decorated NIGS quantum dots, NIGS quantum, CNDs.

5.5.2 Ultraviolet-visible (UV-Vis) spectroscopy

The carbon nanodots decorated NIGS quantum dots were characterized using ultraviolet-visible (UV-Vis) spectroscopy to investigate the optical properties [193]. The Figures 5.2(a) and 5.2(b) displays the UV-Vis absorption spectra and Tauc Plot of NIGS-CND synthesized at reaction times of 15 min and 20 min. The UV-Vis spectroscopy for the nanocomposite synthesized at different reaction time (15 min and 20 min) was performed. The UV-Vis spectra show that the nanocomposite absorbs in the visible region. The bandgap was found to 1.97 eV using the Tauc plot obtained from the UV-Vis spectra. It is observed that the bandgap decreases when the NIGS quantum dots are decorated with carbon nanodots, since the pristine NIGS quantum dots had a bandgap of 2.01 eV. The value of the bandgap of the carbon nanodots decorated NIGS quantum dots is in the range of literature value (1.0-2.4 eV) [181]. Therefore, when NIGS quantum dots are decorated with carbon nanodots, these nanomaterials have a potential to be applied in solar cells [194].
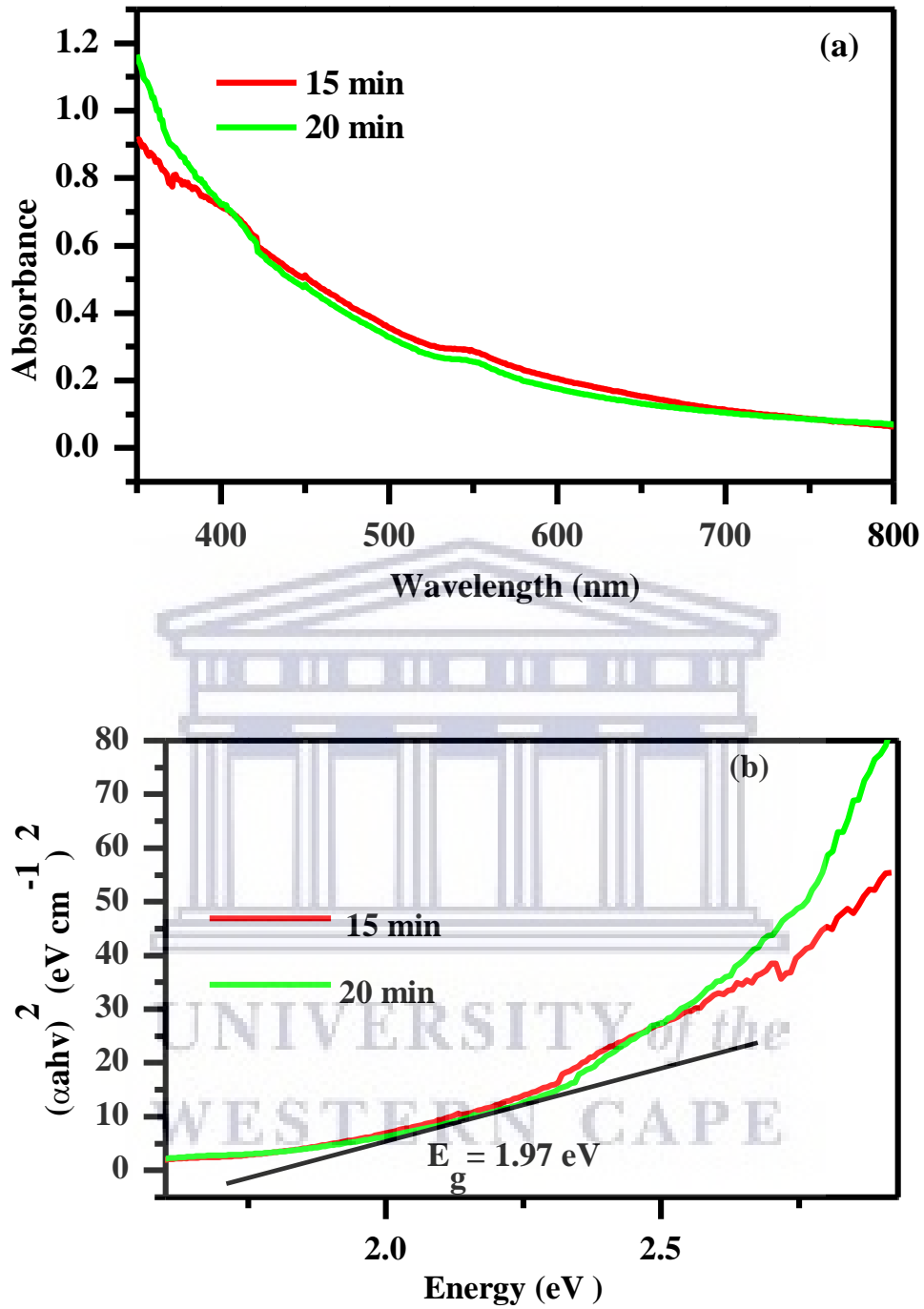
Figure 5.2: UV-Vis spectrum of carbon nanodots -decorated quantum dots (a) and Tauc plot (b).

5.5.3 Photoluminescence spectroscopy

The photoluminescence (PL) emission spectrum of carbon nanodots-decorated NIGS quantum dots is displayed in Figure 5.3 below. The emission spectrum nanomaterials was obtained by dispersing the carbon nanodots decorated NIGS quantum dots material synthesized at different time intervals (15 min and 20 min) in dichlobenzene and the excitation wavelength was set at 350 nm. It was observed from the PL emission spectrum that the prepared carbon nanodots decorated NIGS quantum dots nanomaterial has an emission peak at 444 nm at both time intervals. It was also observed from the PL spectra that the intensity decreases with time.
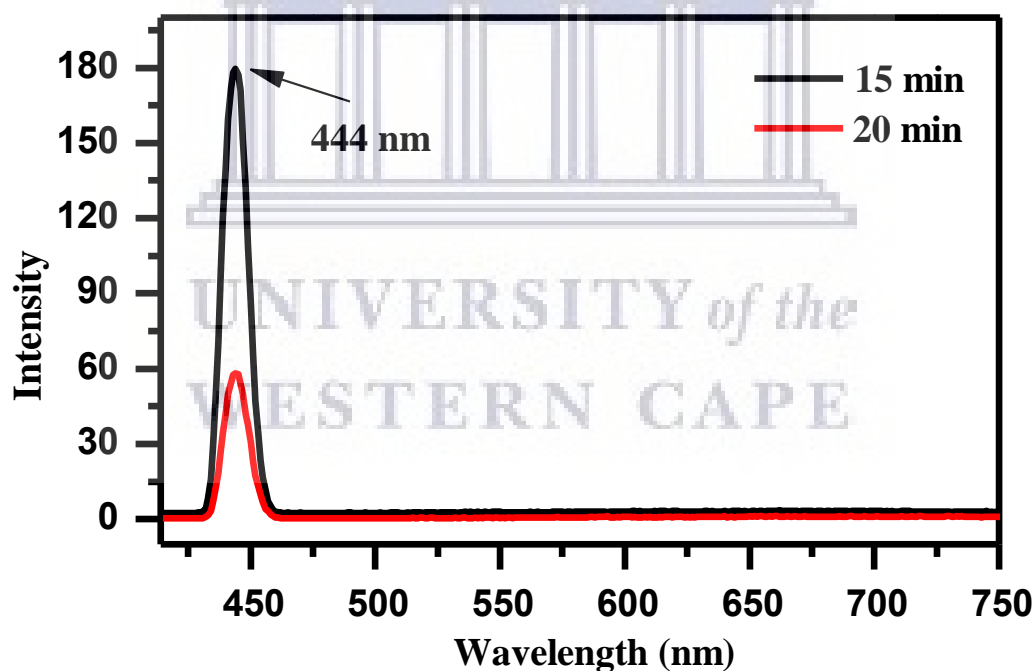
Figure 5.3: Photoluminescence spectrum of carbon nanodots decorated quantum dots.

5.5.4 Analysis of Raman spectroscopy

We have used Raman technique to investigate the phonon properties of the prepared nanomaterials. The Raman measurements for the carbon nanodots decorated NIGS quantum dots synthesized at a reaction time of 20 min were recorded in the Figure 5.4 below, there were three Raman bands observed around 488.53 cm^{-1}, 2432.12 cm^{-1} and 2911.95 cm^{-1}. The Raman peak from 488.53 cm^{-1} is a contribution from a layer of the NIGS quantum dots, this was also observed in the Raman spectra of pristine NIGS quantum dots. On the other hand the Raman peaks around 2432.12 cm^{-1} and 2911.95 cm^{-1} can be speculated as being the Raman peaks contribution from the carbon nanodots. These peaks were not observed in the Raman spectra from the pristine NIGS quantum dots, this is evidence of some successful bonding between the NIGS quantum dots and carbon nanodots. These three broad peaks indicate non-homogeneous of distribution and size of the prepared nanomaterials [195].
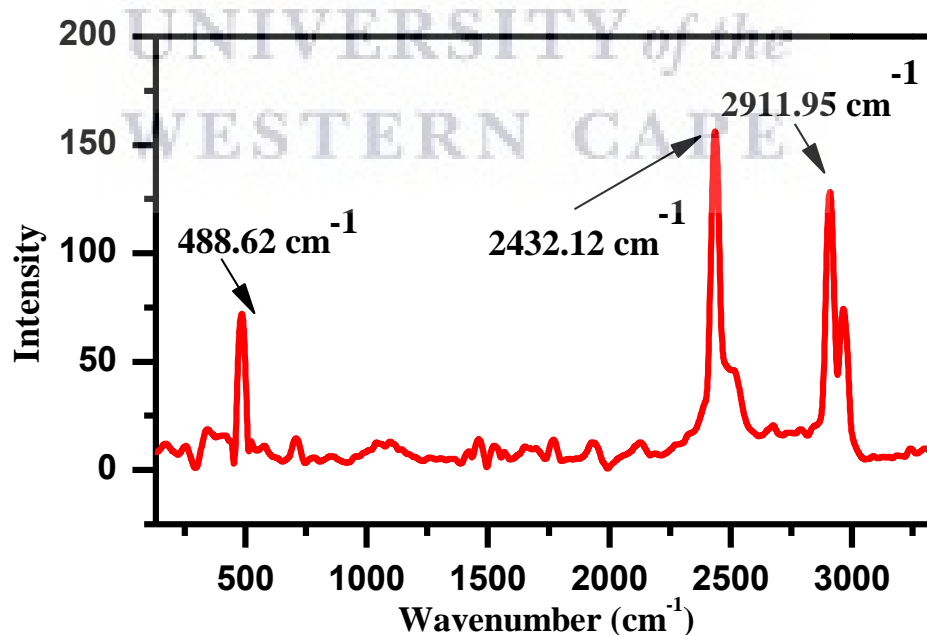
Figure 5.4: Raman spectra of carbon nanodots decorated NIGS quantum dots.

5.5.5 High-resolution transmission electron microscopy (HRTEM)

High-resolution transmission electron microscopy (HRTEM) was employed to investigate the morphology of NIGS-CND nanocomposite [196]. Figures 5.5(a) and 5.5(b) show the HRTEM carbon nanodots decorated NIGS quantum dots and SAED pattern generated from TEM is also inserted in Figure 5.5(a). The NIGS quantum dots attached to CND presents lattice fringes (Figure 5.5(b)), the lattice fringes are assigned to NIGS quantum and CNDs. The HRTEM image in Figure 5.5(a) of the prepared nanomaterials exhibit some shape such as rods and spherical nanoparticles.
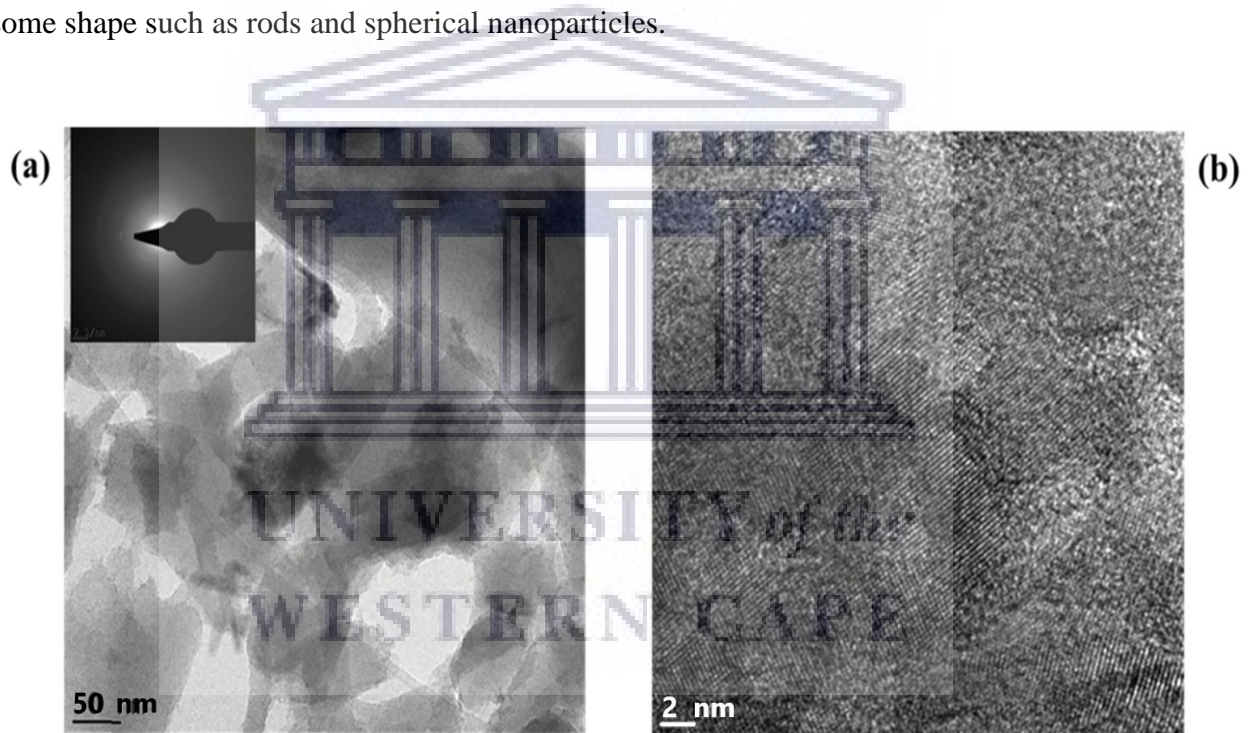
Figure 5.5: HRTEM of carbon nanodots decorated NIGS quantum dots.

5.5.6   Energy-dispersive X-ray spectroscopy (EDS)

The energy-dispersive X-ray spectroscopy (EDS) of the carbon nanodots decorated NIGS quantum dots was generated from TEM, the EDS was used to probe the elemental composition of the synthesized materials. The EDS reveals that the composition prepared material consists of nickel (Ni), indium (In), gallium (Ga) and selenium (Se) from the quantum dots. The material also contains carbon (C) and oxygen (O) from the carbon nanodots.
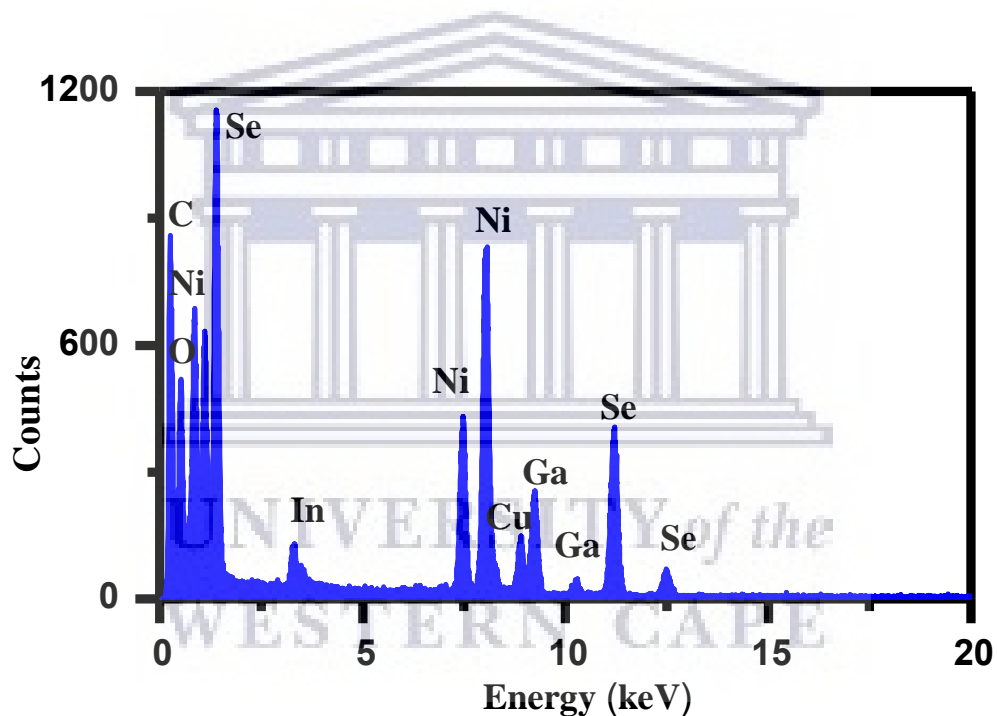
Figure 5.6: EDS of carbon nanodots decorated NIGS quantum dots.

5.5.7   X-ray diffraction (XRD)

The Figure 5.7 below displays the X-ray diffraction (XRD) of carbon nanodots decorated quantum dots. The crystalline nature of the prepared material was investigated by performing the XRD, the XRD is important and a non-destructive technique [197]. The XRD pattern is in agreement with TEM, as it also revealed crystalline carbon nanodots decorated NIGS quantum dots. The XRD pattern revealed that the structure of the carbon nanodots decorated NIGS quantum dots have an Orthorhombic structure [198].
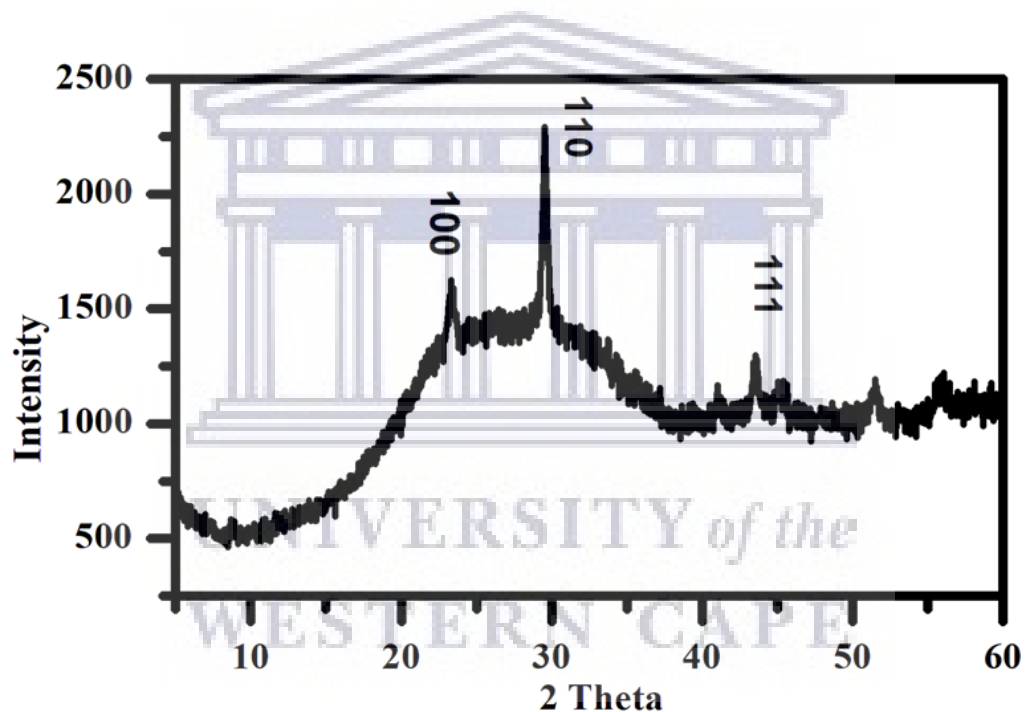
Figure 5.7: XRD of carbon nanodots decorated NIGS quantum dots.

5.5.8   Small-angle X-ray scattering (SAXS) spectroscopy

The shape, size and clustering of nanomaterials in nanocomposite is important in order to gain insight on the microstructure of a heterogeneous material. The small-angle X-ray scattering (SAXS) technique provides important information about the structure of the composite The SAXS technique can be used to elucidate on the information obtained in TEM [199]. The PDDF spectrum in Figure 5.8(a) is used is used to determine shape, this spectrum revealed that the carbon nanodots decorated NIGS quantum dots have a shell, since two curves in the spectrum overlaps to the negative y-axis. This means that there is some degree of success in decorating the NIGS quantum with carbon nanodots [200]. The intensity spectrum in figure 5.8(b) revealed that particles with sizes between 150 nm and 200 nm have more intensity than particles that are close to 100 nm. The spectrum in figure 5.8(c) displays particle size distribution by number, this spectrum showed polydispersity of particles. This means that the carbon nanodots decorated NIGS quantum dots consisted of particles with different sizes which were between 100 nm and 155 nm [201]. The volume by distribution spectrum in Figure 5.8(d) also revealed spherically polydispersed particles. The volume by distribution spectrum also revealed that particles with size of 155 nm are more dominant in the internal structure of carbon nanodots decorated NIGS quantum dots.

.

(a)

77 nm

177 nm

(b)

177 nm
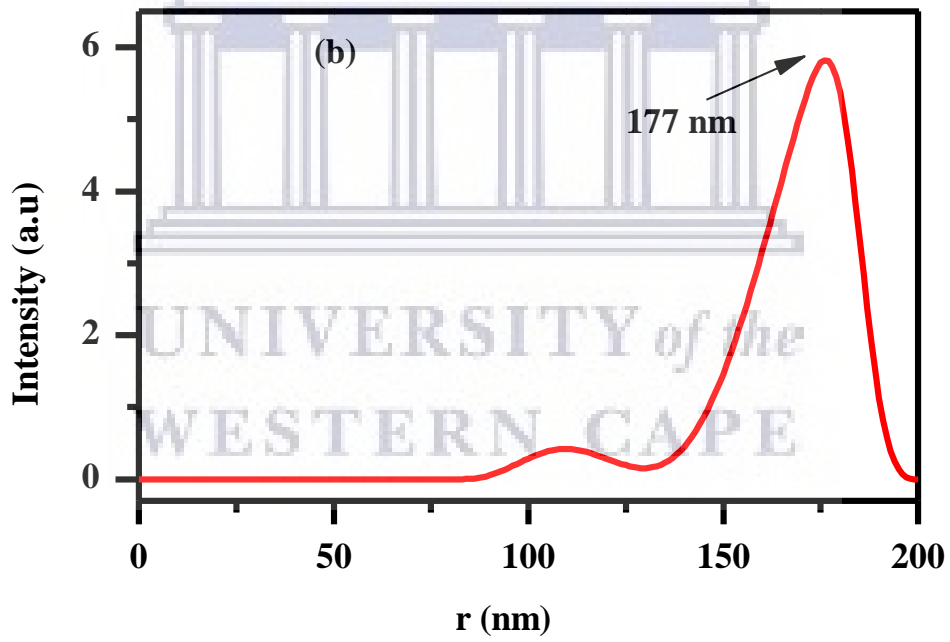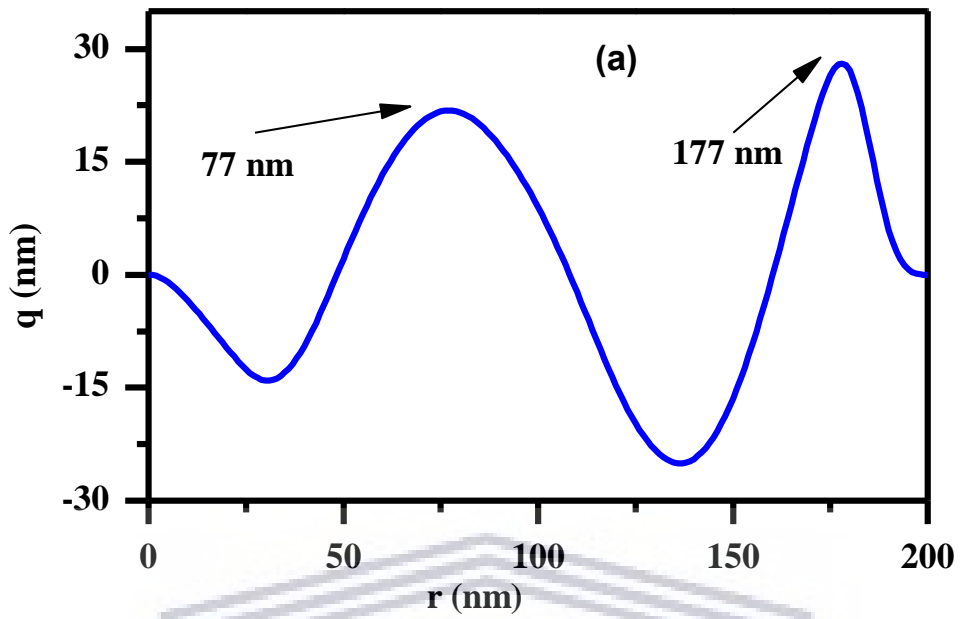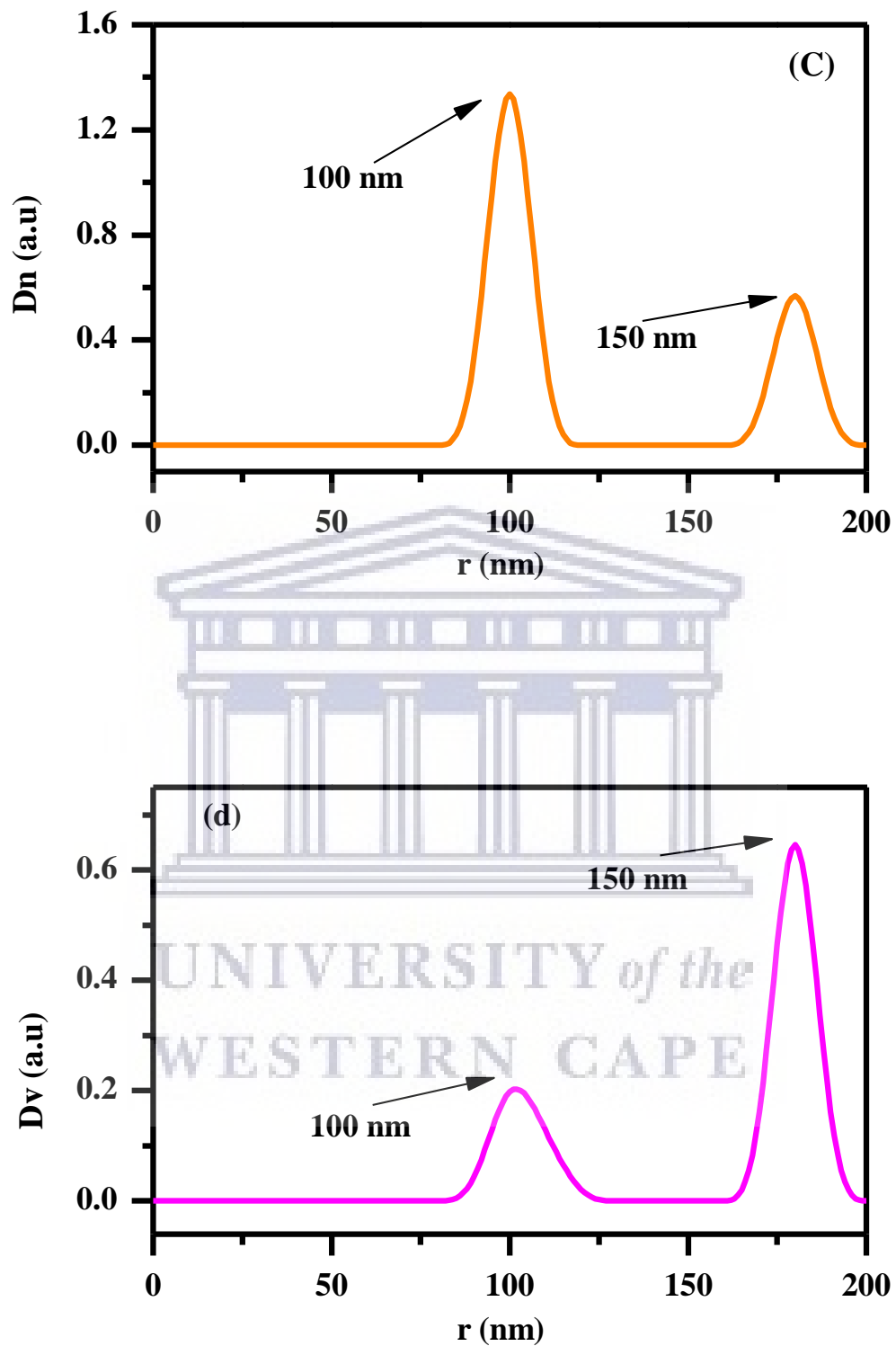
Figure 5.8: SAXS of carbon nanodots-decorated NIGS quantum dots analysed by (a) PDDF, (b) distribution by intensity, (c) distribution by number and (d) distribution by volume.

5.5.9   Cyclic voltammetry (CV)

The electrochemistry of the carbon nanodots decorated NIGS quantum dots was carried out utilizing 0.5 M tetrabutylammonium perchlorate as an electrolyte. The cyclic voltammetry (CV) of the carbon nanodots decorated NIGS quantum dots modified glassy carbon electrode (GCE) was performed using a potential window from -1.10 V to 1.10 V (displayed in Figure 5.10), while the CV of the bare GCE (displayed in Figure 5.9) was performed using a potential window from -1.20 V to 1.20 V. The CV graph of the carbon nanodots- decorated NIGS quantum dots exhibited one oxidation pair, labelled I/I'. This pair, centred at 0.62 V and 1.08 V vs Ag/AgCl is ascribed to the oxidation of carbon nanodots-decorated NIGS quantum dots. The reduction peak (labelled) of the carbon nanodots-decorated NIGS quantum dots was observed at -0.89 V vs Ag/AgCl. It is observed in Figures 5.10(c), that the CV of carbon nanodots-decorated NIGS quantum dots had one oxidation peak (III) at a scan rate of 0.010 V/s which was located at potential of 1.04 V. As the scan rate is increased from 0.01 V/s to 0.05 V/s (Figure 5.10(a)) and from 0.06 V/s to 0.13 V/s (Figure 5.10(b)), an increase in peak current is observed.

Furthermore Figure 5.11 displays cyclic voltammetry of CND, NIGS quantum dots and carbon nanodots decorated NIGS quantum dots obtained at scan rates (0.050 V/s and 0.100 V/s). In Figure 5.11(a) (scan rate of 0.050 V/s) the NIGS quantum dots revealed two oxidation peaks, labeled I and II. These peaks, centred at 0.49 V and 0.91 V ascribed to the oxidation of NIGS quantum dots. The reduction peak (labeled III) appeared at a potential of -0.89 V. The carbon nanodots showed one oxidation peak (labeled VII) at a potential of 0.6 V, while the reduction peak (labeled VI) was observed at a potential of -0.01 V. The carbon nanodots decorated NIGS quantum dots revealed one oxidation pair (labeled V and

IV), which were located at a potential of 0.62 V and 1.08 V. One anodic peak (VIII) was observed at a potential of -0.89 V.

It is observed in Figures 5.11(a) and 5.11(b), that the NIGS quantum dots showed better current response when compared with the carbon nanodots and the carbon nanodots decorated NIGS quantum dots. In Figures 5.11(a) and 5.11(b), the oxidation peaks of NIGS quantum dots shifted to the more positive potentials after decoration with carbon nanodots. This could mean the carbon nanodots act as an oxidizing agent when decorating the NIGS quantum dots. It also observed that after decoration with carbon nanodots the NIGS quantum dots reduction peak did not shift.

The electrochemical bandgap was calculated using the formulae 5.1.

$$Eg= E(HOMO)- E(LUMO) \qquad\qquad 5.1$$

$$E(HOMO)=-e[E_{Ox}^{onset}- 4.4] \qquad\qquad 5.1(a)$$

$$E(LUMO)=-e[E_{Red}^{onset}- 4.4] \qquad\qquad 5.1(b)$$

With an onset oxidation potential of 1.09 V and an onset reduction potential of -0.92 V, the HUMO and LUMO were estimated using equations 5.1 (a) and 5.1 (b), respectively. The HOMO and LUMO were found to be 3.31 eV and 5.32 eV, respectively. This led to an estimated band gap of 2.01 eV for the carbon nanodots decorated NIGS quantum dots.
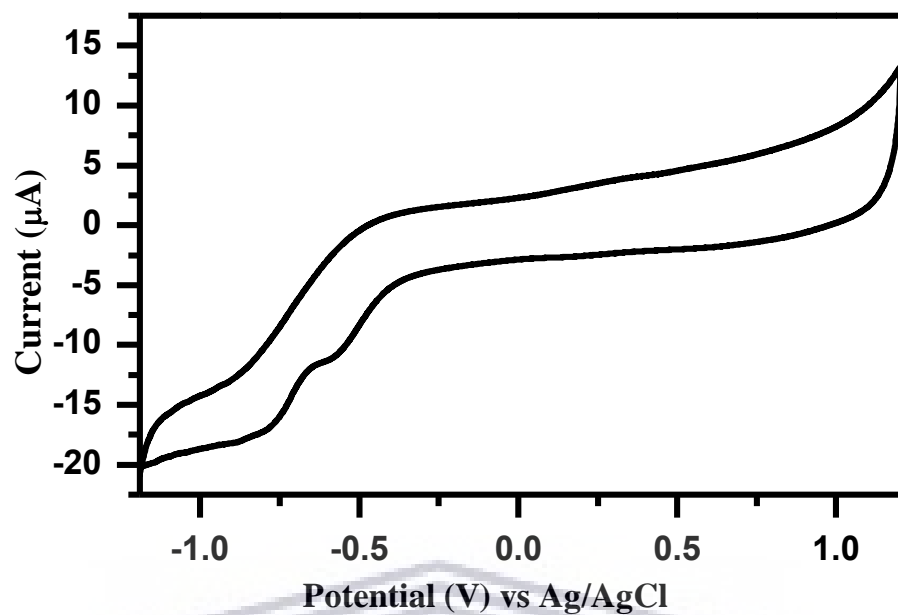
Figure 5.9: Glassy carbon electrode in 0.5 M tetrabutylammonium perchlorate at a scan

rate of 0.050 V/s between -1.20 V and +1.20 V vs Ag/AgCl.
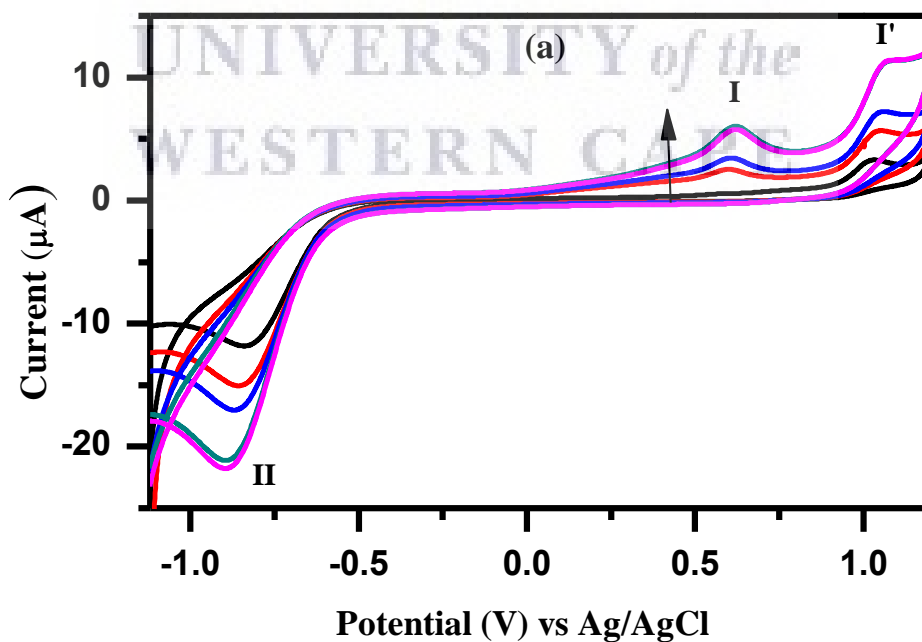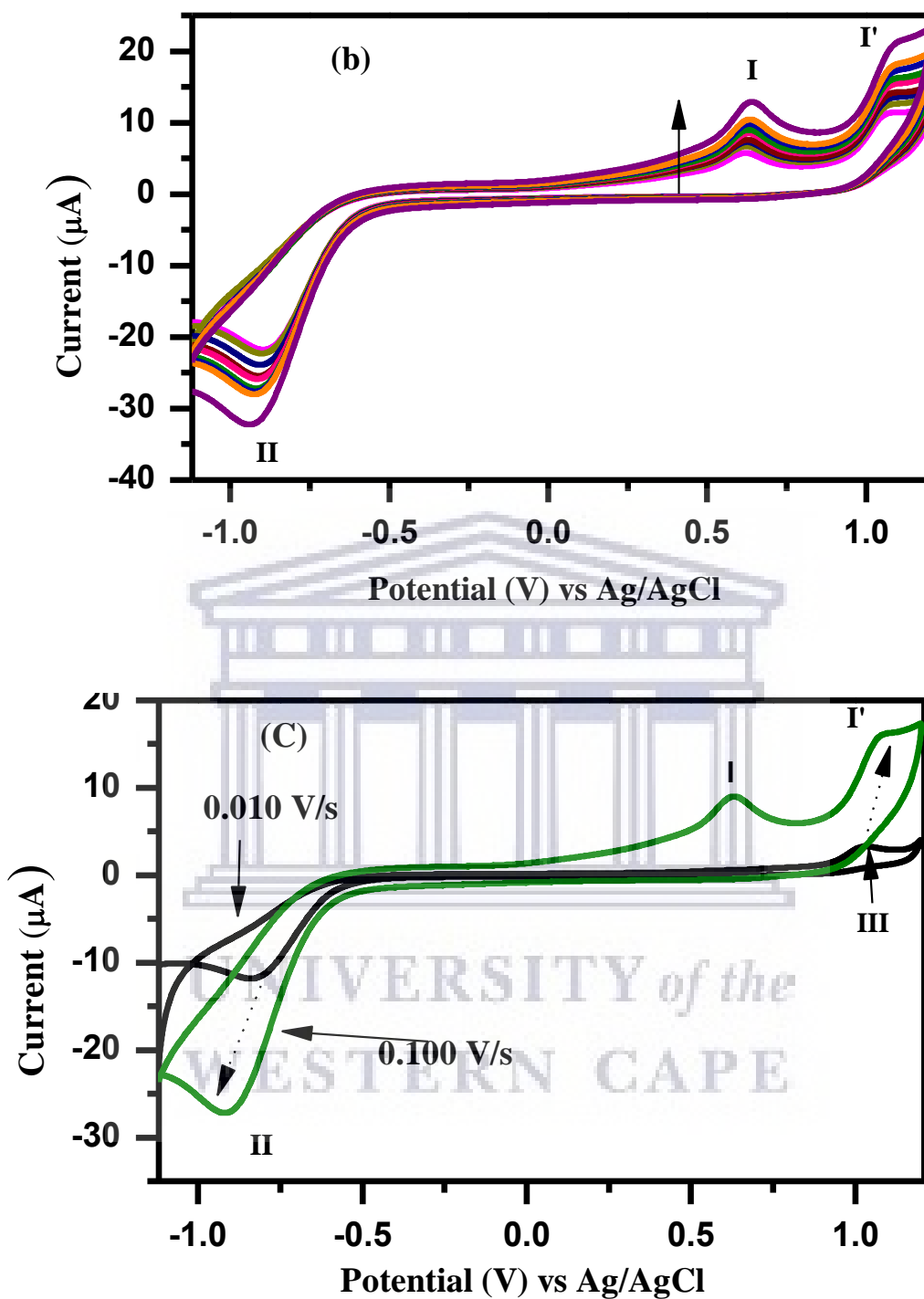
Figure 5.10: Cyclic voltammetry of carbon nanodots -decorated modified GCE between -
1.10 V and +1.10 V in 0.5 M tetrabutylammonium perchlorate at (a) lower
scan rates from 0.010 to 0.050 V/s and (b) higher scan rates from 0.050 to
0.130 V/s in increments of 0.01 V/s (black arrows indicate direction of scan

rate increase), (c) reveals response differences of the carbon nanodots -
decorated NIGS quantum dots (indicated by dashed blue arrows) at the
lowest scan rate (0.010 V/s) and highest scan rate (0.100 V/s).electrode in
0.5 M tetrabutylammonium perchlorate at a scan rate of 0.050 V/s between -
1.20 V and +1.20 V vs Ag/AgCl.
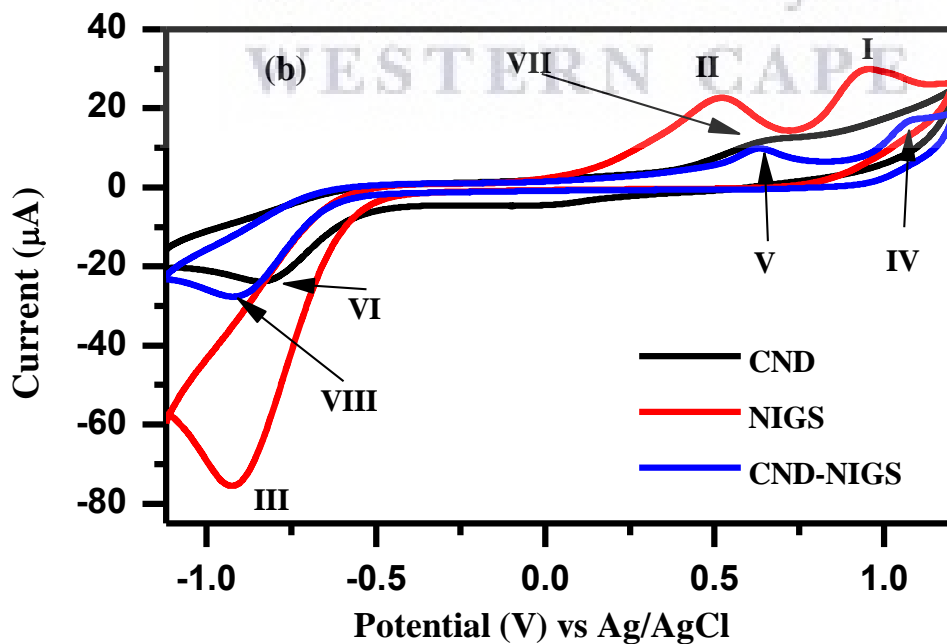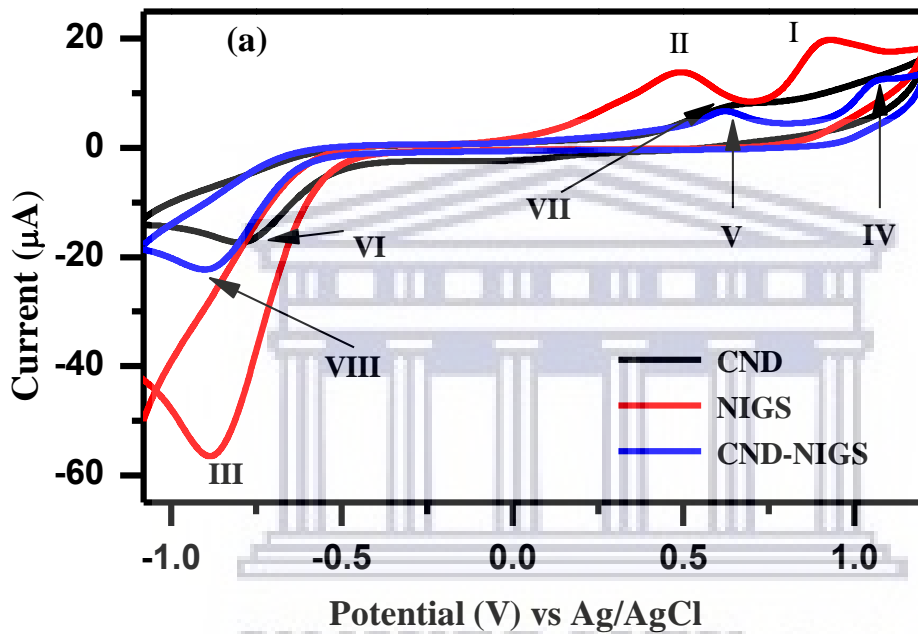
Figure 5.11: CV of carbon nanodots, NIGS quantum dots and carbon nanodots -decorated NIGS quantum dots prepared in 0.5 M tetrabutylammonium perchlorate at scan rates: (a) 0.050 V/s and (b) 0.100 V/s at -1.10 V and +1.10 V vs Ag/AgCl.

5.6 Conclusion

A novel class of nanomaterials known as carbon nanodots decorated nickel, indium, gallium, selenide (NIGS) quantum dots. These novel nanomaterials were prepared using microwave synthesis. All characterization techniques (morphological, optical, structural and electrochemical) showed significant changes and alterations that is due to the interactions between the carbon nanodots and NIGS quantum dots. Particularly, decoration of NIGS quantum dots with carbon nanodots yielded a nanocomposite with improved and enhanced the photophysics while the electrochemistry showed a slight decrease in current response.

The carbon nanodots decorated NIGS quantum exhibited good absorption in the visible region at a wavelength of 400 nm and 750 nm. The nanocomposite reveals maximum peak currents of 98 µA at 0.63 V and 17 µA at 1.0 V, when compared to 29 µA at and 35 µA exhibited by the NIGS quantum dots, respectively. Also, it is notable that these anodic peaks are both shifted towards higher potentials when compared to the pristine NIGS quantum dots where they respectively appear at 0.53 V and 0.95 V. This behaviour firmly confirms interaction between these two materials and the decrease in current response arises from the lower electrochemical activity of CNDs that exhibited a maximum peak current response of 10 µA at 0.6 V. Overall, the carbon nanodots-decorated NIGS quantum

dots had a low bandgap of 1.97 eV which indicates potential application of the nanocomposite in photovoltaic cells.

CHAPTER 6

6.1   Conclusion

In this study, a novel nanocomposite comprising photoluminescent carbon nanodots (CNDs) and quaternary quantum of nickel, indium, gallium and selenium (NIGS), was prepared for photophysical and electrochemical evaluation for future photovoltaic cell applications. The carbon nanodots were prepared from glucose, a readily available, biocompatible and environmentally friendly compound. In addition, the CNDs were prepared using the microwave technique which avoids most drawbacks associated with other conventional techniques that require, amongst others, high temperatures and strong reducing or oxidizing agents. The FT-IR spectrum was used to investigate the structural composition of the CNDs through which the characteristic O-H, C-O-C and C=O bands sourcing from the glucose precursor were identified. Spherical CNDs of diameters between 9-13 nm (from TEM analysis) and 15-20 nm (SAXS analysis using PDDF) absorbed ultraviolet light at 228 nm and 286 nm; with a wide band gap of 4.2 eV. The CNDs also exhibited intense photoluminescence with emission peaks at 445 nm and 636 nm. When cycled in tetrabutylammonium perchlorate at different scan rates, the CNDs showed an oxidation-reduction pair centered at 0.6 V and 0.01 V (vs Ag/AgCl). This pair was attributed to oxidation and reduction of the CNDs, respectively.

The NIGS quantum dots were prepared by solvothermal synthesis, the precursors used were environmentally benign. The spherical NIGS quantum dots with average diameter of 11.55 nm (from HRTEM analysis) and 18-55 nm from (from SAXS analysis) absorb light at 547 nm extending to 700 nm: with optical bandgap of 2.01 eV. The PL analysis revealed

that the NIGS quantum dots emit light at 397 nm. The NIGS quantum dots reveals maximum peak current at 29 µA and at 35 µA.

The carbon nanodots decorated NIGS quantum dots were synthesized using a green synthesis technique known as microwave synthesis which is a fast and cost effective technique. The carbon nanodots decorated NIGS quantum dots showed good absorption properties in the visible region of the solar spectrum at 400 nm and 750 nm: with a bandgap of 2.01 eV. The carbon nanodots decorated NIGS quantum dots exhibit maximum peak currents of 98 µA at 0.63 V and 17 µA at 1.0 V. it is notable that these anodic peaks are both shifted towards higher potentials when compared to the pristine NIGS quantum dots where they respectively appear at 0.53 V and 0.95 V. This behaviour firmly confirms interaction between these two materials and the decrease in current response arises from the lower electrochemical activity of CNDs that exhibited a maximum peak current response of 10 µA at 0.6 V. Overall, the carbon nanodots-decorated NIGS quantum dots had a low bandgap of 1.97 eV which indicates potential application of the nanocomposite in photovoltaic cells.

CHAPTER 7

7.1   References

[1]   E. Kabir, P. Kumar, S. Kumar, A.A. Adelodun, K.H. Kim, Solar energy: Potential and future prospects, Renew. Sustain. Energy Rev. 82 (2018) 894–900.

[2]   T. Blaschke, M. Biberacher, S. Gadocha, I. Schardinger, "Energy landscapes": Meeting energy demands and human aspirations, Biomass and Bioenergy. 55 (2013) 3–16.

[3]   I. Hanif, Impact of fossil fuels energy consumption, energy policies, and urban sprawl on carbon emissions in East Asia and the Pacific: A panel investigation, Energy Strateg. Rev. 21 (2018) 16–24.

[4]   M.-R. Gao, Y.-F. Xu, J. Jiang, S.-H. Yu, Nanostructured metal chalcogenides: synthesis, modification, and applications in energy conversion and storage devices, Chem. Soc. Rev. 42 (2013) 2986.

[5]   N. Abas, A. Kalair, N. Khan, Review of fossil fuels and future energy technologies, Futures. 69 (2015) 31–49.

[6]   S.E. Hosseini, M.A. Wahid, Hydrogen production from renewable and sustainable energy resources: Promising green energy carrier for clean development, Renew. Sustain. Energy Rev. 57 (2016) 850–866.

[7]   A. Gazheli, M. Antal, J. van den Bergh, The behavioral basis of policies fostering long-run transitions: Stakeholders, limited rationality and social context, Futures. 69

(2015) 14–30.

[8] C. Rühl, P. Appleby, J. Fennema, A. Naumov, M. Schaffer, Economic development and the demand for energy: A historical perspective on the next 20 years, Energy Policy. 50 (2012) 109–116.

[9] M. Bhattacharya, S.R. Paramati, I. Ozturk, S. Bhattacharya, The effect of renewable energy consumption on economic growth: Evidence from top 38 countries, Appl. Energy. 162 (2016) 733–741.

[10] L. Olatomiwa, S. Mekhilef, M.S. Ismail, M. Moghavvemi, Energy management strategies in hybrid renewable energy systems: A review, Renew. Sustain. Energy Rev. 62 (2016) 821–835.

[11] P. Bajpai, V. Dash, Hybrid renewable energy systems for power generation in stand-alone applications : A review, Renew. Sustain. Energy Rev. 16 (2012) 2926–2939.

[12] K.L. Sowers, Z. Hou, J.J. Peterson, B. Swartz, S. Pal, O. Prezhdo, T.D. Krauss, Photophysical properties of CdSe / CdS core / shell quantum dots with tunable surface composition, Chem. Phys. 471 (2016) 24–31.

[13] A.F. Palmstrom, P.K. Santra, S.F. Bent, Atomic layer deposition in nanostructured photovoltaics: tuning optical, electronic and surface properties, Nanoscale. 7 (2015) 12266–12283.

[14] R. Giridharagopal, P.A. Cox, D.S. Ginger, Functional scanning probe imaging of nanostructured solar energy materials, Acc. Chem. Res. 49 (2016) 1769–1776.

[15]   H.K. Jun, M.A. Careem, A.K. Arof, Quantum dot-sensitized solar cells — perspective and recent developments : A review of Cd chalcogenide quantum dots as sensitizers, Renew. Sustain. Energy Rev. 22 (2013) 148–167.

[16]   N.I. Ibrahim, F.A. Al-Sulaiman, F.N. Ani, Solar absorption systems with integrated absorption energy storage–A review, Renew. Sustain. Energy Rev. 82 (2018) 1602–1610.

[17]   F. Ongul, S. Aydin, C. Allahverdi, S. Bozar, M. Kazici, S. Gunes, Influences of CdSe NCs on the photovoltaic parameters of BHJ organic solar cells, Spectrochim. Acta Part A Mol. Biomol. Spectrosc. 194 (2018) 50–56.

[18]   A. Abubakar Mas'Ud, A.V. Wirba, F. Muhammad-Sukki, R. Albarracín, S.H. Abu-Bakar, A.B. Munir, N.A. Bani, A review on the recent progress made on solar photovoltaic in selected countries of sub-Saharan Africa, Renew. Sustain. Energy Rev. 62 (2016) 441–452.

[19]   C. Fant, C. Adam Schlosser, K. Strzepek, The impact of climate change on wind and solar resources in southern Africa, Appl. Energy. 161 (2016) 556–564.

[20]   X. Zheng, Y. Yang, S. Chen, L. Zhang, Slow photons for solar fuels, Chinese J. Catal. 39 (2018) 379–389.

[21]   E. Jalali-Moghadam, Z. Shariatinia, Quantum dot sensitized solar cells fabricated by means of a novel inorganic spinel nanoparticle, Appl. Surf. Sci. 441 (2018) 1–11.

[22]   S.K. Cushing, N. Wu, Progress and perspectives of plasmon-enhanced solar energy

conversion, J. Phys. Chem. Lett. 7 (2016) 666–675.

[23]   Z. Ahmad, M.A. Najeeb, R.A. Shakoor, S.A. Al-Muhtaseb, F. Touati, Limits and possible solutions in quantum dot organic solar cells, Renew. Sustain. Energy Rev. 82 (2018) 1551–1564.

[24]   A.K. Hussein, Applications of nanotechnology in renewable energies - A comprehensive overview and understanding, Renew. Sustain. Energy Rev. 42 (2015) 460–476.

[25]   Z. Abdin, M.A. Alim, R. Saidur, M.R. Islam, W. Rashmi, S. Mekhilef, A. Wadi, Solar energy harvesting with the application of nanotechnology, Renew. Sustain. Energy Rev. 26 (2013) 837–852.

[26]   J. Kim, J.L. Rivera, T.Y. Meng, B. Laratte, S. Chen, Review of life cycle assessment of nanomaterials in photovoltaics, Sol. Energy. 133 (2016) 249–258.

[27]   A.K. Hussein, Applications of nanotechnology in renewable energies — A comprehensive overview and understanding, Renew. Sustain. Energy Rev. 42 (2015) 460–476.

[28]   J. Baxter, Z. Bian, G. Chen, D. Danielson, M.S. Dresselhaus, A.G. Fedorov, T.S. Fisher, C.W. Jones, E. Maginn, U. Kortshagen, A. Manthiram, A. Nozik, D.R. Rolison, T. Sands, L. Shi, Y. Wu, Nanoscale design to enable the revolution in renewable energy, Energy Environ. Sci. 2 (2009) 559–588.

[29]   S. Chu, Y. Cui, N. Liu, The path towards sustainable energy, Nat. Mater. 16 (2016)

16–22.

[30] M.A. Green, S.P. Bremner, Energy conversion approaches and materials for high-efficiency photovoltaics, Nat. Mater. 16 (2016) 23–34.

[31] S. Abdelhady, M.S. Abd-Elhady, M.M. Fouad, An understanding of the operation of silicon photovoltaic panels, Energy Procedia. 113 (2017) 466–475.

[32] M.I.H. Ansari, A. Qurashi, M.K. Nazeeruddin, Frontiers, opportunities, and challenges in perovskite solar cells: A critical review, J. Photochem. Photobiol. C Photochem. Rev. 35 (2018) 1–24.

[33] V. Sugathan, E. John, K. Sudhakar, Recent improvements in dye sensitized solar cells: A review, Renew. Sustain. Energy Rev. 52 (2015) 54–64.

[34] H.L. Zhang, T. Van Gerven, J. Baeyens, J. Degrève, Photovoltaics: Reviewing the European feed-in-tariffs and changing PV efficiencies and costs, Sci. World J. 2014 (2014). doi:10.1155/2014/404913.

[35] B. Bajorowicz, M.P. Kobylański, A. Gołąbiewska, J. Nadolna, A. Zaleska-Medynska, A. Malankowska, Quantum dot-decorated semiconductor micro- and nanoparticles: A review of their synthesis, characterization and application in photocatalysis, Adv. Colloid Interface Sci. 256 (2018) 352–372.

[36] Y.A. Wu, J.H. Warner, Shape and property control of Mn doped ZnSe quantum dots : from branched to spherical, J. Mater. Chem. 22 (2012) 417–424.

[37] K. Wu, Y.S. Park, J. Lim, V.I. Klimov, Towards zero-threshold optical gain using

charged semiconductor quantum dots, Nat. Nanotechnol. 12 (2017) 1140–1147.

[38]   J.M. Pietryga, Y.S. Park, J. Lim, A.F. Fidler, W.K. Bae, S. Brovelli, V.I. Klimov, Spectroscopic and device aspects of nanocrystal quantum dots, Chem. Rev. 116 (2016) 10513–10622.

[39]   A.L. Efros, D.J. Nesbitt, Origin and control of blinking in quantum dots, Nat. Nanotechnol. 11 (2016) 661–671.

[40]   A. Manuscript, Nanoscale, (2014). doi:10.1039/C4NR05712K.

[41]   L. Hu, Z. Zhang, R.J. Patterson, Y. Hu, W. Chen, C. Chen, D. Li, C. Hu, C. Ge, Z. Chen, L. Yuan, C. Yan, N. Song, Z.L. Teh, G.J. Conibeer, J. Tang, S. Huang, Achieving high-performance PbS quantum dot solar cells by improving hole extraction through Ag doping, Nano Energy. 46 (2018) 212–219.

[42]   S. Pradhan, F. Di Stasio, Y. Bi, S. Gupta, S. Christodoulou, A. Stavrinadis, G. Konstantatos, High-efficiency colloidal quantum dot infrared light-emitting diodes via engineering at the supra-nanocrystalline level, Nat. Nanotechnol. 14 (2019) 72–79.

[43]   D. Vasudevan, R.R. Gaddam, A. Trinchi, I. Cole, Core-shell quantum dots: Properties and applications, J. Alloys Compd. 636 (2015) 395–404.

[44]   H. Ming, Z. Ma, Y. Liu, K. Pan, H. Yu, F. Wang, Z. Kang, Large scale electrochemical synthesis of high quality carbon nanodots and their photocatalytic property, Dalt. Trans. 41 (2012) 9526.

[45] D. Mo, L. Hu, G. Zeng, G. Chen, J. Wan, Z. Yu, Z. Huang, K. He, C. Zhang, M. Cheng, Cadmium-containing quantum dots: properties, applications, and toxicity, Appl. Microbiol. Biotechnol. 101 (2017) 2713–2733.

[46] A. Valizadeh, S. Mussa Farkhani, Review: three synthesis methods of CdX (X = Se, S or Te) quantum dots, IET Nanobiotechnology. 8 (2014) 59–76.

[47] S. Chand, N. Thakur, S.C. Katyal, P.B. Barman, V. Sharma, P. Sharma, Recent developments on the synthesis, structural and optical properties of chalcogenide quantum dots, Sol. Energy Mater. Sol. Cells. 168 (2017) 183–200.

[48] Y. Yen, Y. Lin, S. Chang, H. Hong, H. Tuan, Y. Chueh, Investigation of bulk hybrid heterojunction solar cells based on Cu(In,Ga)Se2 nanocrystals, Nanoscale Res. Lett. 8 (2013) 329.

[49] J.Y. Park, One pot solvothermal synthesis of colloidal Cu(In1-xGax)Se2(CIGS) quantum dots for solar cell applications, J. Alloys Compd. 629 (2015) 162–166.

[50] A.K. Shukla, K. Sudhakar, P. Baredar, A comprehensive review on design of building integrated photovoltaic system, Energy Build. 128 (2016) 99–110.

[51] H.J. Jeong, Y.C. Kim, S.K. Lee, J.H. Yun, J.H. Jang, Enhanced spectral response of CIGS solar cells with anti-reflective subwavelength structures and quantum dots, Sol. Energy Mater. Sol. Cells. 194 (2019) 177–183.

[52] Y. Meng, Y. Zhang, W. Sun, M. Wang, B. He, H. Chen, Q. Tang, Biomass converted carbon quantum dots for all-weather solar cells, Electrochim. Acta. 257

(2017) 259–266.

[53] D. Sharma, R. Jha, S. Kumar, Quantum dot sensitized solar cell: Recent advances and future perspectives in photoanode, Sol. Energy Mater. Sol. Cells. 155 (2016) 294–322.

[54] M. Liu, W. Chen, Green synthesis of silver nanoclusters supported on carbon nanodots: enhanced photoluminescence and high catalytic activity for oxygen reduction reaction, Nanoscale. 5 (2013) 12558.

[55] K. Dimos, Carbon quantum dots: Surface passivation and functionalization, Curr. Org. Chem. 20 (2016) 682–695.

[56] L. Wang, S.J. Zhu, H.Y. Wang, S.N. Qu, Y.L. Zhang, J.H. Zhang, Q.D. Chen, H.L. Xu, W. Han, B. Yang, H.B. Sun, Common origin of green luminescence in carbon nanodots and graphene quantum dots, ACS Nano. 8 (2014) 2541–2547.

[57] L. Xu, S. Yuan, H. Zeng, J. Song, A comprehensive review of doping in perovskite nanocrystals/quantum dots: evolution of structure, electronics, optics, and light-emitting diodes, Mater. Today Nano. 6 (2019) 100036.

[58] V. Nair, B. Ananthoju, J. Mohapatra, M. Aslam, Photon induced non-linear quantized double layer charging in quaternary semiconducting quantum dots, J. Colloid Interface Sci. 514 (2018) 452–458.

[59] A.A. Chistyakov, M.A. Zvaigzne, V.R. Nikitenko, A.R. Tameev, I.L. Martynov, O. V Prezhdo, Optoelectronic properties of semiconductor quantum dot solids for

photovoltaic applications, J. Phys. Chem. Lett. 8 (2017) 4129−4139.

[60]   A.P. Litvin, I. V. Martynenko, F. Purcell-Milton, A. V. Baranov, A. V. Fedorov, Y.K. Gun'ko, Colloidal quantum dots for optoelectronics, J. Mater. Chem. A. 5 (2017) 13252–13275.

[61]   Z. Yang, J.Z. Fan, A.H. Proppe, F.P.G. De Arquer, D. Rossouw, O. Voznyy, X. Lan, M. Liu, G. Walters, R. Quintero-bermudez, B. Sun, S. Hoogland, G.A. Botton, S.O. Kelley, E.H. Sargent, Mixed-quantum-dot solar cells, Nat. Commun. 8 (2017) 1325.

[62]   M. V Kovalenko, Opportunities and challenges for quantum dot photovoltaics, Nat. Publ. Gr. 10 (2015) 994–997.

[63]   L. Jethi, T.G. Mack, P. Kambhampati, Extending semiconductor nanocrystals from the quantum dot regime to the molecular cluster regime, J. Phys. Chem. C. 121 (2017) 26102–26107.

[64]   C.R. Kagan, C.B. Murray, Bandlike transport in strongly coupled and doped quantum dot solids: A route to high-performance thin-film electronics, Nat. Publ. Gr. 10 (2015) 1013–1026.

[65]   P. Senellart, G. Solomon, A. White, High-performance semiconductor quantum-dot single-photon sources, Nat. Nanotechnol. 12 (2017) 1026–1039.

[66]   T. Ba Hoang, J. Beetz, L. Midolo, M. Skacel, M. Lermer, M. Kamp, S. Höfling, L. Balet, N. Chauvin, A. Fiore, Enhanced spontaneous emission from quantum dots in short photonic crystal waveguides, Appl. Phys. Lett. 100 (2012) 061122.

[67]   C.J. Stolle, T.B. Harvey, D.R. Pernik, J.I. Hibbert, J. Du, D.J. Rhee, V.A. Akhavan, R.D. Schaller, B.A. Korgel, Multiexciton solar cells of CuInSe 2 nanocrystals, J. Phys. Chem. Lett. 5 (2014) 304–309.

[68]   E. Lhuillier, S. Pedetti, S. Ithurria, B. Nadal, H. Heuclin, B. Dubertret, Two-Dimensional colloidal metal chalcogenides semiconductors: Synthesis, spectroscopy, and applications, Acc. Chem. Res. 48 (2015) 22–30.

[69]   D. Kim, Y.K. Lee, D. Lee, W.D. Kim, W.K. Bae, D.C. Lee, Colloidal dual-diameter and core-position-controlled core/shell cadmium chalcogenide nanorods, ACS Nano. 11 (2017) 12461–12472.

[70]   O. Stroyuk, A. Raevskaya, N. Gaponik, Solar light harvesting with multinary metal chalcogenide nanocrystals, Chem. Soc. Rev. 47 (2018) 5354–5422.

[71]   L. Piveteau, T. Ong, A.J. Rossini, L. Emsley, M. V Kovalenko, Structure of colloidal quantum dots from dynamic nuclear polarization surface enhanced NMR spectroscopy, J. Am. Chem. Soc. 137 (2015) 13964–13971.

[72]   S. Dias, K. Kumawat, S. Biswas, S.B. Krupanidhi, Solvothermal synthesis of Cu 2 SnS 3 quantum dots and their application in near-infrared photodetectors, Inorg. Chem. 56 (2017) 2198–2203.

[73]   S.Y. Ã, T. Yoon, K. Lee, S. Yoon, J.M. Ha, S. Choe, Solar energy materials & solar cells nanoparticle-based approach for the formation of CIS solar cells, Sol. Energy Mater. Sol. Cells. 93 (2009) 783–788.

[74] A.J. Nozik, Multiple exciton generation in semiconductor quantum dots, Chem. Phys. Lett. J. 457 (2008) 3–11.

[75] N. Siemons, A. Serafini, Multiple exciton generation in nanostructures for advanced, J. Nanotechnol. 2018 (2018) 1–12.

[76] H. Goodwin, T.C. Jellicoe, N.J.L.K. Davis, M.L. Böhm, Review article Multiple exciton generation in quantum dot-based solar cells, 7 (2018) 111–126.

[77] F. Bertolotti, D.N. Dirin, M. Ibáñez, F. Krumeich, A. Cervellino, R. Frison, O. Voznyy, E.H. Sargent, M. V. Kovalenko, A. Guagliardi, N. Masciocchi, Crystal symmetry breaking and vacancies in colloidal lead chalcogenide quantum dots, Nat. Mater. 15 (2016) 987–994.

[78] S. Zhu, Y. Song, J. Wang, H. Wan, Y. Zhang, Y. Ning, B. Yang, Photoluminescence mechanism in graphene quantum dots: Quantum confinement effect and surface/edge state, Nano Today. 13 (2017) 10–14.

[79] Y. Kim, E. Yassitepe, O. Voznyy, R. Comin, G. Walters, X. Gong, P. Kanjanaboos, A.F. Nogueira, E.H. Sargent, Efficient luminescence from perovskite quantum dot solids, ACS Appl. Mater. Interfaces. 7 (2015) 25007–25013.

[80] D.H. Jara, K.G. Stamplecoskie, P. V. Kamat, Two distinct transitions in CuxInS2 quantum dots. bandgap versus sub-bandgap excitations in copper-deficient structures, J. Phys. Chem. Lett. 7 (2016) 1452–1459.

[81] K. Surana, R.M. Mehra, B. Bhattacharya, H. Rhee, A. Reddy, P.K. Singh, A

comprehensive study of chalcogenide quantum dot sensitized solar cells with a new solar cell exceeding 1 V output, 52 (2015) 1083–1092.

[82]   O. Adegoke, T. Nyokong, P.B.C. Forbes, Photophysical properties of a series of alloyed and non-alloyed water-soluble L-cysteine-capped core quantum dots, J. Alloys Compd. 695 (2017) 1354–1361.

[83]   C. Mongin, P. Moroz, M. Zamkov, F.N. Castellano, Thermally activated delayed photoluminescence from pyrenyl-functionalized CdSe quantum dots, Nat. Chem. 10 (2018) 225–230.

[84]   H. Lu, G.M. Carroll, N.R. Neale, M.C. Beard, Infrared quantum dots: Progress, challenges, and opportunities, ACS Nano. 13 (2019) 939–953.

[85]   A. Zhu, Q. Qu, X. Shao, B. Kong, Y. Tian, Carbon-dot-based dual-emission nanohybrid produces a ratiometric fluorescent sensor for in vivo imaging of cellular copper ions, Angew. Chemie - Int. Ed. 51 (2012) 7185–7189.

[86]   P.K. Bajpai, S. Yadav, A. Tiwari, H.S. Virk, Recent advances in the synthesis and characterization of chalcogenide nanoparticles, 222 (2015) 187–233.

[87]   X. Ji, W. Wang, H. Mattoussi, Controlling the spectroscopic properties of quantum dots via energy transfer and charge transfer interactions: Concepts and applications, Nano Today. 11 (2016) 98–121.

[88]   F. Mirnajafizadeh, D. Ramsey, S. McAlpine, F. Wang, P. Reece, J.A. Stride, Hydrothermal synthesis of highly luminescent blue-emitting ZnSe(S) quantum dots

exhibiting low toxicity, Mater. Sci. Eng. C. 64 (2016) 167–172.

[89] X. Hu, T. Chen, Y. Xu, M. Wang, W. Jiang, W. Jiang, Hydrothermal synthesis of bright and stable AgInS2 quantum dots with tunable visible emission, J. Lumin. 200 (2018) 189–195.

[90] J.K. Cooper, A.M. Franco, S. Gul, C. Corrado, J.Z. Zhang, Characterization of Primary Amine Capped CdSe , ZnSe , and ZnS Quantum Dots by FT-IR : Determination of Surface Bonding Interaction and Identification of Selective Desorption, Langmuir. 27 (2011) 8486–8493.

[91] C. Wang, K. Yang, X. Wei, S. Ding, F. Tian, F. Li, One-pot solvothermal synthesis of carbon dots/Ag nanoparticles/TiO2 nanocomposites with enhanced photocatalytic performance, Ceram. Int. 44 (2018) 22481–22488.

[92] R. Gedye, F. Smith, K. Westaway, H. Ali, L. Baldisera, L. Laberge, J. Rousell, The use of microwave ovens for rapid organic synthesis, Tetrahedron Lett. 27 (1986) 279–282.

[93] A.C. Lokhande, K. V. Gurav, E. Jo, C.D. Lokhande, J.H. Kim, Chemical synthesis of Cu2SnS3 (CTS) nanoparticles: A status review, J. Alloys Compd. 656 (2016) 295–310.

[94] K.M. Omer, M. Sartin, Dual-mode colorimetric and fluorometric probe for ferric ion detection using N-doped carbon dots prepared via hydrothermal synthesis followed by microwave irradiation, Opt. Mater. (Amst). 94 (2019) 330–336.

[95] H. Yang, L. He, Y. Long, H. Li, S. Pan, H. Liu, X. Hu, Fluorescent carbon dots synthesized by microwave-assisted pyrolysis for chromium(VI) and ascorbic acid sensing and logic gate operation, Spectrochim. Acta - Part A Mol. Biomol. Spectrosc. 205 (2018) 12–20.

[96] H. Li, F.Q. Shao, H. Huang, J.J. Feng, A.J. Wang, Eco-friendly and rapid microwave synthesis of green fluorescent graphitic carbon nitride quantum dots for vitro bioimaging, Sensors Actuators, B Chem. 226 (2016) 506–511.

[97] J. Duan, J. Yu, S. Feng, L. Su, A rapid microwave synthesis of nitrogen-sulfur co-doped carbon nanodots as highly sensitive and selective fluorescence probes for ascorbic acid, Talanta. 153 (2016) 332–339.

[98] H. Liu, Z. He, L.P. Jiang, J.J. Zhu, Microwave-assisted synthesis of wavelength-tunable photoluminescent carbon nanodots and their potential applications, ACS Appl. Mater. Interfaces. 7 (2015) 4913–4920.

[99] S. Thambiraj, D.R. Shankaran, Green synthesis of highly fluorescent carbon quantum dots from sugarcane bagasse pulp, Appl. Surf. Sci. 390 (2016) 435–443.

[100] Z. Zhang, W. Sun, P. Wu, Highly photoluminescent carbon dots derived from egg white: facile and green synthesis, photoluminescence properties, and multiple applications, ACS Sustain. Chem. Eng. 3 (2015) 1412–1418.

[101] L. Al Juhaiman, L. Scoles, D. Kingston, B. Patarachao, D. Wang, F. Bensebaa, Green synthesis of tunable Cu(In1−xGax)Se2 nanoparticles using non-organic solvents, Green Chem. 12 (2010) 1248.

[102] C.C. Villarreal, T. Pham, P. Ramnani, A. Mulchandani, Carbon allotropes as sensors for environmental monitoring, Curr. Opin. Electrochem. 3 (2017) 106–113.

[103] V. Ţucureanu, A. Matei, A.M. Avram, FTIR spectroscopy for carbon family study, Crit. Rev. Anal. Chem. 46 (2016) 502–520.

[104] A.A. Kokorina, E.S. Prikhozhdenko, N. V. Tarakina, A. V. Sapelkin, G.B. Sukhorukov, I.Y. Goryacheva, Dispersion of optical and structural properties in gel column separated carbon nanoparticles, Carbon N. Y. 127 (2018) 541–547.

[105] A.B. Siddique, A.K. Pramanick, S. Chatterjee, M. Ray, Amorphous carbon dots and their remarkable ability to detect, Sci. Rep. 8 (2018) 1–10.

[106] J.X. Zheng, X.H. Liu, Y.Z. Yang, X.G. Liu, B.S. Xu, Rapid and green synthesis of fluorescent carbon dots from starch for white light-emitting diodes, New Carbon Mater. 33 (2018) 276–288.

[107] I.Y. Goryacheva, A. V. Sapelkin, G.B. Sukhorukov, Carbon nanodots: Mechanisms of photoluminescence and principles of application, TrAC - Trends Anal. Chem. 90 (2017) 27–37.

[108] V. Strauss, J.T. Margraf, T. Clark, D.M. Guldi, A carbon–carbon hybrid – immobilizing carbon nanodots onto carbon nanotubes, Chem. Sci. 6 (2015) 6878–6885.

[109] V. Strauss, A. Kahnt, E.M. Zolnhofer, K. Meyer, H. Maid, C. Placht, W. Bauer, T.J. Nacken, W. Peukert, S.H. Etschel, M. Halik, D.M. Guldi, Assigning electronic

states in carbon nanodots, Adv. Funct. Mater. 26 (2016) 7975–7985.

[110] A. Sciortino, E. Marino, B. Van Dam, P. Schall, M. Cannas, F. Messina, Solvatochromism unravels the emission mechanism of carbon nanodots, J. Phys. Chem. Lett. 7 (2016) 3419–3423.

[111] L. Bao, C. Liu, Z.L. Zhang, D.W. Pang, Photoluminescence-tunable carbon nanodots: Surface-state energy-gap tuning, Adv. Mater. 27 (2015) 1663–1667.

[112] W. Kwon, S. Do, J.H. Kim, M.S. Jeong, S.W. Rhee, Control of photoluminescence of carbon nanodots via surface functionalization using para-substituted anilines, Sci. Rep. 5 (2015) 1–10.

[113] F. Arcudi, L. Dordevic, M. Prato, Synthesis, separation, and characterization of small and highly fluorescent nitrogen-doped carbon nanodots, Angew. Chemie - Int. Ed. 55 (2016) 2107–2112.

[114] H. Wang, C. Sun, X. Chen, Y. Zhang, V.L. Colvin, Q. Rice, J. Seo, S. Feng, S. Wang, W.W. Yu, Excitation wavelength independent visible color emission of carbon dots, Nanoscale. 9 (2017) 1909–1915.

[115] Y. Park, J. Yoo, B. Lim, W. Kwon, S.W. Rhee, Improving the functionality of carbon nanodots: Doping and surface functionalization, J. Mater. Chem. A. 4 (2016) 11582–11603.

[116] S. Tao, S. Zhu, T. Feng, C. Xia, Y. Song, B. Yang, The polymeric characteristics and photoluminescence mechanism in polymer carbon dots: A review, Mater. Today

Chem. 6 (2017) 13–25.

[117] C. López, M. Zougagh, M. Algarra, E. Rodríguez-Castellón, B.B. Campos, J.C.G. Esteves Da Silva, J. Jiménez-Jiménez, A. Ríos, Microwave-assisted synthesis of carbon dots and its potential as analysis of four heterocyclic aromatic amines, Talanta. 132 (2015) 845–850.

[118] S.Y. Park, N. Thongsai, A. Chae, S. Jo, E.B. Kang, P. Paoprasert, S.Y. Park, I. In, Microwave-assisted synthesis of luminescent and biocompatible lysine-based carbon quantum dots, J. Ind. Eng. Chem. 47 (2017) 329–335.

[119] S. Simsek, M. Ozge Alas, B. Ozbek, R. Genc, Evaluation of the physical properties of fluorescent carbon nanodots synthesized using Nerium oleander extracts by microwave-assisted synthesis methods, J. Mater. Res. Technol. 8 (2019) 2721–2731.

[120] N. Marinova, S. Valero, J.L. Delgado, Organic and perovskite solar cells: Working principles, materials and interfaces, J. Colloid Interface Sci. 488 (2017) 373–389.

[121] K. Wang, Y. Shi, L. Gao, R. Chi, K. Shi, B. Guo, L. Zhao, T. Ma, W(Nb)O x -based efficient flexible perovskite solar cells: From material optimization to working principle, Nano Energy. 31 (2017) 424–431.

[122] P. Huen, W.A. Daoud, Advances in hybrid solar photovoltaic and thermoelectric generators, Renew. Sustain. Energy Rev. 72 (2017) 1295–1302.

[123] Ö. Birel, S. Nadeem, H. Duman, Porphyrin-based dye-sensitized solar cells (DSSCs): a review, J. Fluoresc. 27 (2017) 1075–1085.

[124] P. Reineck, D. Brick, P. Mulvaney, U. Bach, Plasmonic hot electron solar cells: The effect of nanoparticle size on quantum efficiency, J. Phys. Chem. Lett. 7 (2016) 4137–4141.

[125] X. Lan, O. Voznyy, F.P. García De Arquer, M. Liu, J. Xu, A.H. Proppe, G. Walters, F. Fan, H. Tan, M. Liu, Z. Yang, S. Hoogland, E.H. Sargent, 10.6% certified colloidal quantum dot solar cells via solvent-polarity-engineered halide passivation, Nano Lett. 16 (2016) 4630–4634.

[126] J. Du, Z. Du, J.S. Hu, Z. Pan, Q. Shen, J. Sun, D. Long, H. Dong, L. Sun, X. Zhong, L.J. Wan, Zn-Cu-In-Se quantum dot solar cells with a certified power conversion efficiency of 11.6%, J. Am. Chem. Soc. 138 (2016) 4201–4209.

[127] A.J. Labelle, S.M. Thon, S. Masala, M.M. Adachi, H. Dong, M. Farahani, A.H. Ip, A. Fratalocchi, E.H. Sargent, Colloidal quantum dot solar cells exploiting hierarchical structuring, Nano Lett. 15 (2015) 1101–1108.

[128] M. Yuan, M. Liu, E.H. Sargent, Colloidal quantum dot solids for solution-processed solar cells, Nat. Energy. 1 (2016).

[129] D.K. Ko, A. Maurano, S.K. Suh, D. Kim, G.W. Hwang, J.C. Grossman, V. Bulović, M.G. Bawendi, Photovoltaic performance of PbS quantum dots treated with metal salts, ACS Nano. 10 (2016) 3382–3388.

[130] K. Zhao, Z. Pan, X. Zhong, Charge recombination control for high efficiency quantum dot sensitized solar cells, J. Phys. Chem. Lett. 7 (2016) 406–417.

[131] R. Azmi, S.H. Oh, S.Y. Jang, High-efficiency colloidal quantum dot photovoltaic devices using chemically modified heterojunctions, ACS Energy Lett. 1 (2016) 100–106.

[132] Z. Ren, J. Wang, Z. Pan, K. Zhao, H. Zhang, Y. Li, Y. Zhao, I. Mora-Sero, J. Bisquert, X. Zhong, Amorphous TiO 2 buffer layer boosts efficiency of quantum dot sensitized solar cells to over 9%, Chem. Mater. 27 (2015) 8398–8405.

[133] P. V. Kamat, Quantum dot solar cells. The next big thing in photovoltaics, J. Phys. Chem. Lett. 4 (2013) 908–918.

[134] W.A. Badawy, A review on solar cells from Si-single crystals to porous materials and quantum dots, J. Adv. Res. 6 (2015) 123–132.

[135] A.S. Fuhr, H.J. Yun, N.S. Makarov, H. Li, H. McDaniel, V.I. Klimov, Light emission mechanisms in CuInS2 quantum dots evaluated by spectral electrochemistry, ACS Photonics. 4 (2017) 2425–2435.

[136] Y. Li, N. Chopra, Graphene encapsulated gold nanoparticle-quantum dot heterostructures and their electrochemical characterization, Appl. Surf. Sci. 344 (2015) 27–32.

[137] J. Bae, U. Paik, D. Kee Yi, Novel semiconducting CdSe quantum dot based electrochemical capacitors, Mater. Lett. 162 (2016) 230–234.

[138] A.W. Anwar, A. Majeed, N. Iqbal, W. Ullah, A. Shuaib, U. Ilyas, F. Bibi, H.M. Rafique, Specific capacitance and cyclic stability of graphene based metal/metal

oxide nanocomposites: A review, J. Mater. Sci. Technol. 31 (2015) 699–707.

[139] Y. Aniskevich, A. Antanovich, A. Prudnikau, M. V. Artemyev, A. V. Mazanik, G. Ragoisha, E.A. Streltsov, Underpotential deposition of cadmium on colloidal CdSe quantum Dots: effect of particle size and surface ligands, J. Phys. Chem. C. 123 (2019) 931–939.

[140] A. Manjceevan, J. Bandara, Systematic stacking of PbS/CdS/CdSe multi-layered quantum dots for the enhancement of solar cell efficiency by harvesting wide solar spectrum, Electrochim. Acta. 271 (2018) 567–575.

[141] Y. Pu, F. Cai, D. Wang, J.X. Wang, J.F. Chen, Colloidal Synthesis of semiconductor quantum dots toward large-scale production: A review, Ind. Eng. Chem. Res. 57 (2018) 1790–1802.

[142] J.P. Patterson, P. Abellan, M.S. Denny, C. Park, N.D. Browning, S.M. Cohen, J.E. Evans, N.C. Gianneschi, Observing the growth of metal-organic frameworks by in situ liquid cell transmission electron microscopy, J. Am. Chem. Soc. 137 (2015) 7322–7328.

[143] Z. Dang, J. Shamsi, F. Palazon, M. Imran, Q.A. Akkerman, S. Park, G. Bertoni, M. Prato, R. Brescia, L. Manna, In situ transmission electron microscopy study of electron beam-induced transformations in colloidal cesium lead halide perovskite nanocrystals, ACS Nano. 11 (2017) 2124–2132.

[144] F.C.J.M. Van Veggel, Near-infrared quantum dots and their delicate synthesis, challenging characterization, and exciting potential applications, Chem. Mater. 26

(2014) 111–122.

[145] J.A. Sichert, Y. Tong, N. Mutz, M. Vollmer, S. Fischer, K.Z. Milowska, R. García Cortadella, B. Nickel, C. Cardenas-Daw, J.K. Stolarczyk, A.S. Urban, J. Feldmann, Quantum size effect in organometal halide perovskite nanoplatelets, Nano Lett. 15 (2015) 6521–6527.

[146] J.K. Sim, S. Kang, R. Nandi, J.Y. Jo, K.U. Jeong, C.R. Lee, Implementation of graphene as hole transport electrode in flexible CIGS solar cells fabricated on Cu foil, Sol. Energy. 162 (2018) 357–363.

[147] T.A. Swift, M. Duchi, S.A. Hill, D. Benito-Alifonso, R.L. Harniman, S. Sheikh, S.A. Davis, A.M. Seddon, H.M. Whitney, M.C. Galan, T.A.A. Oliver, Surface functionalisation significantly changes the physical and electronic properties of carbon nano-dots, Nanoscale. 10 (2018) 13908–13912.

[148] A.A. Bunaciu, E. gabriela Udriștioiu, H.Y. Aboul-Enein, X-ray diffraction: Instrumentation and applications, Crit. Rev. Anal. Chem. 45 (2015) 289–299.

[149] I.A. Mir, K. Rawat, H.B. Bohidar, Room temperature synthesis of fluorescent band gap tunable Cu1In1 − xGaxSe2.5 nanocrystals, Colloids Surfaces A Physicochem. Eng. Asp. 509 (2016) 182–189.

[150] B.L. Caetano, V. Briois, S.H. Pulcinelli, F. Meneau, C. V. Santilli, Revisiting the ZnO Q-dot formation toward an integrated growth model: From coupled time resolved UV-Vis/SAXS/XAS data to multivariate analysis, J. Phys. Chem. C. 121 (2017) 886–895.

[151] Y. Tian, A. Kelarakis, L. Li, F. Zhao, Y. Wang, W. Wang, Q. Yang, Z. Ye, X. Guo, Facile fluorescence "turn on" sensing of lead ions in water via carbon nanodots immobilized in spherical polyelectrolyte brushes, Front. Chem. 6 (2018).

[152] J. Maes, N. Castro, K. De Nolf, W. Walravens, B. Abécassis, Z. Hens, Size and concentration determination of colloidal nanocrystals by small-angle X-ray scattering, Chem. Mater. 30 (2018) 3952–3962.

[153] X. Hu, Y. Li, J. Tian, H. Yang, H. Cui, Highly efficient full solar spectrum (UV-vis-NIR) photocatalytic performance of Ag2S quantum dot/TiO2 nanobelt heterostructures, J. Ind. Eng. Chem. 45 (2017) 189–196.

[154] D.W. Jeong, J.Y. Park, H.W. Seo, N.V. Myung, T.Y. Seong, B.S. Kim, One-pot synthesis of gradient interface quaternary ZnCdSSe quantum dots, Appl. Surf. Sci. 415 (2017) 19–23.

[155] J.H. Kim, B.Y. Kim, E.P. Jang, S.Y. Yoon, K.H. Kim, Y.R. Do, H. Yang, Synthesis of widely emission-tunable Ag-Ga-S and its quaternary derivative quantum dots, Chem. Eng. J. 347 (2018) 791–797.

[156] O. Zandi, A. Agrawal, A.B. Shearer, L.C. Reimnitz, C.J. Dahlman, C.M. Staller, D.J. Milliron, Impacts of surface depletion on the plasmonic properties of doped semiconductor nanocrystals, Nat. Mater. 17 (2018) 710–717.

[157] Y. Liu, X. Tang, M. Deng, T. Zhu, Y. Bai, D. Qu, X. Huang, F. Qiu, One-step aqueous synthesis of highly luminescent hydrophilic AgInZnS quantum dots, J. Lumin. 202 (2018) 71–76.

[158] K. Hola, Y. Zhang, Y. Wang, E.P. Giannelis, R. Zboril, A.L. Rogach, Carbon dots - emerging light emitters for bioimaging, cancer therapy and optoelectronics, Nano Today. 9 (2014) 590–603.

[159] P. Namdari, B. Negahdari, A. Eatemadi, Synthesis, properties and biomedical applications of carbon-based quantum dots: An updated review, Biomed. Pharmacother. 87 (2017) 209–222.

[160] H. Xu, X. Yang, G. Li, C. Zhao, X. Liao, Green synthesis of fluorescent carbon dots for selective detection of tartrazine in food samples, J. Agric. Food Chem. 63 (2015) 6707–6714.

[161] S.-Y. Song, K.-K. Liu, J.-Y. Wei, Q. Lou, Y. Shang, C.-X. Shan, Deep-ultraviolet emissive carbon nanodots, Nano Lett. 19 (2019) 5553–5561.

[162] Z. Kang, Y. Liu, J. Gao, M. Zhu, Advances, challenges and promises of carbon dots, Inorg. Chem. Front. 4 (2017) 1963–1986.

[163] L. Sai, X. Wang, Q. Chang, W. Shi, L. Huang, Selective determination of acetone by carbon nanodots based on inner filter effect, Spectrochim. Acta - Part A Mol. Biomol. Spectrosc. 216 (2019) 290–295.

[164] S. Wang, Y. Zhu, B. Liu, C. Wang, R. Ma, Introduction of carbon nanodots into SnO2 electron transport layer for efficient and UV stable planar perovskite solar cells, J. Mater. Chem. A. 7 (2019) 5353–5362.

[165] T. Yoshinaga, Y. Iso, T. Isobe, Particulate , structural , and optical properties of D-

glucose-derived Carbon dots synthesized by microwave-assisted hydrothermal treatment, J. Solid State Sci. Technol. 7 (2018) 3034–3039.

[166] T. Yoshinaga, Y. Iso, T. Isobe, Optimizing the microwave-assisted hydrothermal synthesis of blue-emitting L-cysteine-derived carbon dots, J. Lumin. 213 (2019) 6–14.

[167] L. Đorđević, F. Arcudi, M. Prato, Preparation, functionalization and characterization of engineered carbon nanodots, Nat. Protoc. 14 (2019) 2931–2953.

[168] P.M. Gharat, H. Pal, S. Dutta Choudhury, Photophysics and luminescence quenching of carbon dots derived from lemon juice and glycerol, Spectrochim. Acta - Part A Mol. Biomol. Spectrosc. 209 (2019) 14–21.

[169] Z.C. Su, H.G. Ye, Z. Xiong, Q. Lou, Z. Zhang, F. Tang, J.Y. Tang, J.Y. Dai, C.X. Shan, S.J. Xu, Understanding and manipulating luminescence in carbon nanodots, Carbon N. Y. 126 (2018) 58–64.

[170] N. Papaioannou, A. Marinovic, N. Yoshizawa, A.E. Goode, M. Fay, A. Khlobystov, M.M. Titirici, A. Sapelkin, Structure and solvents effects on the optical properties of sugar-derived carbon nanodots, Sci. Rep. 8 (2018) 1–10.

[171] Y. Kamura, K. Imura, Space-selective fabrication of light-emitting carbon dots in polymer films using electron-beam-induced chemical reactions, ACS Omega. 4 (2019) 3380–3384.

[172] N. Mas, J.L. Hueso, G. Martinez, A. Madrid, R. Mallada, M.C. Ortega-Liebana, C.

Bueno-Alejo, J. Santamaria, Laser-driven direct synthesis of carbon nanodots and application as sensitizers for visible-light photocatalysis, Carbon N. Y. 156 (2020) 453–462.

[173] A. Sciortino, M. Gazzetto, G. Buscarino, R. Popescu, R. Schneider, G. Giammona, D. Gerthsen, E.J. Rohwer, N. Mauro, T. Feurer, A. Cannizzo, F. Messina, Disentangling size effects and spectral inhomogeneity in carbon nanodots by ultrafast dynamical hole-burning, Nanoscale. 10 (2018) 15317–15323.

[174] J. Manioudakis, F. Victoria, C.A. Thompson, L. Brown, M. Movsum, R. Lucifero, R. Naccache, Effects of nitrogen-doping on the photophysical properties of carbon dots, J. Mater. Chem. C. 7 (2019) 853–862.

[175] Z.L. Wu, Z.X. Liu, Y.H. Yuan, Carbon dots: materials, synthesis, properties and approaches to long-wavelength and multicolor emission, J. Mater. Chem. B. 5 (2017) 3794–3809.

[176] Y. Tian, L. Li, X. Guo, A. Wójtowicz, L. Estevez, M.J. Krysmann, A. Kelarakis, Dramatic photoluminescence quenching in carbon dots induced by cyclic voltammetry, Chem. Commun. 54 (2018) 9067–9070.

[177] Z. Du, Z. Pan, F. Fabregat-Santiago, K. Zhao, D. Long, H. Zhang, Y. Zhao, X. Zhong, J.S. Yu, J. Bisquert, Carbon counter-electrode-based quantum-dot-sensitized solar cells with certified efficiency exceeding 11%, J. Phys. Chem. Lett. 7 (2016) 3103–3111.

[178] S. Yu, Y. Gong, J. Jiang, S. Wu, W. Yan, X. Li, W. Huang, H. Xin, Over 10%

efficient CuIn(S,Se) 2 solar cells fabricated from environmentally benign solution in air, Sol. RRL. 3 (2019) 1900052.

[179]   L. Chen, W. Tian, L. Min, F. Cao, L. Li, Si/CuIn 0.7 Ga 0.3 Se 2 core–shell heterojunction for sensitive and self-driven UV–vis–NIR broadband photodetector, Adv. Opt. Mater. 7 (2019) 1–10.

[180]   M. Langenhorst, B. Sautter, R. Schmager, J. Lehr, E. Ahlswede, M. Powalla, U. Lemmer, B.S. Richards, U.W. Paetzold, Energy yield of all thin-film perovskite/CIGS tandem solar modules, Prog. Photovoltaics Res. Appl. 27 (2019) 290–298.

[181]   A. Khorasani, M. Marandi, R. Khosroshahi, M. Malekshahi Byranvand, M. Dehghani, A.I. Zad, F. Tajabadi, N. Taghavinia, Optimization of CuIn1-XGaXS2 nanoparticles and their application in the hole-transporting layer of highly efficient and stable mixed-halide perovskite solar cells, ACS Appl. Mater. Interfaces. 11 (2019) 30838–30845.

[182]   A. Attanzio, A. Sapelkin, F. Gesuele, A. van der Zande, W.P. Gillin, M. Zheng, M. Palma, Carbon nanotube-quantum dot nanohybrids: Coupling with single-particle control in aqueous solution, Small. 13 (2017) 1–5.

[183]   Y. Li, H. Lin, J. Zeng, J. Chen, H. Chen, Enhance short-wavelength response of CIGS solar cell by CdSe quantum disks as luminescent down-shifting material, Sol. Energy. 193 (2019) 303–308.

[184]   R. Marin, A. Vivian, A. Skripka, A. Migliori, V. Morandi, F. Enrichi, F. Vetrone, P.

Ceroni, C. Aprile, P. Canton, Mercaptosilane-passivated CuInS2 quantum dots for luminescence thermometry and luminescent labels, ACS Appl. Nano Mater. 2 (2019) 2426–2436.

[185] D.W. Houck, E.I. Assaf, H. Shin, R.M. Greene, D.R. Pernik, B.A. Korgel, Pervasive cation vacancies and antisite defects in copper indium diselenide (CuInSe2) nanocrystals, J. Phys. Chem. C. 123 (2019) 9544–9551.

[186] G. Jia, B. Liu, K. Wang, C. Wang, P. Yang, J. Liu, W. Zhang, R. Li, S. Zhang, J. Du, CuInTe 2 nanocrystals : Shape and size control , formation mechanism and application , and use as photovoltaics, Nanomaterials. 9 (2019) 409.

[187] L. Wang, J. Feng, Y. Tong, J. Liang, A reduced graphene oxide interface layer for improved power conversion efficiency of aqueous quantum dots sensitized solar cells, Int. J. Hydrogen Energy. 44 (2018) 128–135.

[188] H. Limborço, P.M.P. Salomé, R. Ribeiro-andrade, J.P. Teixeira, N. Nicoara, K. Abderrafi, J.P. Leitão, J.C. Gonzalez, S. Sadewasser, CuInSe 2 quantum dots grown by molecular beam epitaxy on amorphous SiO 2 surfaces, Beilstein J. Nanotechnol. 10 (2019) 1103–1111.

[189] M.P. Weir, D.T.W. Toolan, R.C. Kilbride, N.J.W. Penfold, A.L. Washington, S.M. King, J. Xiao, Z. Zhang, V. Gray, S. Dowland, J. Winkel, N.C. Greenham, R.H. Friend, A. Rao, A.J. Ryan, R.A.L. Jones, Ligand shell structure in lead sulfide–oleic acid colloidal quantum dots revealed by small-angle scattering, J. Phys. Chem. Lett. 10 (2019) 4713–4719.

[190] Y. V Kuznetsova, I. Letofsky-papst, B. Sochor, B. Schummer, A.A. Sergeev, F. Hofer, A.A. Rempel, Greatly enhanced luminescence efficiency of CdS nanoparticles in aqueous solution, Colloids Surfaces A. 581 (2019) 123814.

[191] A. Attanzio, A. Sapelkin, F. Gesuele, A. van der Zande, W.P. Gillin, M. Zheng, M. Palma, Carbon Nanotube-Quantum Dot Nanohybrids: Coupling with Single-Particle Control in Aqueous Solution, Small. 13 (2017) 1–5.

[192] S. Sharma, S.K. Mehta, A.O. Ibhadon, S.K. Kansal, Fabrication of novel carbon quantum dots modified bismuth oxide (α-Bi 2 O 3 /C-dots): Material properties and catalytic applications, J. Colloid Interface Sci. 533 (2019) 227–237.

[193] L. Hu, S. Huang, R. Patterson, J.E. Halpert, Enhanced mobility in PbS quantum dot films: Via PbSe quantum dot mixing for optoelectronic applications, J. Mater. Chem. C. 7 (2019) 4497–4502.

[194] M. Suri, A. Hazarika, B.W. Larson, Q. Zhao, M. Vallés-Pelarda, T.D. Siegler, M.K. Abney, A.J. Ferguson, B.A. Korgel, J.M. Luther, Enhanced open-circuit voltage of wide-bandgap perovskite photovoltaics by using alloyed (FA1- xCsx)Pb(I1- xBrx)3 quantum dots, ACS Energy Lett. 4 (2019) 1954–1960.

[195] X. Miao, S. Wen, Y. Su, J. Fu, X. Luo, P. Wu, C. Cai, R. Jelinek, L.P. Jiang, J.J. Zhu, Graphene quantum dots wrapped gold nanoparticles with integrated enhancement mechanisms as sensitive and homogeneous substrates for surface-enhanced raman spectroscopy, Anal. Chem. 91 (2019) 7295–7303.

[196] B. Babu, V.V.N. Harish, R. Koutavarapu, J. Shim, K. Yoo, Enhanced visible-light-

active photocatalytic performance using CdS nanorods decorated with colloidal SnO
2 quantum dots: Optimization of core–shell nanostructure, J. Ind. Eng. Chem. 76
(2019) 476–487.

[197] A.C. Badgujar, R.O. Dusane, S.R. Dhage, Sonochemical synthesis of
CuIn0.7Ga0.3Se2 nanoparticles for thin film photo absorber application, Mater. Sci.
Semicond. Process. 81 (2018) 17–21.

[198] X. Zhang, S. Liu, F. Wu, X. Peng, B. Yang, Y. Xiang, Phase-selective synthesis of
CIGS nanoparticles with metastable phases through tuning solvent composition,
Nanoscale Res. Lett. 13 (2018) 1–7.

[199] Y. Yu, G. Fan, A. Fermi, R. Mazzaro, V. Morandi, P. Ceroni, D.M. Smilgies, B.A.
Korgel, Size-dependent photoluminescence efficiency of silicon nanocrystal
quantum dots, J. Phys. Chem. C. 121 (2017) 23240–23248.

[200] E. Marino, T.E. Kodger, G.H. Wegdam, P. Schall, Revealing driving forces in
quantum dot supercrystal assembly, Adv. Mater. 1803433 (2018) 1–6.

[201] Q. Li, K. Tong, J. Qiu, M. Yan, Q. Tian, X. Chen, X. Yue, Molecular packing of
surface active ionic liquids in a deep eutectic solvent: A small angle X-ray scattering
(SAXS) study, Soft Matter. 15 (2019) 5060–5066.